University of Alberta

Arsenic Binding to Hemoglobin and Its Role in Arsenic Distribution, Metabolism, and Toxicity

by

Meiling Lu 

A thesis submitted to the Faculty of Graduate Studies and Research in partial fulfillment of the requirements for the degree of *Doctor of Philosophy*

Department of *Chemistry*

Edmonton, Alberta

Spring 2006

Your file Votre référence
ISBN: 0-494-14014-3
Our file Notre référence
ISBN: 0-494-14014-3

To my husband Hailin Wang, my son Huidong Wang, and my parents

For your love and encouragement throughout my program

Abstract

The metabolism, disposition, and toxicity of arsenic are dramatically different in humans and rats. To better understand the chemical and biochemical basis of these differences and the modes of action of arsenic, here I studied the interaction of arsenic species with hemoglobin (Hb) of both humans and rats.

Fast gel filtration chromatography combined with inductively coupled plasma mass spectrometry, nanoelectrospray mass spectrometry, and tandem mass spectrometry methods have been developed to facilitate the study. The three metabolically reactive trivalent arsenic species, inorganic arsenite (iAs^{III}), monomethylarsonous acid (MMA^{III}), and dimethylarsinous acid (DMA^{III}), showed increasing binding affinity with the Hb of rats and humans, with relative binding constants of 1:20:95 for rat Hb and 1:6.5:17 for human Hb. Rat Hb has a binding affinity for these arsenic species 3–16 times stronger than human Hb.

In vitro exposure of human and rat red blood cells (RBC) to iAs^{III}, MMA^{III}, and DMA^{III} showed that rat RBC can take up 1.5–4.5-fold more arsenic than human RBC; about 10–34-fold more arsenic species were bound to the Hb of rat RBC than to that of human RBC, consistent with the higher binding affinity of rat Hb to arsenic species.

Rats exposed to arsenic compounds accumulated arsenic in their RBC, with arsenic levels in the RBC being 185–1393-fold higher than in the plasma. Further investigation demonstrated that about 99% of arsenic in RBC of rats was bound to cys-13 in the α unit of rat Hb in the form of Hbα-DMA^{III} complex irrespective of whether rats were fed inorganic, monomethyl, or dimethyl arsenicals. The amount of rat Hbα-DMA^{III} is well correlated with the occurrence of hyperplasia and urothelial lesion severity in the

rat bladder. In contrast, RBC from acute promyelocytic leukemia patients under arsenic treatment only showed 2.5–4.5-fold higher arsenic in the RBC than in the plasma, with ~53% of arsenic in the RBC in the protein-bound form. The presence of the unique cysteine-13 in the α chain of rat Hb may be responsible for the apparent significant differences in arsenic disposition, metabolism, and toxicity between rats and humans.

Acknowledgements

I would like to express my gratitude to my supervisor, Dr. X. Chris Le, for his guidance and support throughout my PhD program. His expertise and patience added considerably to my graduate experience. With his support, I had terrific opportunities to collaborate with excellent researchers in toxicology, biochemistry, blood chemistry, and environmental health, through which I have greatly broadened my knowledge from pure analytical chemistry to environmental health-related fields.

I would also like to thank my committee members, Dr. Charles A. Lucy, Dr. John S. Klassen, Dr. Robert E. Campbell, Dr. Jason P. Acker, and Dr. David D. Y. Chen, for serving on my committee.

I would like to thank my collaborators: Dr. Xing-Fang Li (Department of Public Health Sciences) for her collaboration, discussions, suggestions, and support through my program; Dr. Samuel M. Cohen and Ms. Lora L. Arnold (University of Nebraska Medical Center) for their collaboration in the rat-related experiments and for providing the toxicological data; Dr. Jason P. Acker (Canadian Blood Services) for providing the human red blood cells and the facility for oxygen binding affinity measurement and for collaborating on the project examing the effect of arsenic on human blood cells; Dr. William R. Cullen (University of British Columbia) for providing his precious arsenic species; Dr. Jin Zhou (Harbin Medical University of China) for his collaboration on the project of acute promyelocytic leukemia patients under arsenic trioxide treatment.

I would like to thank Ms. Katerina Carastathis and Dr. Jeff Guthrie for copy-editing and proofreading my thesis.

I would like to thank all the other faculty and staff members, research associates, post-doctoral fellows, and students from Environmental Health Sciences for their discussions, suggestions, collaboration, and friendship.

I would like to thank Mrs. Ilona Baker and Ms. Jeannette Loiselle at the General Office of the Department of Chemistry for always being there and providing general support for me.

I would like to acknowledge the Graduate Teaching Assistantship and Graduate Research Assistantship from the Department of Chemistry and the Province of Alberta Graduate Fellowship from the Province of Alberta.

I would like to acknowledge the financial support provided for this project by the Natural Sciences and Engineering Research Council of Canada (NSERC), the Canadian Water Network (CWN-NCE), the Canada Research Chairs Program, and Alberta Health and Wellness.

I would like to thank my parents for their constant love and support.

Finally, I want to thank my husband and colleague, Dr. Hailin Wang, for his endless love, encouragement, patience, and great suggestions through my PhD research.

TABLE OF CONTENTS

LIST OF TABLES

LIST OF FIGURES

LIST OF SCHEMES

LIST OF ABBREVIATIONS

AFS	atomic fluorescence spectrometry
APL	acute promyelocytic leukemia
CAD	collision activated dissociation
Cys	cysteine
DMA^{III}	dimethylarsinous acid
DMA^{V}	dimethylarsinic acid
DNA	deoxyribonucleic acid
GFC	gel filtration chromatography
GSH	glutathione
Hb	hemoglobin
HGAFS	hydride generation atomic fluorescence spectrometry
hHb	human hemoglobin
HPLC	high performance liquid chromatography
iAs^{III}	inorganic arsenite
iAs^{V}	inorganic arsenate
ICPMS	inductively coupled plasma mass spectrometry
MMA^{III}	monomethylarsonous acid
MMA^{V}	monomethylarsonic acid
MS	mass spectrometry
MS/MS	tandem mass spectrometry
NanoESI	nanoelectrospray ionization

PBS	phosphate buffered saline
RBC	red blood cells
rHb	rat hemoglobin
SEM	scanning electron microscopy
TMA^{III}	trimethyl arsine
TMAO	trimethylarsine oxide
TOF	time-of-flight

Chapter 1 Literature Review

1.1 Introduction

Humans are exposed to various environmental contaminants during their life-span. Increasing health awareness and new developments in science and technology have spurred more research activities focusing on identification of environmental contaminants, characterization of their chemical, biological, and geographical properties, and assessment of their toxicological impacts. Various geographical and epidemiological surveys, chemical analyses, biological studies, and experimental animal models have been applied to understand the distribution, exposure, mechanisms, and health effects of these contaminants. My specific interest is to study one of the most notorious environmental contaminants: arsenic.

1.2 Environmental concern of arsenic

1.2.1 Arsenic exposure

Arsenic is a naturally occurring element. It is widely present in water and food (1). It is also used commercially as a preservative, pesticide, medicine, and in the manufacture of glass and semiconductors (1-3). Humans are exposed to arsenic mainly by ingestion of contaminated drinking water and food (4). Groundwater, the major source of drinking water in some geographic regions, may contain high levels of arsenic. Bangladesh is one of the countries most severely affected by arsenic. In most regions of Bangladesh (50 out of 64 districts), the arsenic concentration in groundwater is greater than 50 μg/L, affecting more than 35 million people in those areas (5). In West Bengal of

India, more than six million people are at risk from arsenic-contaminated drinking water, and more arsenic-affected areas have been identified in India (6). In the Blackfoot-disease (BFD) area of Taiwan, the average arsenic (predominantly As^{III}) concentration in wells is 671±149 μg/L compared to 0.7μg/L outside the BFD area (1). In China, a population of more than three million is exposed to high amounts of arsenic (>50 μg/L), and the endemic areas involve up to eight provinces and 37 counties across the country (7). High levels of arsenic (higher than the 10 μg/L World Health Organization guideline) in drinking water were also found in Argentina, Australia, Chile, Hungary, Mexico, Peru, Thailand, and the United States (1, 8, 9). Approximately nine million Canadians rely on groundwater as their drinking water source. It is not known how many Canadians are exposed to arsenic in drinking water at levels above the 25 μg/L Canadian interim guideline.

1.2.2 Health effects of arsenic

Chronic exposure to high levels of arsenic can cause a range of adverse health effects. Epidemiological studies have provided strong evidence that arsenic causes cancers in the bladder, liver, skin, lung, digestive tract, kidneys, and the lymphatic and hematopoietic systems (10-12). Arsenic also causes various noncancerous effects. Skin lesions are the most visible effect, such as the arsenicosis found in Bangladesh, India, and China (6, 7). A unique peripheral vascular disease, known as Blackfoot disease, was identified in Taiwan (1). Arsenic was also reported to increase the risk of hypertension, diabetes, and infant mortality, and to reduce the intellectual function of children (10, 13-16). No other environmental contaminant causes such extensive health effects.

1.2.3 Arsenic metabolism

The major species of arsenic in nature is inorganic arsenic (penta- or trivalent). It can be metabolized in the human body after ingestion; the organs most likely involved are the liver and kidneys (17). The widely accepted arsenic metabolism pathway is an alternate reduction followed by a sequential oxidative methylation process (18), which forms a series of arsenic metabolites such as monomethylarsonic acid (MMA^V), monomethylarsonous acid (MMA^{III}), dimethylarsinic acid (DMA^V), dimethylarsinous acid (DMA^{III}), trimethylarsine oxide (TMAO), and even trimethylarsine (TMA) (Scheme 1-1). Generally, dimethyl arsenicals are the final metabolites for most mammals. Some bacteria can further methylate arsenic to TMAO and TMA. Even among mammal species, the methylation efficiency can vary greatly. For example, rats can methylate arsenic to TMAO (19).

DMA^V and MMA^V were found to be the major metabolites in human urine two decades ago (1), and soon it was discovered that these two species were less toxic than their inorganic parent compounds (1). This led to the conclusion that arsenic metabolism is a detoxification pathway. The intermediate trivalent arsenic species (MMA^{III} and DMA^{III}) are chemically unstable, and are easily oxidized to their pentavalent forms *in vitro* (20). Following recent developments in arsenic speciation analysis, MMA^{III} and DMA^{III} were repeatedly observed in the urine of humans exposed to high levels of arsenic from drinking water (21-23), which confirms that the intermediate arsenic species do indeed circulate *in vivo*. Therefore, it is very important to understand the toxicity of each individual metabolite and its relative contribution to the overall arsenic toxicity. It

has recently been found that DMA^{III} and MMA^{III} may be more toxic than inorganic arsenic (24-27), which suggests that inorganic arsenic may be bioactivated *in vivo*.

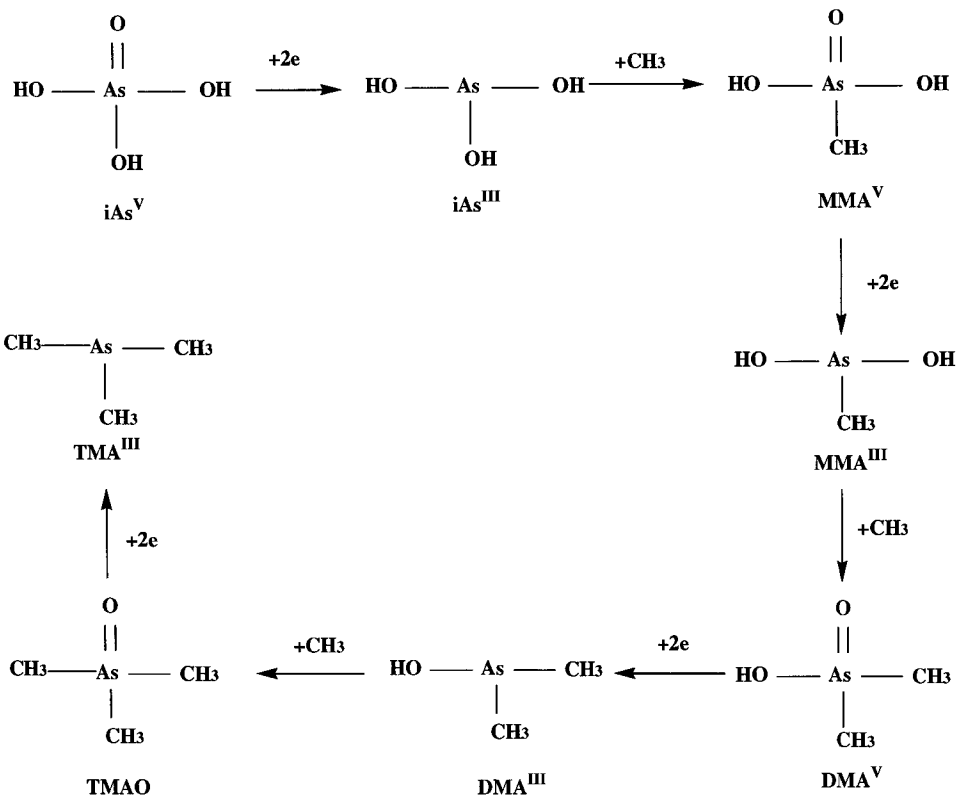

Scheme 1-1. Pathway of arsenic metabolism. Enzyme involved: methyltransferase; methyl donor: S-adenosylmethionine (SAM); reducing agents: possibly glutathione (1).

1.2.4 Possible mechanisms of arsenic action

How arsenic causes toxicity has always been the focus of arsenic research, but this has not yet been well-established. A number of possible mechanisms have been proposed in the past two decades. The earliest theory of arsenic toxicity is that arsenic can break down energy metabolism by forming an unstable arsenate ester instead of a

phosphate ester (1). Oxidative stress is one of the newer theories and has recently been paid increasing attention. In 1989, Yamanaka et al. (28) found a high degree of DNA damage in the lungs of ICR male mice exposed to 1500 mg/kg of DMA^V, which suggested that active oxygen species could be involved. Subsequently, more and more experimental evidence was reported. For example, the oxidative DNA damage indicator, 8-hydroxy-2'-deoxyguanosine, was detected in significantly enhanced levels in rats exposed to DMA^V, MMA^V, or TMAO, compared to the control rats (29-31). The free radicals trapped by the trapping reagent (DMSO) were detected by electron paramagnetic spectroscopy in mice exposed to arsenic, and inhibition of free radical generation by co-administration of a free radical scavenger such as superoxide dismutase was also observed (32). This evidence indicates that the generation of reactive oxygen species is likely to play an important role in the arsenic induction of carcinogenesis in the early phase. Other mechanisms include the alteration of chromosomal abnormalities, promotion of carcinogenesis, alteration in growth factors, induction of cell proliferation, inhibition of DNA repair and several key enzymes, and modulation of DNA methylation and gene expression (33, 34). All these mechanisms are interrelated, and no single mechanism can explain the complex consequences of arsenic exposure so far.

1.2.5 Animal models for arsenic-induced cancers

Arsenic has been confirmed as a complete carcinogen in humans. It is able to induce cancer without inducement by other agents that promote tumor growth or development. However, most experimental animals used to evaluate the carcinogenesis of arsenic, such as hamsters, beagles, and cynomolgus monkeys, displayed tolerance to

arsenic after long-term administration (1, 31). Distinct exceptions were rats and mice. DMA^V, the major arsenic metabolite in most mammals including humans, was shown to have a carcinogenic effect on the bladder of male and female F344 rats during two-year bioassays (35, 36). The carcinogenic effects of DMA^V were also observed in mice (37). In addition, DMA^V was shown to have promotion effects on a medium-term multi-organ (including the urinary bladder, kidneys, liver, and thyroid gland) carcinogenesis bioassay in male F344 rats (31).

DMA^V is a complete carcinogen for the rat bladder. However, a number of issues remain unclear, such as why rats are unique in the induction of bladder cancer by DMA^V, what effects the environmentally present inorganic arsenic would have on rats, and how to extrapolate the toxicological data obtained from rats to humans. Therefore, it would be very interesting to examine the possible contributions that lead to the unique carcinogenic effects of arsenic on rats.

1.2.6 Arsenic in blood

When arsenic is absorbed and enters the blood stream, it undergoes distribution throughout the body via systematic blood circulation, and causes adverse effects in specific locations of the body. The transportation of arsenic in the blood would certainly have critical effects on the toxicokinetics and toxicodynamics of arsenic. The differences in the blood transport of a specific toxin between experimental animals and humans may be a critical factor to consider for understanding the experimental data and extrapolating this data to humans. It has been found that arsenic in the blood of humans and rats is significantly different. Rats can accumulate arsenic for a long time (related to the life

cycle of the red blood cells) with a significant amount of arsenic in red blood cells (RBC), as seen from previous studies (1, 17, 38), while humans clear arsenic very quickly (1, 39). The retention of arsenic in blood is probably due to the strong binding of arsenic to the proteins in the RBC. This may alter the metabolism pathway, change the *in vivo* biotransformation fate of arsenic, and furthermore change the toxicity profile since different arsenic species have different toxicities. Therefore, the interaction of arsenic with blood proteins is of particular interest.

1.3 Hemoglobin adduct and its application in biomonitoring

1.3.1 Hemoglobin structure and function

Hemoglobin (Hb) is the most abundant blood protein present in the RBC. It has been studied for more than half a century, and it still attracts much attention. Hb basically consists of four units, two α units and two β units. There is one prosthetic group, heme, in each unit (Figure 1-1). Each unit has a molecular weight of ~16 kDa. The main function of Hb is to transport oxygen (O_2) from the lungs to other tissues and carry carbon dioxide (CO_2) back to the lungs. The distinct quaternary structure of Hb allows its conformation to change when it is exposed to different environments. In the lungs where there is more O_2 and less CO_2, the Hb is oxygenated. In the tissues where there is more CO_2 and less O_2, the Hb is deoxygenated. The dissociation/association isotherm curve of Hb indicates the affinity of oxygen binding and the cooperativity of the four units in Hb molecules (Figure 1-2). Significant changes in the dissociation curve of Hb may indicate that the function of oxygen transport has been affected.

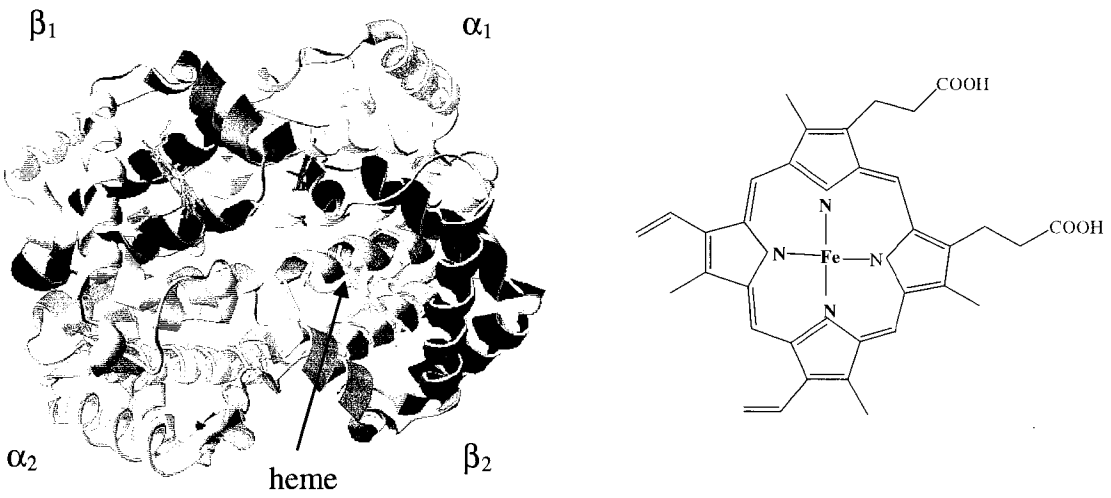

(a) (b)

Figure 1-1. Structure of hemoglobin. (a) three dimensional structure of hemoglobin; (b) structure of the heme prosthetic group. The three dimensional structure of hemoglobin was displayed using DeepView/Swiss PdbView (http://www. Expasy.org/spdbv, 40). The structure of heme was drawn using ChemDraw 6.0 (CambridgeSoft, Cambridge, MT).

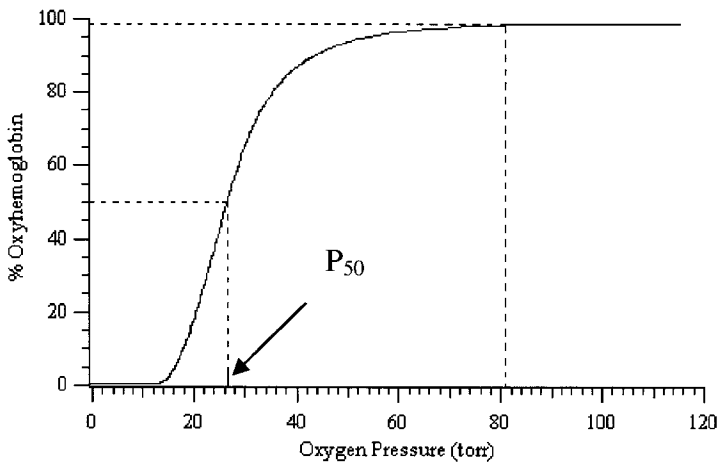

Figure 1-2. Dissociation curve of hemoglobin. Data was generated from hemoglobin of a healthy human volunteer using Hemox Analyzer.

1.3.2 Modification of hemoglobin

Hb possesses several nucleophilic sites such as cysteine, lysine, and histidine residues that make it a target for electrophilic attack by toxins, and allow the formation of Hb complexes. In fact, it has been found that Hb is a target for interaction with various xenobiotics since it is abundantly distributed in the blood and is in constant contact with the pulmonary blood supply. Such interactions may have an influence on the distribution and toxicity of toxins.

Hb complexes were originally suggested as biochemical markers of carcinogen exposure and measures of genotoxic risk three decades ago (41, 42). Subsequently, a number of studies have demonstrated that carcinogenic compounds can bind covalently to Hb (43-45). There are a number of advantages to use Hb complexes as biomarkers. Hb is relatively easy to obtain and the associated Hb complexes are generally stable at physiological conditions. Hb and RBC have no mechanism to repair Hb complexes, so the binding kinetics is relatively simple. The lifetime of the RBC in the circulation of blood is approximately 120 days in humans. Therefore, Hb complexes would accumulate in the blood, thereby enhancing their detection and allowing them to be used as biomarkers of exposure to various agents. The level of Hb complexes may reflect the exposure within the last several months.

1.4 Study hypothesis and objectives

1.4.1 Study hypothesis

The above review has shown that reactive arsenic metabolites may interact with some proteins by binding to them. Arsenic retention in RBC may be due to arsenic-protein binding in the RBC, which cannot transport across the cell membrane freely. Therefore, I made the following three hypotheses:

1. The reactive arsenic metabolite may bind to the most abundant protein, Hb, in the RBC, leading to significant accumulation of arsenic in rat blood.
2. The binding of arsenic to Hb could stabilize the reactive arsenic metabolites, providing an effective way to trace these reactive metabolites *in vivo*.
3. The reactive arsenic metabolites binding to Hb could play a critical role in arsenic distribution, metabolism, and overall toxicity.

1.4.2 Study objectives

Based on the above hypotheses, the primary objective of this thesis is to develop analytical methods and apply them to evaluate the reactivity of each arsenic species involved in the metabolic pathway to Hb in humans and rats, from which the chemical basis of arsenic accumulation in blood may be elucidated. With the achievement of the primary objective, further study focuses on: determination of the factor(s) governing the reactivity; demonstration of arsenic distribution, accumulation, and dose response of the arsenic binding in blood; and elucidation of the relationship between arsenic-Hb binding and the occurrence of adverse health effect(s).

1.5 Study methods

1.5.1 Gel filtration chromatography-inductively coupled plasma mass spectrometry

To facilitate the arsenic-protein interaction study, a gel filtration chromatography-inductively coupled plasma mass spectrometry (GFC-ICPMS) method has been developed.

Gel filtration chromatography (GFC) (46) separates molecules based on molecular size. The matrix stationary-microbeads in the column contain pores and internal channels. Small molecules easily diffuse into the pores and the internal channels, and therefore take longer to be eluted out of the column (Figure 1-3). Larger molecules diffuse with more difficulty into the small pores. They tend to flow around and between the beads, and so are eluted out of column faster (with shorter retention time). GFC is biocompatible, and is widely applied in separation, purification, and preparation of proteins.

Inductively coupled plasma mass spectrometry (ICPMS) (47) is a powerful analytical tool for analysis of trace and ultra-trace elements. In ICPMS, a plasma of high temperature (6000–8000 K) is first generated from argon gas. A sample (usually aerosol or gas) is introduced into the plasma. The plasma then atomizes and ionizes the elements in the sample. The resulting ions are transferred to a mass spectrometer (typically a quadrupole) and analyzed according to the mass-to-charge ratios. The intensity of a specific elemental ion in the mass spectrum is proportional to the amount of that element in the original samples, which is the basis for quantitative analysis.

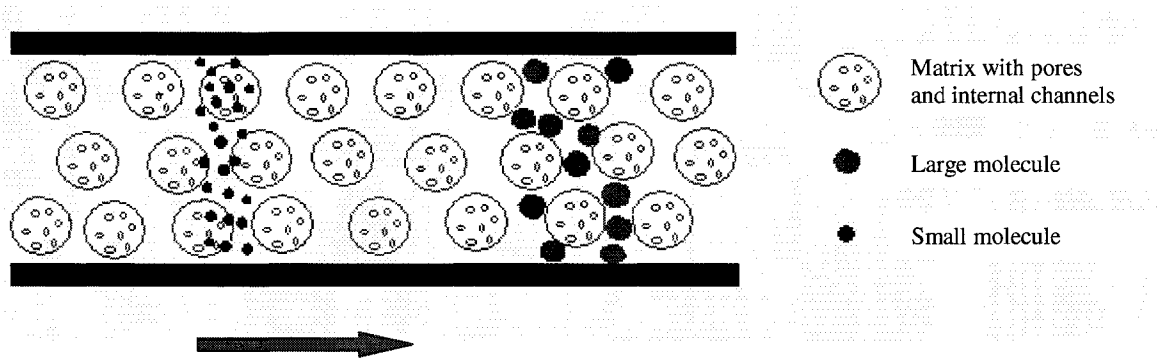

Figure 1-3. Schematic diagram showing the separation of molecules of different sizes by gel filtration chromatography

Hyphenating gel filtration chromatography (GFC) with inductively coupled plasma mass spectrometry (GFC-ICPMS) (Figure 1-4) takes the advantages of both techniques. When applying this hyphenated technique in arsenic-protein interaction studies, GFC facilitates separation of protein-bound arsenic from free arsenic, and ICPMS allows sensitive, selective, and quantitative detection of arsenic. With the quantitation of both protein-bound arsenic and free arsenic, the binding constants between arsenic and protein can be determined. This technique also allows speciation of protein-bound arsenic and free arsenic in the blood and other biological samples.

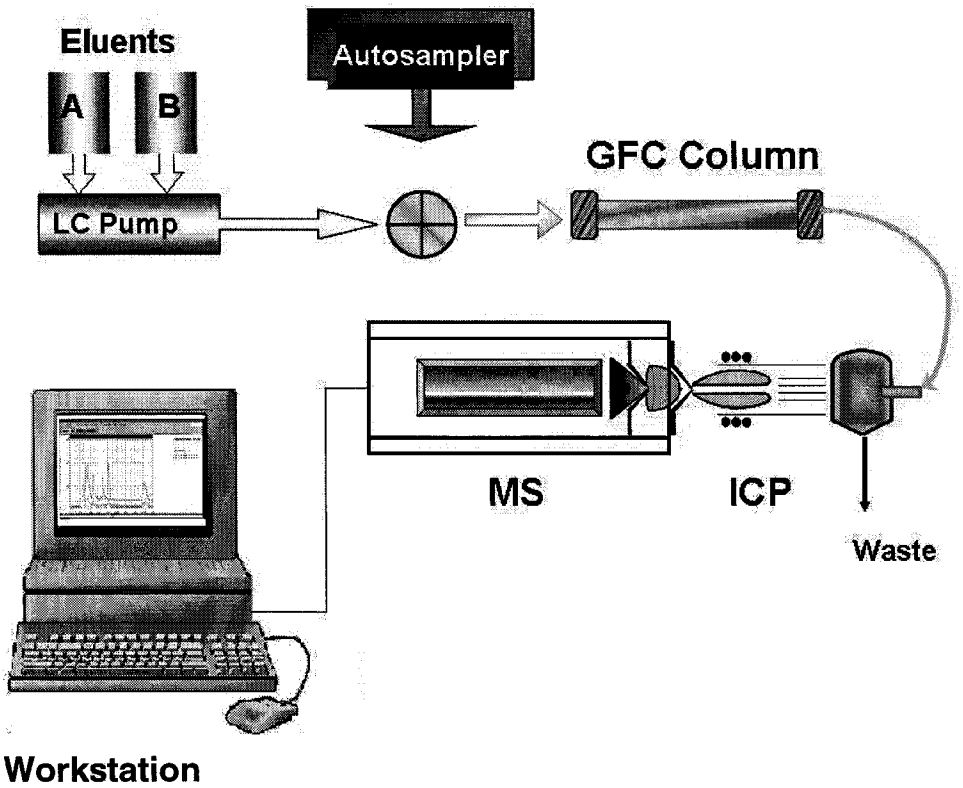

Figure 1-4. Diagram of a GFC-ICPMS system

1.5.2 Nanoelectrospray ionization hybrid quadrupole time-of-flight mass spectrometry

To characterize the arsenic-protein interaction product and identify the binding site of arsenic in the protein, a nanoelectrospray ionization hybrid quadrupole time-of-flight mass spectrometry (nanoESI-Q/TOF-MS) method has been developed.

Electrospray ionization (ESI) (48) is a soft ionization method that transfers ions in solution to gas phase molecular ions. It causes little interruption of the distinct structure of biomolecules. It uses a conductive capillary tip and a high voltage, and the process is carried out at atmospheric pressure. The analyte solution in the capillary tip is transferred

into the gas phase by applying a high voltage (Figure 1-5). The droplets in the gas phase undergo solvent evaporation and droplet fission processes, and eventually multiply charged ions are formed (Figure 1-5). Using a capillary tip with smaller diameter and lower diffusion rate allows the spraying of the solution at the rate of nanolites per minute; this is termed nanoelectrospray ionization (nanoESI). NanoESI has high sensitivity, which is particularly useful for the analysis of samples with very small amount. It also allows the use of low voltage for the ion spray, which is suitable for maintaining weak associations such as noncovalent complexes.

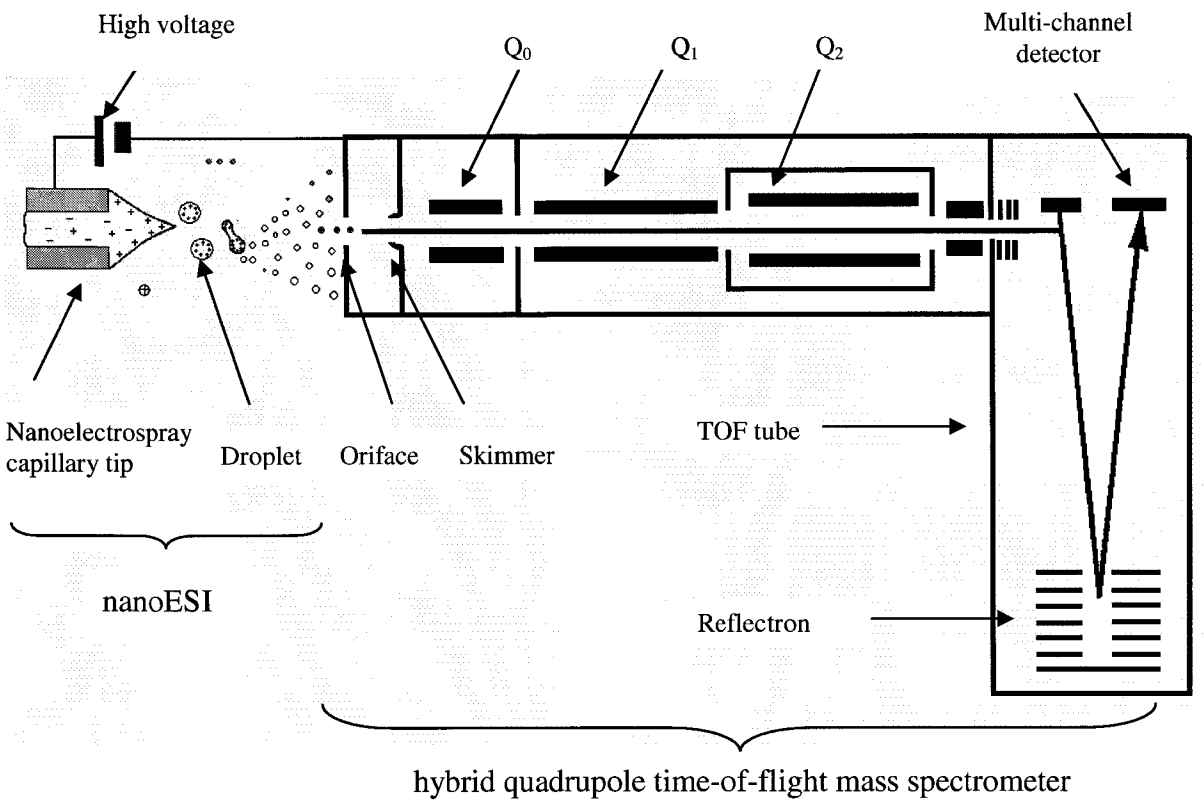

Figure 1-5. A schematic diagram showing the nanoESI-hybrid Q/TOF mass spectrometer. Q_0, Q_1, and Q_2 are the three quadrupoles in series. TOF is the mass analyzer in both the TOF-MS mode and the MS/MS modes.

The nanoESI typically produces multiply charged ions in the gas phase. The ions are transferred into a mass spectrometer for analysis. In the settings of hybrid quadrupole time-of-flight mass spectrometry (Q/TOF-MS) such as the QSTAR system (Applied Biosystems/MDS Sciex, Concord, Ontario) (Figure 1-5), there are three quadrupoles in series (Q_0, Q_1, and Q_2) and a time-of-fight mass analyzer orthogonal to the quadrupoles. Q_0 acts as a mass filter by applying characteristic electric voltage, which allows ions in a specified range of mas-to-charge ratio to pass through. When the instrument is operated in TOF-MS mode, Q_1 and Q_2 work the same way as Q_0, allowing the ions to pass through the three quadrupoles and fly into the TOF region. In TOF the ions are separated according to the flight time and detected by a multichannel detector. When the setting is operated in MS/MS mode, quadrupole Q_1 is used as a mass selector to select the parent ions of interest, and quadrupole Q_2 is used as a collision cell where nitrogen gas is introduced to collide with the parent ions and generate fragment ions. The fragment ions are then transferred to the TOF region, separated on the basis of flight time, and detected by a multi-channel detector.

Use of the nannies hybrid quadruple time-of-flight mass spectrometry in TOFMS mode allows the characterization of protein-arsenic complex, including the bound protein species, bound arsenic species, and binding stoichiometry; use of this system in MS/MS mode allows the identification of the binding site of arsenic species in the protein.

1.6 Design of project and overview of the contents of the thesis

The project was designed in three phases, as follows.

The first phase developed the above analytical methods and applied them to study the interaction of the model protein, Hb, from humans and rats with arsenic species, in order to evaluate the reactivity of each arsenic species to Hb and to determine the possible binding stoichiometries and the targeting amino acid residues (Chapter 2).

The second phase applied both analytical methods to study the interaction of arsenic species with the RBC of humans and rats and to identify the possible interaction products (Chapter 2).

The third phase applied a series of analytical and bioanalytical methods to study arsenic in blood *in vivo*. In the rat model system, arsenic distribution, accumulation, dose effect, binding stoichiometry, the relevance to the occurrence of health effects (Chapter 3), and the binding site (Chapter 4) were systematically studied after exposing rats to arsenic compounds. To further extend this research in humans, a preliminary study based on acute promyelocytic leukemia (APL) patients under arsenic trioxide treatment was also carried out (Chapter 5).

The major conclusions arising from this project are discussed in Chapter 6 and some potential future projects are proposed.

1.7 References

1. National Research Council (1999) *Arsenic in the Drinking Water,* National Academy Press, Washington, DC.
2. Basu, A., Mahata, J., Gupta, S., and Giri, A. K. (2001) Genetic toxicology of a paradoxical human carcinogen, arsenic: a review. *Mutat. Res.* **488**, 171-194.

3. Zhang, T.-D., Chen, G.-Q., Wang, Z.-G., Wang, Z.-Y., Chen, S.-J., and Chen, Z. (2001) Arsenic trioxide, a therapeutic agent for APL. *Oncogene* **20**, 7146-7153.
4. Wu, M.-M., Chiou, H.-Y., Wang, T.-W., Hsueh, Y.-M., Wang, I.-H., Chen, C.-J., and Lee, T.-C. (2001) Association of blood arsenic levels with increased reactive oxidants and decreased antioxidant capacity in a human population of northeastern Taiwan. *Environ. Health Perspect.* **109**, 1011-1017.
5. BGS (2001) *Arsenic contamination of groundwater in Bangladesh.* BGS technical report WC/00/19, Keyworth, UK: British Geological Survey.
6. Chakraborti, D., Mukherjee, S.C., Pati, S., Sengupta, M. K., Rahman, M. M., Chowdhury, U. K., Lodh, D., Chanda, C. R., Chakraborty, A. K., and Basul, G. K. (2003) Arsenic groundwater contamination in Middle Ganga Plain, Bihar, India: a future danger? *Environ. Health Perspect.* **111**,1194-1201.
7. Sun, G. (2004) Arsenic contamination and arsenicosis in China. *Toxicol. Appl. Pharmacol.* **198**, 268-271.
8. Graziano, J. H. and van Geen, A. (2005) Reducing arsenic exposure from drinking water: Different settings call for different approaches. *Environ. Health Perspect.* **113**, A360-A361.
9. WHO (2001) Arsenic in drinking water. *WHO Fact Sheet*, **No 210**, World Health Organization.
10. National Research Council (2001) *Arsenic in the Drinking Water,* (update) National Academy Press, Washington, DC.
11. Abernathy, C. O., Liu, Y. P., Longfellow, D., Aposhian, H. V., Beck, B. D., Fowler, B. A., Goyer, R. A., Menzer, R., Rossman, T., Thompson, C., and

Waalkes, M. (1999) Arsenic: health effects, mechanisms of actions, and research issues. *Environ. Health Perspect.* **107**, 593-597.

12. U.S. Department of Health and Human Services, Public Health Service, National Toxicology Program (2005) Substance profiles: arsenic compounds, inorganic. *11th Carcinogen Report.*
13. Tseng, C. H., Tseng, C. P., Chiou, H. Y., Hsueh, Y. M., Chong, C. K., and Chen, C. J. (2002) Epidemiologic evidence of diabetogenic effect of arsenic. *Toxicol Lett.* **133**, 69-76.
14. Rahman, M. (2002) Arsenic and hypertension in Bangladesh. *Bull. WHO* **80**, 173.
15. Hopenhayn-Rich, C., Browning, S. R., Hertz-Picciotto, I., Ferreccio, C., Peralta, C., and Gibb, H. (2000) Chronic arsenic exposure and risk of infant mortality in two areas of Chile. *Environ. Health Perspect.***108**, 667-673.
16. Wasserman, G. A., Liu, X. H., Parvez, F., Ahsan, H., Factor-Litvak, P., van Geen, A., Slavkovich, V., Lolacono, N. J., Cheng, Z. Q., Hussain, L., Momotaj, H., and Graziano, J. H. (2004) Water arsenic exposure and children's intellectual function in Araihazar, Bangladesh. *Environ. Health Perspect.* **112**, 1329-1333.
17. Lerman, S. A. and Clarkson, T. W. (1983) The metabolism of arsenite and arsenate by the rat. *Fundam. Appl. Toxicol.* **3**, 309-314.
18. Challenger, F. (1945) Biological methylation. *Chem. Rev.* **36**, 315-361.
19. Lu, X., Arnold, L.L., Cohen, S.M., Cullen,W.R., and Le, X.C. (2003) Speciation of dimethylarsinous acid and trimethylarsine oxide in urine from rats fed with dimethylarsinic acid and dimercaptopropane sulfonate. *Anal. Chem.* **75**, 6463-6468.

20. Gong, Z., Lu, X., Cullen, W. R., and Le, X.C. (2001) Unstable trivalent arsenic metabolites, monomethylarsonous acid and dimethylarsinous acid. *J. Anal. At. Spectrom.* **16**, 1409-1413.

21. Aposhian, H. V., Gurzau, E. S., Le, X. C., Gurzau, A., Healy, S. M., Lu, X. F., Ma, M. S., Yip, L., Zakharyan, R. A., Maiorino, R. M., Dart, R. C., Tircus, M. G., Gonzalez-Ramirez, D., Morgan, D. L., Avram, D., and Aposhian, M. M. (2000) Occurrence of monomethylarsonous acid in urine of humans exposed to inorganic arsenic. *Chem. Res. Toxicol.* **13**, 693-697.

22. Le, X. C., Lu, X., Ma, M., Cullen, W. R., Aposhian, H. V., and Zheng, B. (2000) Speciation of key arsenic metabolic intermediates in human urine. *Anal. Chem.* **72**, 5172-5177.

23. Mandal, B. K., Ogra, Y., and Suzuki, K. T. (2001) Identification of dimethylarsinous and monomethylarsonous acids in human urine of the arsenic-affected areas in West Bengal, India. *Chem. Res. Toxicol.* **14**, 371-378.

24. Aposhian, H. V., Zakharyan, R. A., Avram, M. D., Kopplin, M. J., and Wollenberg, M. L. (2003) Oxidation and detoxification of trivalent arsenic species. *Toxicol. Appl. Pharmacol.* **193,** 1-8.

25. Styblo, M., Del Razo, L. M., Vega, L., Germolec, D. R., LeCluyse, E. L., Hamilton, G. A., Reed, W., Wang, C., Cullen, W. R., and Thomas, D. J. (2000) Comparative toxicity of trivalent and pentavalent inorganic and methylated arsenicals in rat and human cells. *Arch. Toxicol.* **74**, 289–299.

26. Kitchin, K. T. and Ahmad, S. (2003) Oxidative stress as a possible mode of action for arsenic carcinogenesis. *Toxicol. Lett.* **137**, 3-13.

27. Mass, M. J., Tennant, A., Roop, B. C., Cullen, W. R., Styblo, M., Thomas, D. J., and Kligerman, A. D. (2001) Methylated trivalent arsenic species are genotoxic. *Chem. Res. Toxicol.* **14,** 355-361.

28. Yamanaka, K., Hasegawa, A., Sawamura, R., and Okada, S. (1989) Dimethylated arsenics induce DNA strand breaks in lung via the production of active oxygen in mice. *Biochem. Biophys. Res. Commun.* **165**, 43-50.

29. Wei, M., Wanibuchi, H., Morimura, K., Iwai, S., Yoshida, K., Endo, G., Nakae, D., and Fukushima, S. (2002) Carcinogenicity of dimethylarsinic acid in male F344 rats and genetic alterations in induced urinary bladder tumors. *Carcinogenesis* **23**, 1387-1397.

30. Nishikawa, T., Wanibuchi, H., Ogawa, M., Kinoshita, A., Morimura, K., Hiroi, T., Funae, Y., Kishida, H., Nakae, D., and Fukushima, S. (2002) Promoting effects of monomethylarsonic acid, dimethylarsinic acid and trimethylarsine oxide on induction of rat liver preneoplastic glutathione S-transferase placental form positive foci: A possible reactive oxygen species mechanism. *Int. J. Cancer* **100**, 136-139.

31. Wanibuchi, H., Salim, E. I., Kinoshita, A., Shen, J., Wei, M., Morimura, K., Yoshida, K., Kuroda, K., Endo, G., and Fukushima, S. (2004) Understanding arsenic carcinogenicity by the use of animal models. *Toxicol. Appl. Pharmocol.* **198**, 366-376.

32. Liu, S. X., Athar, M., Lippai, I., Waldren, C., and Hei, T. K. (2001) Induction of oxyradicals by arsenic: Implication for mechanism of genotoxicity. *Proc. Natl. Acad. Sci. USA* **98**, 1643-1648.

33. Kitchin, K. T. (2001) Recent advances in arsenic carcinogenesis: Modes of action, animal model systems, and methylated arsenic metabolites. *Toxicol. Appl. Pharmacol.* **172**, 249-261.

34. Miller, W. H., Schipper, H. M., Lee, J. S., Singer, J., and Waxman, S. (2002) Mechanisms of action of arsenic trioxide. *Cancer Res.* **62**, 3893-3903.

35. Wei, M., Wanibuchi, H., Yamamoto, S., Li, W., and Fukushima, S. (1999) Urinary bladder carcinogenicity of dimethylarsinic acid in male F344 rats. *Carcinogenesis* **20**, 1873-1876.

36. Arnold, L. L., Cano, M., St John, M., Eldan, M., van Gemert, M., and Cohen, S. M. (1999) Effects of dietary dimethylarsinic acid on the urine and urothelium of rats. *Carcinogenesis* **20**, 2171-2179.

37. Salim, E.T., Wanibuchi, H., Morimura, K., Wei, M., Yashida, K., Endo, G., and Fukushima, S. (2003) Carcinogenicity of dimethylarsince acid in $p53^{+/-}$ heterozygous knockout and wild type C57BL/6J mice. *Carcinogenesis* **24**, 335-342.

38. Odanaka, Y., Matano, O., and Goto, S. (1980) Biomethylation of inorganic arsenic by the rat and some laboratory animals. *Bull. Environ. Contam. Toxicol.* **24**, 452-459.

39. Pomroy, C., Charbonneau, S. M., McCullough, R. S., and Tam, G. K. H. (1980) Human retention studies with ^{74}As. *Toxicol. Appl. Pharmacol.* **53**, 550-556.

40. Guex, N. and Peitsch, M.C. (1997) Swiss-Model and the Swiss-PdbViewer: An environment for comparative protein modeling. *Electrophoresis* **18**, 2714-2723.

41. Ehrenberg, L., Ostermangolkar, S., Segermangolkar, S., Segerback, D., and Svensson, K., and Calleman, C. J. (1977) Evaluation of genetic risks of alkyation-agents. 3. Alkaylation of hemoglobin after metabolic conversion of ethane to ethane oxide in vivo. *Mutat. Res.* **45**, 175-184.

42. Segerback, D., Calleman, C. J., Ehrenberg, L., Lofroth, G., and Ostermangolkar, S. (1978) Evaluation of genetic risks of alkylation-agents. 4. Quantitative-determination of alkylated amino-acids in hemoglobin as a measure of dose after treatment of mice with methyl methanesulfonate. *Mutat. Res.* **49**, 71-82.

43. Day, B. W., Naylor, S., Gan, L. S., Sahali, Y., Nguyen, T. T., Skipper, P. L., Wishnok, J. S., and Tannenbaum, S. R. Molecular dosimetry of polycyclic aromatic hydrocarbon epoxides and diol epoxides via hemoglobin adducts. *Cancer Res.* **50**, 4611-4618.

44. Calleman, C. J., Wu, Y., He, F., Tian, G., Bergmark, E., Zhang, S., Deng, H., Wang, Y., Crofton, K. M., Fennell, T., and Costa, L. G. (1994) Relationships between biomarkers of exposure and neurological effects in a group of workers exposed to acrylamide. *Toxicol. Appl. Pharmacol.* **126**, 361-371.

45. Osterman-Golkar, S. M., Moss, O., James, A., Bryant, M. S., Turner, M., and Bond, J. A. (1998) Epoxybutene-hemoglobin adducts in rats and mice: Dose response for formation and persistence during and following long-term low-level exposure to butadiene. *Toxicol. Appl. Pharmacol.* **150**, 166-173.

46. Fischer, L. (1980) *Gel filtration chromatography,* Elsevier/North-Holland Biomedical Press, Amsterdam.

47. Thomas, R. (2004) *Practical guide to ICP-MS,* Marcel Dekker, New York.

48. Cole, R. B. (1997) *Electrospray ionization mass spectrometry: fundamentals, instrumentation, and applications* Wiley, New York.

Chapter 2 Evidence of hemoglobin binding to arsenic as a basis for the accumulation of arsenic in rat blood[1]

2.1 Introduction

Epidemiological studies from several arsenic endemic regions have provided clear evidence that chronic exposure to arsenic can lead to a range of adverse health effects (1-7). Studies of populations from Taiwan, Argentina, and Chile exposed to high levels of arsenic from ingestion of drinking water have shown an association between arsenic ingestion and the prevalence of skin, lung, and bladder cancers (1-4). Numerous reports from other areas of the world, such as India, Bangladesh, Inner Mongolia (China), and Mexico, have also attributed cancer etiology to high levels of arsenic in drinking water (1, 2, 5-7). In addition, there is increasing evidence demonstrating that various non-cancerous effects, such as hypertension, diabetes, and cardiovascular disease, may result from exposure to arsenic (1, 2, 8, 9). Although arsenic in drinking water affects tens of millions of people worldwide (10), the mechanism(s) of action by which arsenic causes adverse health effects is not clear (2, 7).

The limitation of animal models for arsenic-induced carcinogenicity makes it more difficult to understand arsenic health effects (11). Nonetheless, an intriguing difference between humans and rats has been observed. Studies have shown that arsenic was cleared from human blood with a short half-life of 1 h (12-13). In contrast, arsenic

[1] *A version of this chapter has been published. Lu et al. 2004. Chem. Res. Toxicol. 17: 1733-1742.*

displayed a longer retention in rat blood (14-17). The hemoglobin (Hb) in red blood cells (RBC) was considered to be a possible target protein (18-19). However, the biochemical basis for arsenic accumulation in the RBC of rats required examination. Rat Hb binding directly to trivalent arsenicals may lead to the retention of arsenic in the RBC. To test this hypothesis, the binding between rat Hb and human Hb with various arsenic species have been examined, and the affinity of rat Hb and human Hb for arsenic species have been compared in this chapter.

The interaction of Hb with three major trivalent arsenic species, inorganic arsenite (iAs^{III}), monomethylarsonous acid (MMA^{III}), and dimethylarsinous acid (DMA^{III}), have been chosen in this study because of their recognized toxicity (20-24). MMA^{III} and DMA^{III} are two major reactive trivalent arsenic metabolites that have recently been found to be present in biological systems (25-29). They are among the most toxic arsenic species to humans and experimental animals (20-24, 30). The relative reactivity of these trivalent arsenic species with hHb and rHb has been demonstrated in this chapter. By using three systems — pure Hb, RBC, and rats fed with arsenic-supplemented diet — it has shown that differences in the binding affinity of these arsenic species to the Hb of rats and humans are responsible for the difference in arsenic retention in rat and human blood. The results provide a chemical basis for understanding how and why arsenic accumulates in blood.

2.2 Materials and Methods

2.2.1 Materials

Standard iAs^{III} solution (1000 mg/L arsenic) was obtained from Sigma (St. Louis, MO). Phenylarsine oxide ($PhAs^{III}O$) (C_6H_5AsO) and dimethylarsinic acid (DMA^V) [$(CH_3)_2As(O)OH$] (hydroxyldimethylarsine oxide) were obtained from Aldrich (Milwaukee, WI). Methylarsine oxide (CH_3AsO) and iododimethylarsine [$(CH_3)_2AsI$] were prepared following literature procedures (31-32), and were kept at -20 °C. Dilute solutions of these precursors were prepared fresh in deionized water to form MMA^{III} [$CH_3As(OH)_2$] and (DMA^{III}) [$(CH_3)_2AsOH$], respectively.

Standard human hemoglobin (hHb, purity 98%)) and rat hemoglobin (rHb, purity 98%) were purchased from Sigma (St. Louis, MO) and used without further purification. Another rHb was obtained from the frozen RBC of a female F344 rat (University of Nebraska Medical Center). The rat RBC (64 mg, wet weight) were thawed and lysed. The lysate was suspended in 1 mL phosphate buffer (5 mM, pH 7.2) and centrifuged at 12000 rpm for 10 min. The concentration of rHb in the supernatant solution was measured by absorbance at 523 nm and calibrated against the commercial rHb from Sigma. Stock solutions of rHb or hHb (100 μM or 6.45 mg/mL) were prepared in 20 mM ammonium acetate aqueous solution (pH 7.0). They were kept at 4 °C and diluted to appropriate concentrations with 20 mM ammonium acetate solution (pH 7.0).

Methanol, formic acid, and water (all HPLC grade) were purchased from Fisher Scientific (Fair Lawn, NJ). All other reagents used in the experiments were HPLC grade or analytical grade.

2.2.2 Instrumentation and procedures

2.2.2.1 Gel filtration chromatography separation with ICPMS detection (GFC-ICPMS)

A Perkin-Elmer 200 series HPLC system (PE Instruments, Shelton, CT) fitted with an autosampler was part of the system used for the quantitative detection of arsenic. A Sephadex desalting column (10 mm internal diameter, 26 mm long) with an exclusion limit of 5000 Da (Amersham Biosciences, CA) was used as the GFC column to separate the protein-bound arsenic from the unbound arsenic species. A volatile buffer, ammonium acetate (20 mM, pH 7.0), was chosen as the mobile phase, and its flow rate was 1.0 mL/min. The effluent from the GFC column was introduced directly to the spray chamber of an inductively coupled plasma mass spectrometry (ICPMS) system (Elan 6100 DRC plus, PE Sciex, Concord, ON). The operating parameters of ICPMS were optimized to RF power of 1150 W, plasma gas flow of 15 L/min, auxiliary gas flow of 1.2 L/min, and nebulizer gas flow of 0.89 L/min.

In order to study the interaction of standard Hb with arsenic species, iAs^{III}, MMA^{III}, DMA^{III}, and $PhAs^{III}O$ (1 μM each) were incubated separately with hHb or rHb (up to 20 μM) in 20 mM ammonium acetate (pH 7.0) at room temperature for 1-24 h. The reaction mixtures were subjected to GFC-ICPMS analysis. The sample injection volume was 30 μL. Arsenic and iron were detected using the peak-hopping mode of the ICPMS at m/z of 75 and 57, respectively (Iron 57 was used to monitor the retention time where hemoglobin is eluted out and monitor the integrity of hemoglobin). Data was acquired at a rate of 1 data point per second. The resulting chromatograms were processed using

TurboChrom Workstation (Perkin Elmer) and Igor Pro (WaveMetrics, Lake Oswego, OR).

To test whether the presence of oxygen affects interactions between Hb and trivalent arsenicals, the binding of MMA^{III} and DMA^{III} with rHb have been compared when the incubation was carried out either under nitrogen or under aerobic conditions for 2 h. It was found that the presence of oxygen had no significant effect on the binding of rHb to these arsenicals. The percentage of arsenicals bound to the rHb was approximately 1-3% lower under nitrogen than under aerobic conditions. Therefore, subsequent *in vitro* incubation of Hb with arsenicals was carried out under aerobic conditions.

2.2.2.2 Nanoelectrospray mass spectrometry (nanoESI-MS)

A QSTAR Pulsar i mass spectrometer (Applied Biosystems/MDS Sciex, Concord, ON) was equipped with a nanoelectrospray source (Protana, Denmark). The schematic diagram of this mass spectrometry system is shown in Figure 1-5. The conductive capillary tips for nanoelectrospray were purchased from Proxeon Biosystems (Denmark). The system was operated in the positive ionization mode with an ion spray voltage of 1100 V, first declustering potential (DP1) of 65 V, second declustering potential (DP2) of 10 V, and focusing potential (FP) of 215 V. The operational vacuum was ~10^{-7} torr. The flow rate of the curtain gas (nitrogen) used to help evaporation of the solvent was ~1.31 L/min.

In order to characterize the interaction products between standard Hb and arsenic species by nanoESI-MS, all reaction solutions were prepared in 5 mM sodium phosphate buffer (pH 7.2). A desired concentration of Hb (e.g., 20 μM) was incubated with arsenic

species (0-1000 μM) at room temperature for 5 min. The reaction solution was then desalted to remove the salt and the unbound arsenic species using a BioSpin-6 column (Bio-Rad Laboratories, CA). The resulting protein fraction was then diluted 10 times by addition of methanol (to a final concentration of 50% methanol) and formic acid (to a final concentration of 1%) and immediately loaded into a nanoelectrospray capillary tip and subjected to nanoESI-MS analysis. Each spectrum (m/z 600-1500) was collected for 2 min (120 cycles). The instrument was routinely calibrated using standard horse skeletal apo-myoglobin (Sigma, St. Louis, MO) as an external standard. Multi-charged ions (with 14^+ to 17^+ charges) of the α unit of hHb and rHb were also used as internal standards for mass calibration. The resulting spectra were further deconvoluted to zero charge mass spectra using Bioanalyst software (Applied Biosystems/MDS Sciex).

2.2.2.3 *In vitro* exposure of RBC to arsenic species

Fresh human and rat blood samples were collected from healthy human volunteers and rats according to protocols approved by the University of Alberta Health Research Ethics Board and the Institutional Animal Care and Use Committee of the University of Nebraska Medical Center, respectively. The blood samples were then centrifuged at 4000 rpm at 4 °C for 10 min. The plasma and buffy coat were removed, and the packed RBC were washed three times by phosphate buffered saline (PBS) (137 mM NaCl, 2.7 mM KCl, and 10 mM phosphate buffer, pH 7.4). Suspensions of the human and rat RBC (10%) in PBS were separately incubated with DMA^{III}, MMA^{III}, or iAs^{III} (1, 10, or 100 μM) at 37 °C for 14 h. After incubation, the cells were precipitated by centrifugation at 4000 rpm for 10 min at 4 °C. The cells were then subjected to lysis in

ten-fold excess water and further centrifugation at 12000 rpm at 4 °C for 10 min. The supernatant solution was analyzed for protein-bound and unbound arsenic species by GFC-ICPMS. Another portion of the supernatant solution was subjected to BioSpin-6 column centrifugation. The protein fraction collected was further diluted 10-fold with water, methanol, and formic acid (to a final methanol concentration of 10% and formic acid concentration of 0.002%), and immediately loaded into the nanoelectrospray capillary and subjected nanoESI-MS analysis.

The concentration of total arsenic in the RBC was obtained from the measurements of total arsenic concentration in the cell lysate by ICPMS, the volume of the lysate, and the volume of the packed cells, using the following equation:

$$C_1 = (C_2V_2)/(V_1 - V_m) \approx (C_2V_2)/V_1 \qquad (2.1)$$

where V_1 is the volume of the packed cells, C_1 is the concentration of arsenic species in the packed cells, V_2 is the volume of the lysate, C_2 is the concentration of arsenic species in the lysate, and V_m is the volume of the cell membrane of the packed cells.

2.2.2.4 *In vivo* exposure of rats to DMA^V from diet (rat treatment and blood collection done by Lora L. Arnold at UNMC)

Eight female F344 rats, 4 weeks old, were purchased from Charles River Breeding Laboratories (Raleigh, NC). The animals were housed in polycarbonate cages (4/cage) on dry corncob bedding in a room with a targeted temperature of 22 °C, humidity of 50%, and a 12 h light/dark cycle, as described previously (33). They were fed pelleted Certified Rodent Diet 5002 (PMI Nutrition International, St. Louis, MO). Food and water were available *ad libitum* throughout the study. Following quarantine, rats

were randomized into two groups of 4 each: group 1 was fed the basal diet and group 2 was fed the basal diet supplemented with 100 μg/g DMA^V. The DMA^V was supplied by Luxembourg Industries (Pamol, Tel Aviv, Israel) and certified to be 99.5% pure. The purity was confirmed by NMR at the University of Nebraska Medical Center. The rat diet supplemented with DMA^V was obtained from Dyets (Bethlehem, PA). The desired amount of DMA^V was mixed into Certified Purina 5002 and then pelleted. Seventy-two days after the rats were fed the DMA^V-supplemented diet, the rats were sacrificed and blood was collected. RBC were separated from plasma by centrifugation at 4000 rpm at 4 °C for 10 min. The resultant packed RBC were immediately frozen at -80 °C, and kept on dry ice during shipping. The RBC was then lysed and prepared the same way as that in Section 2.2.2.3 and subjected to both GFC-ICPMS and nanoESI-MS analyses.

2.3 Results

2.3.1 Characterization of arsenic binding with rat and human Hb

The binding of commercially available standard Hb (from Sigma) with three metabolically important trivalent arsenic species, DMA^{III}, MMA^{III}, or iAs^{III}, was initially studied by GFC-ICPMS. Figure 2-1 shows typical chromatograms from GFC-ICPMS analysis of reaction mixtures containing 20 μM Hb and 1 μM trivalent arsenic species (DMA^{III}, MMA^{III} or iAs^{III}). In a comparison of rHb with hHb, it is clear that a higher fraction of all three trivalent arsenic species is bound to rHb (Figures 2-1B and 2-1C) than to hHb (Figures 2-1A and 2-1C). Even without incubation with arsenic, the commercially available rHb contains traces of arsenic bound to the protein (Figure 2-1B).

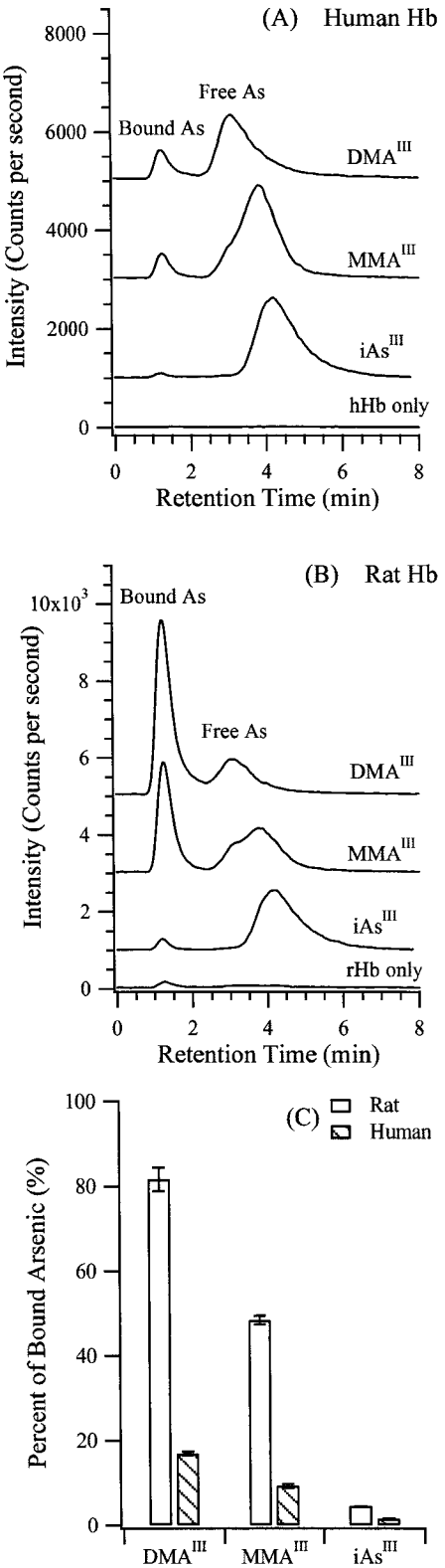

Figure 2-1. Binding of the trivalent arsenic species to human and rat hemoglobin. hHb or rHb (20 μM) was incubated with iAs^{III}, MMA^{III}, or DMA^{III} (1 μM) at room temperature for 24 h in 20 mM ammonium acetate solution (pH 7.0). An aliquot (30 μL) of each reaction mixture was subjected to GFC separation with a mobile phase containing 20 mM ammonium acetate solution (pH 7.0). The flow rate of the mobile phase was 1.0 mL/min and the separation was carried out at room temperature. The eluent was introduced directly to the ICPMS to selectively detect arsenic at m/z 75. (A) chromatograms obtained from hHb interaction with three arsenicals, (B) chromatograms obtained from rHb interaction with three arsenicals, and (C) comparison of the fraction of each arsenic species that is bound to rHb and hHb.

In contrast, no arsenic is detectable in hHb (Figure 2-1A). These results support rHb having a higher affinity for trivalent arsenicals than hHb.

The apparent binding constants (Table 2-1) obtained from binding studies using a range of arsenic and Hb concentrations analyzed by GFC-ICPMS also show stronger arsenical binding for rHb than hHb. For the four arsenic species tested, the binding constants with rHb are 3–16-fold higher than those with hHb.

Table 2-1. Apparent binding constants (n·K) for trivalent arsenicals binding to rat hemoglobin (rHb) and human hemoglobin (hHb)

Arsenic species	n·K (M^{-1})	
	rHb	hHb
iAs^{III}	2.33×10^3	7.69×10^2
MMA^{III}	4.69×10^4	5.00×10^3
DMA^{III}	2.22×10^5	1.36×10^4
$PhAs^{III}O$	5.35×10^5	7.75×10^4

The apparent binding constants (n·K) were calculated according to the following equation:

$$n \cdot K = \frac{[bound\ As]M}{(P_t - \frac{[bound\ As]}{n})M \cdot [free\ As]M} \cong \frac{[bound\ As]}{P_t \cdot [free\ As]} M^{-1} \quad (\text{when } P_t >> \frac{[bound\ As]}{n}) \tag{2.2}$$

where $[bound\ As]$ is the concentration (M) of protein-bound arsenic, P_t is the total concentration (M) of protein, $[free\ As]$ is the concentration (M) of free (unbound) arsenic species, and n is the number of binding sites in each Hb molecule. Assumption: binding of one arsenical molecule does not affect the binding of the second arsenical molecule.

It is believed that cysteine is the likely binding site for the trivalent arsenic species because of the affinity of trivalent arsenicals for sulfhydryl groups. This was further supported by tandem MS analysis of arsenic-bound protein in Chapter 4. It was found that cysteine residues are the unique binding sites for trivalent arsenic species.

To characterize the binding products between Hb and the arsenic species, the molecular species resulting from arsenic binding to the α and the β units of Hb was identified by nanoESI-MS. Figure 2-2A shows typical deconvoluted mass spectra from the nanoESI-MS analysis of rHb with or without reaction to DMA^{III}. In the absence of DMA^{III} (bottom spectrum of Figure 2-2A), the mass spectrum of rHb shows two major species (peak 1 at 15197 Da and peak 5 at 15835 Da), corresponding to the normal α and β units, respectively. Several small peaks are due to α and β variants that are known to exist in rHb. After reaction with DMA^{III}, three new peaks (2*, 3*, and 4*) having molecular mass of 15301 Da, 15405 Da, and 15509 Da are detected. They have mass shifts of 104, 208, and 312 Da, respectively, from the normal α unit (15197 Da), and they represent the complexes of one α with one, two, and three DMA^{III} molecules, respectively. Two other new peaks (6* and 7*) have molecular mass of 15939 Da and 16043 Da, 104 and 208 Da higher than the β unit (15835 Da). The mass shifts of 104 and 208 from that of the β unit suggest that they are complexes of one β unit with one and two DMA^{III} molecules, respectively. The mass shift of 104 Da is characteristic of the addition of one DMA^{III} with loss of a water molecule, as illustrated in Scheme 2-1. Excellent agreement between the expected and measured mass values (Table 2-2) supports the assignment of the mass spectral peaks. The results show that each α unit can bind with up to three DMA^{III} molecules, and each β unit can bind with up to two DMA^{III}

molecules. These binding stoichiometries are consistent with the number of sulfhydryl groups in rHb. rHb consists of three cysteines (Cys13, Cys104, and Cys111) in each α unit, and two cysteines (Cys93 and Cys125) in each β unit. With a total of two α and two β units in the rHb tetramer, a maximum of 10 DMA^{III} molecules may be bound to each rHb, occupying all 10 sulfhydryl groups in the rHb molecule (2α2β).

Table 2-2. Characterization of Hb complexes with three trivalent arsenic species and comparison between the measured and expected mass values according to the protein sequence. The measured values for DMA^{III} and MMA^{III} were averages (± standard deviation) from three individual spectra. One spectrum was used for values for iAs^{III}. Mass shift was calculated as the difference between the average mass of complexes and the average mass of Hb subunits. The β chain of Hb from F344 rat is a variant that is not reported in the protein database. Although it has the same number of cysteine residues as that in the database, the expected mass value is not available. For iAs^{III}, the mass shift was calculated from the globin chain containing a heme group (apo-Hb +616.20 Da).

HHb	α chain (1 cysteine)				β chain (2 cysteines)			
	Measured (Da)	Expected (Da)	Error (ppm)	Mass shift (Da)	Measured (Da)	Expected (Da)	Error (ppm)	Mass shift (Da)
Apo-Hb	15126.09±0.03	15126.37	-18	-	15866.85±0.07	15867.24	-24	-
DMA^{III}	15229.68±0.10	15230.61	-44	103.82±0.19	15970.39±0.20	15971.22	-52	103.78±0.28
					16073.70±0.04	16075.20	-93	207.54±0.82
MMA^{III}	-	-	-	-	15954.39±0.16	15955.18	-49	87.69±0.30
iAs^{III}	-	-	-	-	16573.82	16573.35	28	90.77

rHb	α chain (3 cysteines)				β chain (2 cysteines)	
	Measured (Da)	Expected (Da)	Error (ppm)	Mass shift (Da)	Measured (Da)	Mass shift (Da)
Apo-Hb	15197.07±0.22	15197.30	-15	104.24±0.19	15834.54±0.58	-
DMA^{III}	15301.20±0.40	15301.35	-10	208.34±0.35	15938.20±0.47	103.98±0.20
	15405.17±0.33	15405.33	-11	312.84±0.10	16042.63±0.44	208.32±0.11
	15509.67±0.08	15509.32	-22	88.13±0.22	-	-
MMA^{III}	15285.03±0.18	15285.31	-18	90.41	15922.02±0.24	88.17±0.18
iAs^{III}	15903.68	15903.48	14	90.42	16540.35	89.61

Note: "-" indicates no data available because of no complex of the particular species was observed.

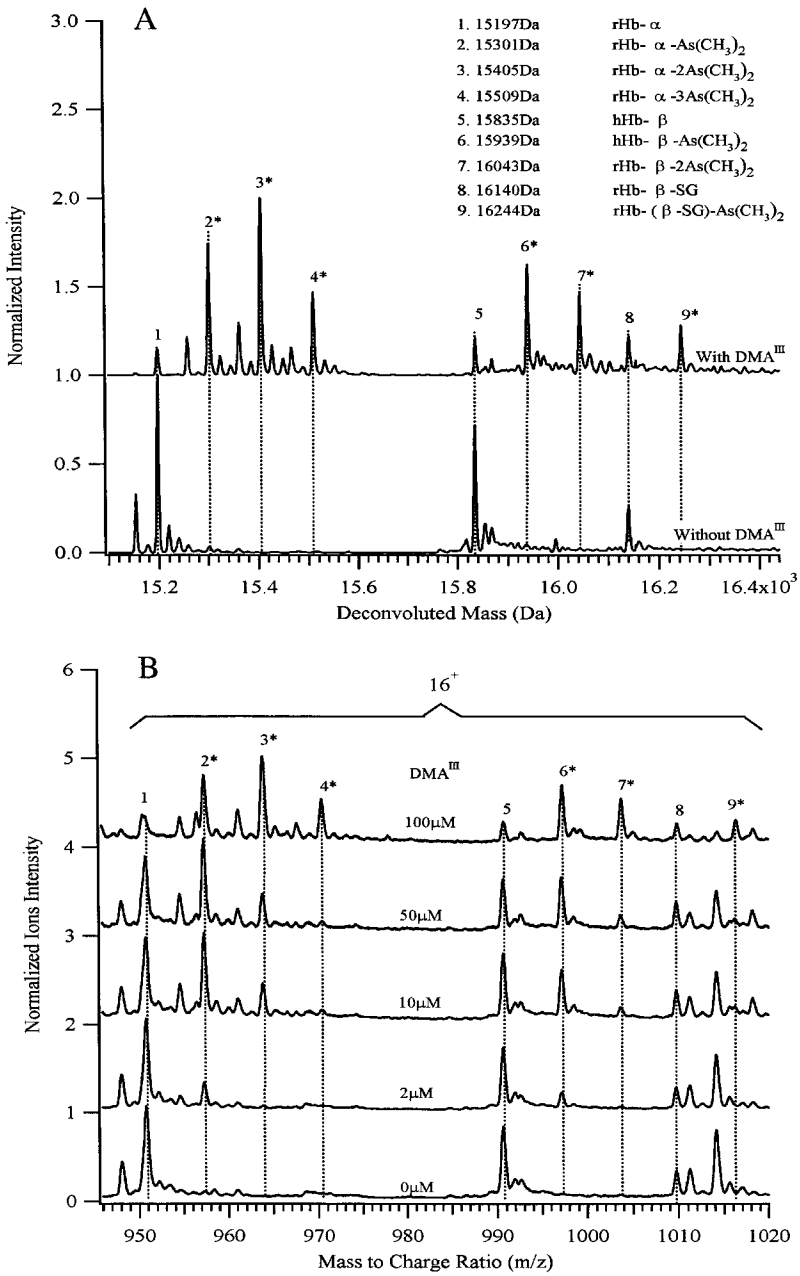

Figure 2-2. Nanoelectrospray mass spectra showing the interaction products between the α and the β units of rHb and DMA^{III}. The detailed experimental conditions are shown in Section 2.2.2.2. (A): deconvoluted mass spectra showing molecular mass of the species. (B): mass spectra showing relative changes in the interaction products between rHb and DMA^{III} with increasing concentration of DMA^{III}. The ions carry 16 positive charges. Peaks 1 and 5 correspond to the α and the β units, respectively. Peaks 2*, 3*, and 4* are due to complexes of one α unit with one, two, and three DMA^{III} species, respectively. Peaks 6* and 7* are due to complexes of one β unit with one and two DMA^{III} species, respectively. Peak 8 is the complex of a β unit with a glutathione. Peak 9* is the complex of a β unit with a glutathione and a DMA^{III} molecule. Unlabeled peaks primarily result from the variants of rHb.

DMA^{III}-Protein

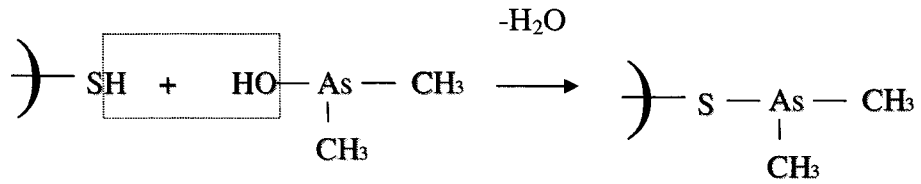

Protein DMA^{III} +104 Da

MMA^{III}-Protein

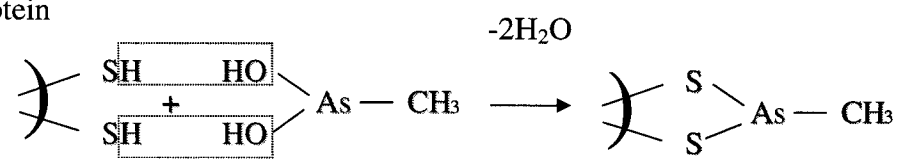

Protein MMA^{III} +88 Da

Scheme 2-1. Schematic diagram showing changes in molecular mass after protein binding with DMA^{III} and MMA^{III}.

In addition to the unmodified α and β chains in the rHb (without treatment with arsenicals), a peak appearing at 16140 Da (peak 8) has a mass shift of 305 Da from the unreacted β chain (15835 Da). This is probably a β complex of glutathione (GSH) (Figure 2-2). The mass shift of 305 is the result of the loss of two protons and the formation of a disulfide bond between the sulfhydryl groups of one cysteine residue in the β unit and another in GSH. An Hb-GSH complex from rabbit erythrocytes has been observed previously using NMR (19). Our experiments show that the β-GSH complex

can additionally bind with one DMA^{III} molecule to form a tertiary complex (16244 Da, peak 9*). This is reasonable because the β chain of rHb has two cysteines, and DMA^{III} can only bind with the cysteine that is not bound to GSH. There is no complex of the β chain with one GSH and two DMA^{III} molecules, indicating that GSH conjugation on the β chain reduces the number of sites available for binding of DMA^{III}, and further supports that the DMA^{III} directly reacts with sulfhydryl groups in the cysteines of proteins.

The complexes of DMA^{III} with both the α and the β units of rHb are dependent on the relative concentrations of rHb and DMA^{III} (Figure 2-2B). Because rHb has three cysteines in the α chain and two cysteines in the β chain, several complexes with different stoichiometries are formed when the concentration of DMA^{III} is changed. With increasing DMA^{III} concentration, increasing amounts of DMA^{III} are bound to the α unit (up to three DMA^{III}, peak 4*) and to the β unit (up to two DMA^{III}, peak 7*). The maximum numbers of bound DMA^{III} are consistent with the numbers of sulfhydryl groups in the α and β chains of rHb. These results suggest that all cysteines in rHb can be accessed by excess amounts of DMA^{III}.

While one DMA^{III} molecule is able to bind with only one sulfhydryl group, one MMA^{III} molecule can bind in principle to two sulfhydryl groups (Scheme 2-1). Figure 2-3A illustrates the deconvoluted mass spectra obtained from rHb incubated with MMA^{III}. Both the α chain and the β chain of rHb can bind MMA^{III} because of the presence of three cysteines in the α chain (Cys104, Cys111, and Cys13) and two cysteines in the β chain (Cys93 and Cys125). The mass shifts of 88 Da from the unbound α unit (15197 Da) and the unbound β unit (15835 Da) to the complexes (15285 Da and 15923 Da, respectively) correspond to the addition of one MMA^{III} molecule and the loss of two H_2O

molecules (Scheme 2-1). The complexes (peaks 2* and 4*) of MMA^{III} with the α and β units of rHb increase with an increase in MMA^{III} concentration (Figure 2-3B). When one of the cysteines in the β unit is bound to GSH (peak 5 at 16140 Da), there is no complex of the β unit with GSH and MMA^{III}, suggesting that MMA^{III} does not form a stable complex when only one cysteine in the β unit is free and the other is blocked.

Similarly, interaction products between hHb and the arsenicals were characterized, and the main complexes of hHb-As are compared with those of rHb-As (Table 2-2). The α chain of rHb is able to bind with up to three DMA^{III} molecules or one MMA^{III} molecule because of the presence of three cysteines in the α chain of rHb. The β chain of rHb is able to bind with two DMA^{III} molecules or one MMA^{III} molecule because of the presence of two cysteines in the β chain of rHb. In contrast, the α chain of hHb, which binds with only one DMA^{III} molecule, does not bind to MMA^{III}. The β chain of hHb is able to bind with two DMA^{III} molecules or one MMA^{III} molecule. These binding stoichiometries are consistent with the number of available cysteines in the α and β chains of hHb.

2.3.2 Binding of arsenicals to Hb after incubation of RBC with arsenicals

The preferential binding of arsenic to rHb over hHb is further confirmed by studying rat and human RBC that have been exposed to arsenicals. Following the separate incubation of rat RBC with 1-100 μM iAs^{III}, MMA^{III}, and DMA^{III} for 14 h, the concentration of arsenic in the RBC is up to 5-fold higher than in the initial incubation medium (Figure 2-4).

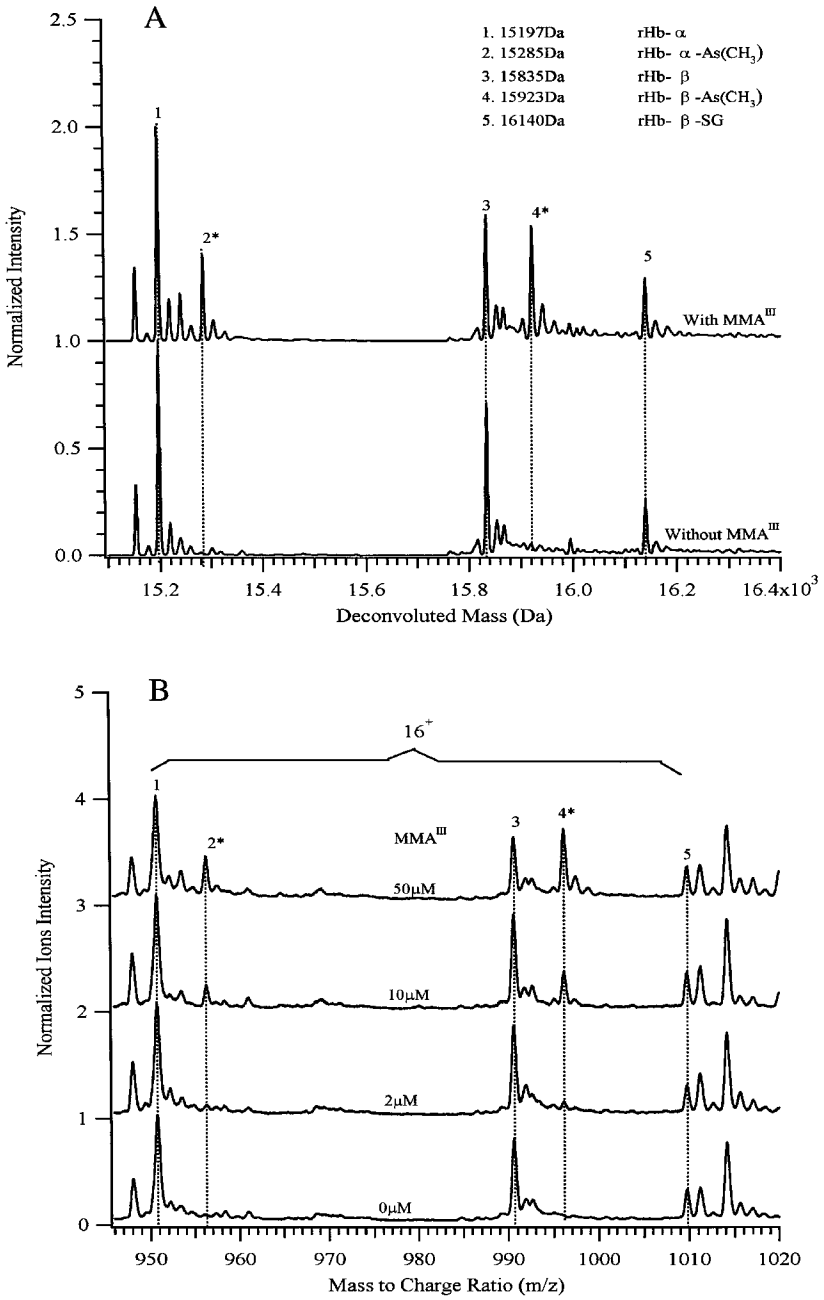

Figure 2-3. Nanoelectrospray mass spectra showing the interaction products between the α and the β units of rHb and MMA^{III}. The experimental conditions are shown in Section 2.2.2.2. (A): Deconvoluted mass spectra showing the molecular mass of the species. (B): Mass spectra showing relative changes in the interaction products between rHb and MMA^{III} with increasing concentration of MMA^{III}. The ions carry 16 positive charges. Peaks 1 and 3 correspond to the α and the β units, respectively. Peak 2* is due to the complex of one α unit with one MMA^{III} species. Peak 4* is due to the complex of one β unit with one MMA^{III} species. Peak 5 is the complex of a β unit with glutathione. Unlabeled peaks result primarily from the variants of rHb.

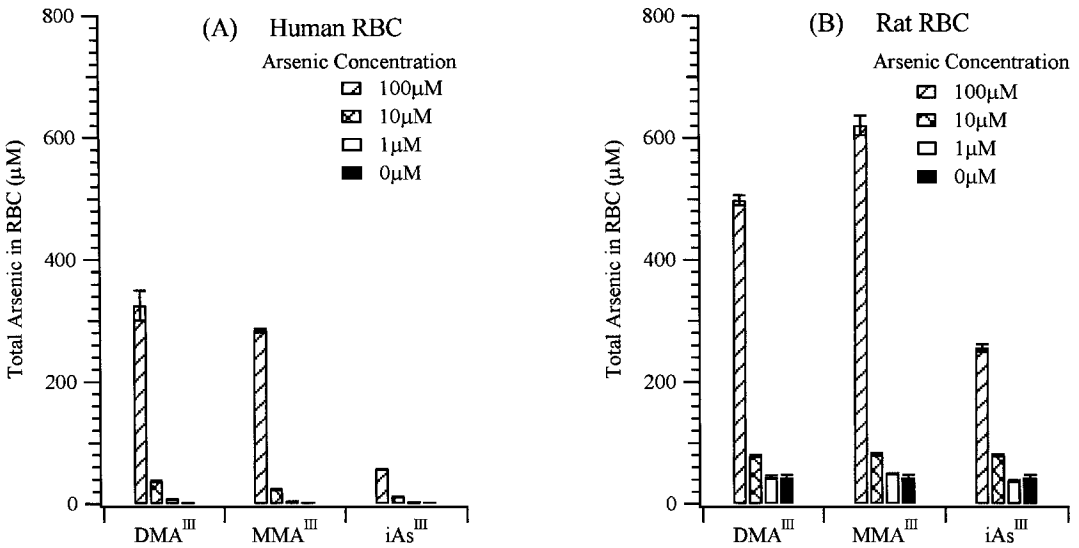

Figure 2-4. Concentration of total arsenic in human and rat RBC after exposing of RBC to arsenic species. Suspensions of human and rat RBC (10%) in phosphate buffered saline (pH 7.4) were separately incubated with DMA^{III}, MMA^{III}, and iAs^{III} (1, 10, and 100 μM). Following precipitation and lysis of the cells, the supernatant was analyzed for total arsenic concentration using ICPMS. (A) human RBC; (B) rat RBC.

At low (subtoxic) concentrations, both the uptake and efflux mechanisms probably determine in part the amount of arsenicals found in rat and human RBC. The highest concentrations used are cytotoxic. It is not clear how cytotoxicity affects the uptake and retention of arsenicals and the binding to Hb.

Furthermore, the majority of the arsenic has been found to accumulate in the RBC of rat is bound to proteins (Figure 2-5B). However, only a small fraction of arsenic present in human RBC is bound to proteins (Figure 2-5A). The protein-bound arsenic in

rat RBC is 15-30 times higher than that in human RBC. Further characterization by nanoelectrospray mass spectrometry of the protein-bound arsenic from rat RBC exposed to DMA^{III} and MMA^{III} suggests that both DMA^{III} and MMA^{III} were bound to the α chain of rHb, respectively (Figure 2-6 and Table 2-3).

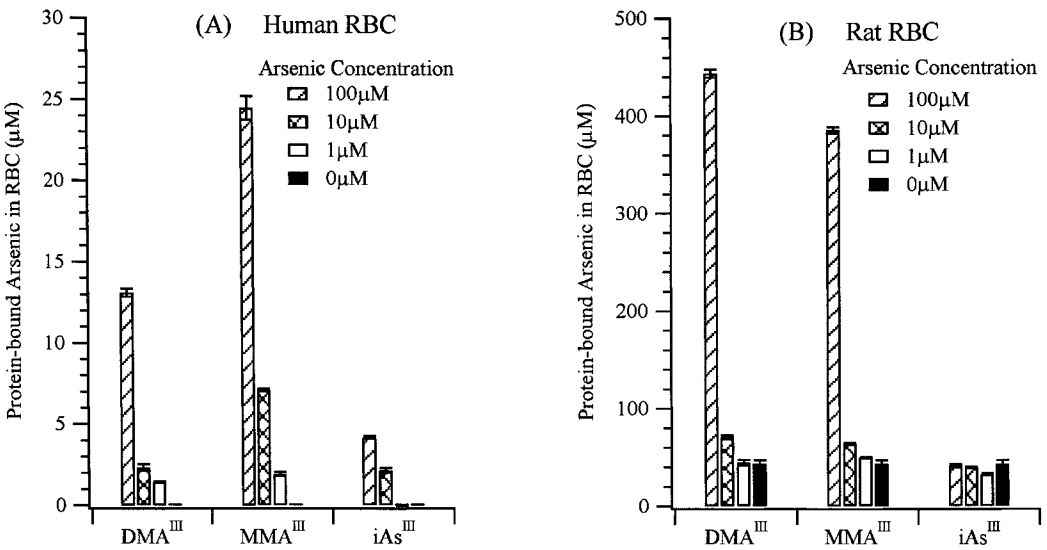

Figure 2-5. Concentration of protein-bound arsenic in human and rat RBC after exposure of RBC to arsenic species. Suspensions of human and rat RBC (10%) in phosphate buffered saline (pH 7.4) were separately incubated with DMA^{III}, MMA^{III}, and iAs^{III} (1, 10, and 100 μM). Following precipitation and lysis of the cells, the supernatant was analyzed for protein-bound and free arsenic species using GFC-ICPMS. (A) human RBC; (B) rat RBC.

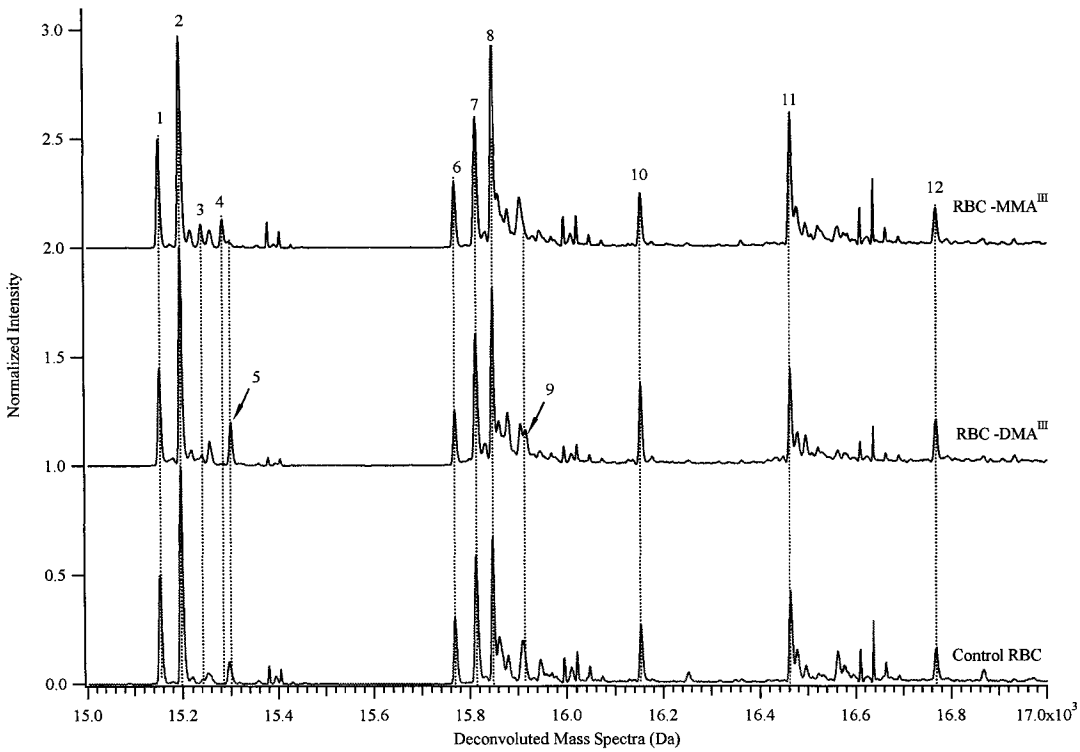

Figure 2-6. Nanoelectrospray mass spectra from the lysate of rat RBC exposed to 100 μM DMA^{III} or MMA^{III} for 14 hours. The lysate of RBC were desalted using a Bio-Spin 6 column. Immediately prior to nanoESI-MS analysis, the desalted protein solution was diluted 10-fold with water, methanol, and formic acid to a final methanol concentration of 10% and formic acid concentration of 0.002%. The major arsenic species in RBC were the α unit bound with one DMA^{III} or one MMA^{III} molecule with a mass shift from the α unit of 104 and 88 Da, respectively. The identified species are shown in Table 2-3.

Table 2-3. The identified species with measured and expected molecular weight from Figure 2-6. Error was calculated as the relative deviation of the measured value from the expected value in ppm.

		Measured MW	Expected MW	Error	Rat RBC treatment		
#	Species	(Da)	(Da)	(ppm)	Control	DMA^{III}	MMA^{III}
1	Hb α_1	15153.5	N/A	N/A	yes	yes	yes
2	Hb α	15197.1	15197.3	-13	yes	yes	yes
3	Hb α_1-MMA^{III}	15241.5	N/A	N/A	**no**	**no**	**yes**
4	Hb α-MMA^{III}	15285.5	15285.31	12.4	**no**	**no**	**yes**
5	Hb α-DMA^{III}	15301.0	15301.35	-23	**no**	**yes**	**no**
6	Hb α_1^h	15769.4	N/A	N/A	yes	yes	yes
7	Hb α^h	15813.2	15813.5	-19	yes	yes	yes
8	Hb β	15848.3	15848.1	13	yes	yes	yes
9	Hb α^h-DMA^{III}	15917.2	15917.4	-13	**no**	**yes**	**no**
10	Hb β-GSH	16153.6	16153.4	12	yes	yes	yes
11	Hb β^h	16464.7	16464.3	24	yes	yes	yes
12	Hb β^h-GSH	16769.3	16769.6	-18	yes	yes	yes

Note: α_1 is a variant of the rat Hb α unit, observed in our experiment, and its expected molecular weight is not available.

2.3.3 Arsenic binding to Hb in rats fed with DMA^V

The binding of arsenic to Hb and the accumulation of arsenic in the RBC of rats are further confirmed by *in vivo* experiments with rats. Five-week-old rats were fed with a diet supplemented with 100 μg/g DMA^V continuously for 72 days and then they were

sacrificed. Blood samples were collected and separated into plasma and RBC. Arsenic speciation analysis was focused on the RBC because initial analysis showed that the major fraction of the arsenic was present in the rat RBC, which is consistent with previous findings (14-15). GFC-ICPMS analyses of the RBC samples show that arsenic is predominantly present in a protein-bound form (refer to Figure 3-2). Further characterization of the arsenic species in the RBC of these rats by nanoESI-MS confirms that most of the arsenic is bound to the α chain of rHb as one DMA^{III} bound with 1 α unit (Figure 2-7).

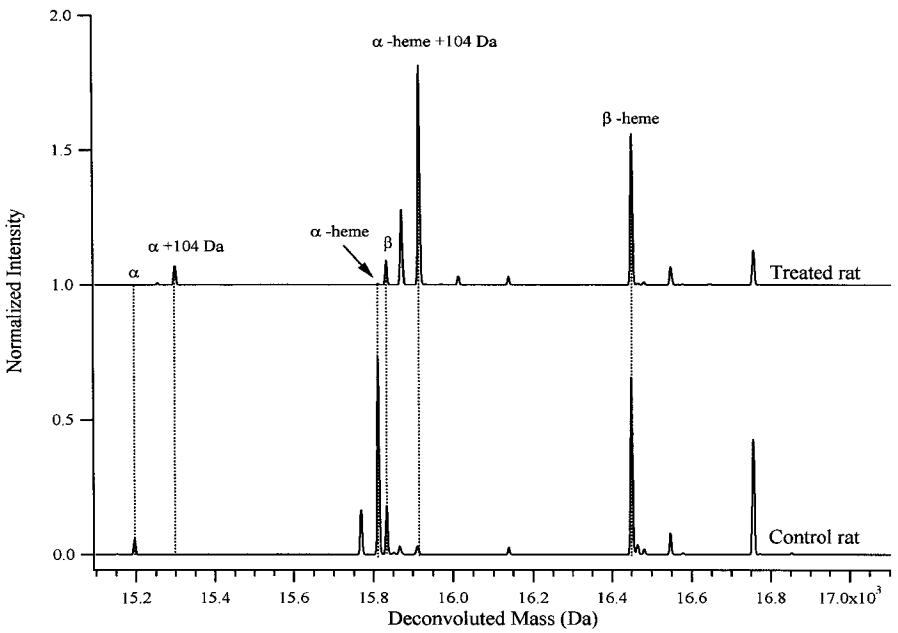

Figure 2-7. Nanoelectrospray mass spectra of RBC lysate from rats that were fed either a basal diet or a diet supplemented with 100 μg/g DMA^{V} for 72 days. The major arsenic species in the RBC of the treated rat is one α unit bound with one DMA^{III} species. The solution preparation for nanoelectrospray was the same as that in Figure 2-6, and the other conditions are described in Section 2.2.2.2.

The total arsenic concentration in both plasma and RBC of the blood samples from the DMA^V-fed rats was measured. Arsenic concentration in the plasma was 7.3±1.0 μM and that in RBC was 1101±130 μM. Thus, the arsenic concentration in RBC was approximately 150 times higher than that in plasma.

2.4 Discussion

Previous studies showed that the retention time of arsenic in the blood of rats was much longer than in the blood of humans (1, 12-17). However, the biochemical basis for this binding and accumulation in RBC had not been established. In this study, direct evidence of the binding between arsenic species and Hb in RBC is presented. When comparing the ability of rHb and hHb to bind to arsenic species, rHb shows a consistently higher binding affinity (Figure 2-1). The apparent binding constants for rHb binding to the trivalent arsenic species are 3–16-fold higher than those for hHb binding to the same arsenic species (Table 2-1). These results provide a chemical basis for the observed accumulation of arsenic in the RBC of rats. The higher binding affinity of rHb for trivalent arsenicals is probably due to the larger number of cysteine residues (and their preferred position) in rHb compared to hHb. Both rHb and hHb are tetramers, each consisting of two α chains and two β chains. The rHb has three cysteines in each α chain (Cys104, Cys111, and Cys13) and two cysteines in each β chain (Cys93 and Cys125). The hHb contains only one cysteine in each α chain (Cys104) and two cysteines in each β chain (Cys93 and Cys112). Because trivalent arsenicals bind to sulfhydryl groups, the difference in the number of cysteine residues and the preferred binding site between rHb

and hHb are probably the primary reason for the observed difference in the binding affinity.

The binding affinity of Hb to arsenic varies with different arsenic species at constant concentrations. The fraction of DMA^{III}, MMA^{III}, and iAs^{III} that is bound to rHb is 82%, 48%, and 4.5%, respectively, and to hHb it is 17%, 9.3%, and 1.6%, respectively (Figure 2-1C). Thus, the relative ability to bind with both rHb and hHb increases from iAs^{III} to MMA^{III} to DMA^{III}.

There has been much speculation about the stability of the binding of arsenicals with the molecular formula $RAsX_2$ to proteins. The claim has been made that these arsenicals would react with two sulfhydryl (-SH) groups on the protein to form compounds in which the arsenic is part of a ring and hence the strength of the binding would be enhanced (1). However, this stabilizing effect of "chelation," an entropy effect, would play little role when the ring contains more than 6 atoms, and is unlikely to enhance the binding of arsenicals to proteins. In the present work, DMA^{III}, which reacts with one SH group, can bind to Hb better than MMA^{III}, which reacts with two SH groups. These results suggest that factors such as hydrophobicity may contribute to the affinity of arsenicals with proteins (probably by allowing access to the cysteine residues that may be partially buried in the protein). This notion was examined by exposing a more hydrophobic arsenic compound, phenylarsine oxide ($PhAs^{III}O$), to both rHb and hHb. $PhAs^{III}O$ showed the strongest binding to both rHb and hHb of all the arsenicals tested (Table 2-1). The relative binding affinity of iAs^{III}, MMA^{III}, DMA^{III}, and $PhAs^{III}O$ is 1:20:95:230 for rHb and 1:6:18:101 for hHb.

The partition coefficient (P) of the four trivalent arsenic species in n-octanol/water was further estimated using Chemoffice software (CambridgeSoft, Cambridge, MA). Logarithmic values of the n-octanol/water partition coefficient (logP) correlated well with the logarithmic binding constant values, with correlation coefficients (r) of 0.98 for rHb binding to the four arsenic species and 0.93 for hHb binding to the same four arsenic species (Figure 2-8). These results indicate that hydrophobicity is an important factor affecting the interaction between arsenic species and Hb.

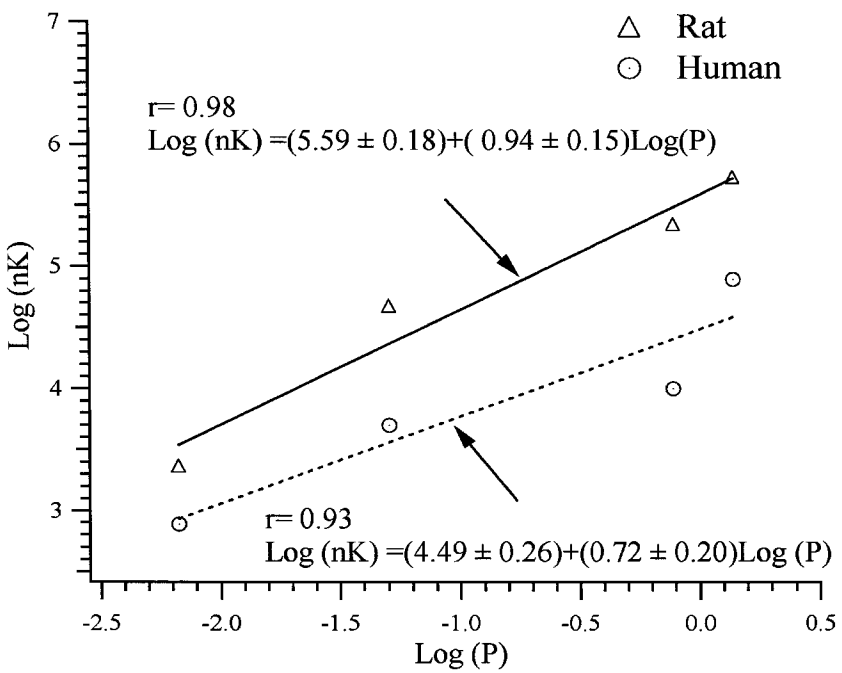

Figure 2-8. Correlation of the binding constants with n-octanol/water partition coefficients. Values of n·K were from Table 2-1. The partition coefficients in n-octanol/water (P values) were obtained from Chemoffice software (CambridgeSoft, Cambridge, MA).

Inorganic arsenite (iAs^{III}) and arsenate (iAs^{V}) are the main arsenic species commonly found in water. These arsenic species are readily metabolized in the body (1, 14-17, 31, 34-41). The metabolic process involves 2-electron reduction steps to afford trivalent arsenic species followed by the oxidative addition of a methyl group to afford pentavalent arsenic species (31, 39, 42). The major biomethylation products include the pentavalent monomethylarsonic acid (MMA^{V}) and dimethylarsinic acid (DMA^{V}) and the trivalent MMA^{III} and DMA^{III}. The trivalent methyl arsenic species, MMA^{III} and DMA^{III}, have been found to be much more toxic than their pentavalent counterparts (20, 21, 23, 43). Furthermore, MMA^{III} and DMA^{III} are more toxic than iAs^{III} in a range of tests, including acute toxicity to animals (LD_{50}) (30) and mammalian cells (21, 44), genotoxicity (23, 24), and inhibition of enzyme activities (45). Consequently, studies on protein interactions with these toxic arsenic species have been focused.

Ironically, As^{III} has been successfully used as a chemotherapeutic agent to treat acute promyelocytic leukemia (APL) (46-48). Preliminary *in vitro* experiments show that MMA^{III} may be more effective than As^{III} in causing apoptosis of APL cells (49). Extensive research has been devoted to the effect of arsenic on apoptosis (48-51), although little has been learned about how the binding of arsenic with proteins may facilitate the apoptotic process.

There has been extensive research toward understanding the mechanisms of the actions responsible for arsenic transport, metabolism, and chronic health effects. Some of these studies have recently been reviewed (50-59). Because the uptake of arsenic is

important for its action, the transport of arsenic has been extensively studied (60-63). The binding of arsenic to proteins could conceivably play a role in mediating the transport.

Oxidative damage to DNA and chromosomes has been studied as a possible mechanism of arsenic carcinogenicity (22, 64-67). Electron spin resonance (ESR) with spin trapping has detected free radicals produced in cells incubated with iAs^{III} (24, 66). It is believed that the observed oxidative damage induced by arsenicals happens through the action of free radicals. The effect of arsenic on the repair of DNA damage is another possible mechanism under extensive study (58, 68, 69). Because the trivalent arsenic species can bind with sulfhydryl groups in proteins, as shown in this study, it is possible that the trivalent arsenic species may alter the conformation and function of DNA repair proteins.

Arsenic has been shown to inhibit the activities of glutathione reductase (GR) (70, 71), glutathione S-transferase (71), glutathione peroxidase (GPx) (72), thioredoxin reductase (TR) (45), thioredoxin peroxidase (73), and Arg-tRNA protein transferase (74). How arsenic species inhibit the activity of these enzymes has not been clearly elucidated. The techniques and methodological approaches described in this study can be extended to understanding arsenic interactions with these and other functional proteins.

2.5 References

1. National Research Council (1999) *Arsenic in the Drinking Water*, National Academy Press, Washington, DC.

2. National Research Council (2001) *Arsenic in the Drinking Water* (update), National Academy Press, Washington, DC.
3. Chen, C. J., Chuang, Y. C., Lin, T. M., and Wu, H. Y. (1985) Malignant neoplasms among residents of a blackfoot disease endemic area in Taiwan — high arsenic artesian well water and cancers. *Cancer Res.* **45**, 5895-5899.
4. Smith, A. H., Goycolea, M., Haque, R., and Biggs, M. L. (1998) Marked increase in bladder and lung cancer mortality in a region of Northern Chile due to arsenic in drinking water. *Am. J. Epidemiol.* **147**, 660-669.
5. Bagla, P. and Kaiser, J. (1996) Epidemiology — India's spreading health crisis draws global arsenic experts. *Science* **274**, 174-175.
6. Chakraborti, D., Rahman, M. M., Paul, K., Chowdhury, U. K., Sengupta, M. K., Lodh, D., Chanda, C. R., Saha, K. C., and Mukherjee, S. C. (2002) Arsenic calamity in the Indian subcontinent — What lessons have been learned? *Talanta* **58**, 3-22.
7. Abernathy, C. O., Liu, Y. P., Longfellow, D., Aposhian, H. V., Beck, B. D., Fowler, B. A., Goyer, R. A., Menzer, R., Rossman, T., Thompson, C., and Waalkes, M. (1999) Arsenic: health effects, mechanisms of actions, and research issues. *Environ. Hlth. Perspect.* **107**, 593-597.
8. Lee, M. Y., Jung, B. I., Chung, S. M., Bae, O. N., Lee, J. Y., Park, J. D., Yang, J. S., Lee, H., and Chung, J. H. (2003) Arsenic-induced dysfunction in relaxation of blood vessels. *Environ. Hlth. Perspect.* **111,** 513-517.
9. Tseng, C. H., Tseng, C. P., Chiou, H. Y., Hsueh, Y. M., Chong, C. K., and Chen, C. J. (2002) Epidemiologic evidence of diabetogenic effect of arsenic. *Toxicol. Lett.* **133**, 69-76.

10. Nordstrom, D. K. (2002) Worldwide occurrences of arsenic in ground water. *Science* **296**, 2143-2145.

11. Rossman, T. G. (2003) Mechanism of arsenic carcinogenesis: an integrated approach. *Mutat. Res.* **533**, 37-65.

12. Mealey, J., Brownell, G. L., and Sweet, W. H. (1959) Radioarsenic in plasma, urine, normal tissue, and intracranial neoplasms. *Arch. Neurol. Psychiatr.* **81**, 310-320.

13. Pomroy, C., Charbonneau, S. M., McCullough, R. S., and Tam, G. K. H. (1980) Human retention studies with ^{74}As. *Toxicol. Appl. Pharmacol.* **53**, 550-556.

14. Odanaka, Y., Matano, O., and Goto, S. (1980) Biomethylation of inorganic arsenic by the rat and some laboratory animals. *Bull. Environ. Contam. Toxicol.* **24**, 452-459.

15. Lerman, S. A. and Clarkson, T. W. (1983) The metabolism of arsenite and arsenate by the rat. *Fundam. Appl. Toxicol.* **3**, 309-314.

16. Lerman, S. A., Clarkson, T. W., and Gerson, R. J. (1983) Arsenic uptake and metabolism by liver cells is dependent on arsenic oxidation state. *Chem. Biol. Interact.* **45**, 401-406.

17. Styblo, M., Del Razo, L. M., LeCluyse, E. L., Hamilton, G. A., Wang, C., Cullen, W. R., and Thomas, D. J. (1999) Metabolism of arsenic in primary cultures of human and rat hepatocytes. *Chem. Res. Toxicol.* **12**, 560-565.

18. Winski, S. L. and Carter, D. E. (1995) Interactions of rat red blood cell sulfhydryls with arsenate and arenite. *J. Toxicol. Environ. Health* **46**, 379-397.

19. Delnomdedieu, M., Basti, M. M., Styblo, M., Otvos, J. D., and Thomas, D. J. (1994) Complexation of arsenic species in rabbit erythrocytes. *Chem. Res. Toxicol.* **7**, 621-627.

20. Aposhian, H. V., Zakharyan, R. A., Avram, M. D., Kopplin, M. J., and Wollenberg, M. L. (2003) Oxidation and detoxification of trivalent arsenic species. *Toxicol. Appl. Pharmacol.* **193,** 1-8.

21. Styblo, M., Del Razo, L. M., Vega, L., Germolec, D. R., LeCluyse, E. L., Hamilton, G. A., Reed, W., Wang, C., Cullen, W. R., and Thomas, D. J. (2000) Comparative toxicity of trivalent and pentavalent inorganic and methylated arsenicals in rat and human cells. *Arch. Toxicol.* **74**, 289–299.

22. Kitchin, K. T. and Ahmad, S. (2003) Oxidative stress as a possible mode of action for arsenic carcinogenesis. *Toxicol. Lett.* **137**, 3-13.

23. Mass, M. J., Tennant, A., Roop, B. C., Cullen, W. R., Styblo, M., Thomas, D. J., and Kligerman, A. D. (2001) Methylated trivalent arsenic species are genotoxic. *Chem. Res. Toxicol.* **14,** 355-361.

24. Nesnow, S., Roop, B. C., Lambert, G., Kadiiska, M., Mason, R. P., Cullen, W. R., and Mass, M. J. (2002) DNA damage induced by methylated trivalent arsenicals is mediated by reactive oxygen species. *Chem. Res. Toxicol.* **15**, 1627-1634.

25. Aposhian, H. V., Gurzau, E. S., Le, X. C., Gurzau, A., Healy, S. M., Lu, X. F., Ma, M. S., Yip, L., Zakharyan, R. A., Maiorino, R. M., Dart, R. C., Tircus, M. G., Gonzalez-Ramirez, D., Morgan, D. L., Avram, D., and Aposhian, M. M. (2000) Occurrence of monomethylarsonous acid in urine of humans exposed to inorganic arsenic. *Chem. Res. Toxicol.* **13**, 693-697.

26. Le, X. C., Lu, X., Ma, M., Cullen, W. R., Aposhian, H. V., and Zheng, B. (2000) Speciation of key arsenic metabolic intermediates in human urine. *Anal. Chem.* **72**, 5172-5177.

27. Lu, X. F., Arnold, L. L., Cohen, S. M., Cullen, W. R., and Le, X. C. (2003) Speciation of dimethylarsinous acid and trimethylarsine oxide in urine from rats fed with dimethylarsinic acid and dimercaptopropane sulfonate. *Anal. Chem.* **75**, 6463-6468.

28. Del Razo, L. M., Styblo, M., Cullen, W. R., and Thomas, D. J. (2001) Determination of trivalent methylated arsenicals in biological matrices. *Toxicol. Appl. Pharmacol.* **174**, 282–293.

29. Mandal, B. K., Ogra, Y., and Suzuki, K. T. (2001) Identification of dimethylarsinous and monomethylarsonous acids in human urine of the arsenic-affected areas in West Bengal, India. *Chem. Res. Toxicol.* **14**, 371-378.

30. Petrick, J. S., Jagadish, B., Mash, E. A., and Aposhian, H. V. (2001) Monomethylarsonous acid (MMA(III)) and arsenite: LD50 in hamsters and in vitro inhibition of pyruvate dehydrogenase. *Chem. Res. Toxicol.* **14,** 651-656.

31. Cullen, W. R., McBridge, B. B., Manji, H., Pickett, A. W., and Reglinski, J. (1989) The metabolism of methylarsine oxide and sulfide. *Appl. Organomet. Chem.* **3**, 71-78.

32. Burrows, G. J. and Turner, E. E. (1920) A new type of compound containing arsenic. *J. Chem. Soc. Trans.* **117**, 1373-1383.

33. Cohen, S. M., Arnold, L. L., Uzvolgyi, E., Cano, M., John, M. S., Yamamoto, S., Lu, X. F., and Le, X. C. (2002) Possible role of dimethylarsinous acid in dimethylarsenic acid-induced urothelial toxicity and regeneration in the rat. *Chem. Res. Toxicol.* **15,** 1150-1157.

34. Chappell, W. R., Abernathy, C. O., and Cothern, C. R. (Editors). (1994) *Arsenic Exposure and Health Effects*, Science and Technology Letters, Northwood, U. K.

35. Charbonneau, S. M., Tam, G. K. H., Bryce, F., Zawidzka, Z., and Sandi, E. (1979) Metabolism of orally administered inorganic arsenic in the dog. *Toxicol. Lett.* **3**, 107-114.

36. Vahter, M. (1981) Biotransformation of trivalent and pentavalent inorganic arsenic in mice and rats. *Environ. Res.* **25**, 286-293.

37. Vahter, M., Marafante, E., and Dencker, L. (1984) Tissue distribution and retention of ^{74}As-dimethylarsinic acid in mice and rats. *Arch. Environ. Contam. Toxicol.* **13**, 259-264.

38. Kaise, T., Yamauchi, H., Horiguchi, Y., Tani, T., Watanabe, S., Hirayama, T., and Fukui, S. (1989) A comparative study on acute toxicity of methylarsonic acid, dimethylarsenic acid and trimethlarsine oxide in mice. *Appl. Organomet. Chem.* **3**, 273-277.

39. Cullen, W. R. and Reimer, K. J. (1989) Arsenic speciation in the environment. *Chem. Rev.* **89**, 713-764.

40. Aposhian, H. V. (1997) Enzymetic methylation of arsenic species and other new approaches to arsenic toxicity. *Annu. Rev. Pharmacol. Toxicol.* **3**, 397-419.

41. Le, X. C., Lu, X. F., and Li, X. F. (2004) Arsenic speciation. *Anal. Chem.* **76**, 27A-33A.

42. Challenger, F. (1945) Biological methylation. *Chem. Rev.* **36**, 315-361.

43. Vega, L., Styblo, M., Patterson, R., Cullen, W. R., Wang, C., and Germolec, D. (2001) Differential effects of trivalent and pentavalent arsenicals on cell proliferation and cytokine secretion in normal human epidermal keratinocytes. *Toxicol. Appl. Pharmacol.* **172**, 225-232.

44. Petrick, J. S., Ayala-Fierro, F., Cullen, W. R., Carter, D. E., and Aposhian, H. V. (2000) Monomethylarsonous acid (MMA^{III}) is more toxic than arsenite in Chang human hepatocytes. *Toxicol. Appl. Pharmacol.* **163**, 203-207.

45. Lin, S., Del Razo, L. M., Styblo, M., Wang, C., Cullen, W. R., and Thomas, D. J. (2001) Arsenicals inhibit thioredoxin reductase in cultured rat hepatocytes. *Chem. Res. Toxicol.* **14**, 305-311.

46. Shen, Z. X., Chen, G. Q., Ni, J. H., Li, X. S., Xiong, S. M., Qiu, Q. Y., Zhu, J., Tang, W., Sin, G. L., Yang, K. Q., Chen, Y., Zhou, L., Fang, Z. W., Wang, Y. T., Ma, J., Zhang, P., Zhang, T. D., Chen, S. J., Chen, Z., and Wang, Z. Y. (1997) Use of arsenic trioxide (As_2O_3) in the treatment of acute promyelocytic leukemia (APL): II. Clinical efficacy and pharmacokinetics in relapsed patients. *Blood* **89**, 3354-3360.

47. Soignet, S. L., Maslak, P., Wang, Z. G., Jhanwar, S., Calleja, E., Dardashti, L. J., Corso, D., DeBlasio, A., Gabrilove, J., Scheinberg, D. A., Pandolfi, P. P., and Warrell, R. P. (1998) Complete remission after treatment of acute promyelocytic leukemia with arsenic trioxide. *N. Engl. J. Med.* **339**, 1341-1348.

48. Shen, Z. X., Shi, Z. Z., Fang, J., Gu, B. W., Li, J. M., Zhu, Y. M., Shi, J. Y., Zheng, P. Z., Yan, H., Liu, Y. F., Chen, Y., Shen, Y., Wu, W., Tang, W., Waxman, S., de The, H., Wang, Z. Y., Chen, S. J., and Chen, Z. (2004) All-trans retinoic acid/As2O3 combination yields a high quality remission and survival in newly diagnosed acute promyelocytic leukemia. *Proc. Natl. Acad. Sci. USA.***101**, 5328-5335.

49. Chen, G. Q., Zhou, L., Styblo, M., Walton, F., Jing, Y. K., Weinberg, R., Chen, Z., and Waxman, S. (2003) Methylated metabolites of arsenic trioxide are more potent

than arsenic trioxide as apoptotic but not differentiation inducers in leukemia and lymphoma cells. *Cancer Res.* **63**, 1853-1859.

50. Miller, W. H., Schipper, H. M., Lee, J. S., Singer, J., and Waxman, S. (2002) Mechanisms of action of arsenic trioxide. *Cancer Res.* **62**, 3893-3903.
51. Zhu, J., Chen, Z., Lallemand-Breitenbach, V., and de The, H. (2002) How acute promyelocytic leukaemia revived arsenic. *Nat. Rev. Cancer* **2**, 705-713.
52. Oremland, R. S., and Stolz, J. F. (2003) The ecology of arsenic. *Science* **300**, 939-944.
53. Rosen, B. P. (2002) Biochemistry of arsenic detoxification. *FEBS Lett.* **529**, 86-92.
54. Kitchin, K. T. (2001) Recent advances in arsenic carcinogenesis: Modes of action, animal model systems, and methylated arsenic metabolites. *Toxicol. Appl. Pharmacol.* 172, 249-261.
55. Hughes, M. F. (2002) Toxicity and potential mechanisms of action. *Toxicol. Lett.* **133**, 1-16.
56. Vahter, M. (2002) Mechanisms of arsenic biotransformation. *Toxicology* 181, 211-217.
57. Styblo, M., Drobna, Z., Jaspers, I., Lin, S., and Thomas, D. J. (2002) The Role of biomethylation in toxicity and carcinogenicity of arsenic: a research update. *Environ. Health Perspect.* **110 (Suppl.)**, 767-777.
58. Rossman, T. G., Uddin, A. N., Burns, F. J., and Bosland, M. C. (2002) Arsenite cocarcinogenesis: An animal model derived from genetic toxicology studies. *Environ. Health Perspect.* **110 (Suppl.)**, 749-752.

59. Bode, A. M. and Dong, Z. G. (2002) The paradox of arsenic: molecular mechanisms of cell transformation and chemotherapeutic effects. *Crit. Rev. Oncol. Hematol.* **42**, 5-24.

60. Rosen, B. P. (1999) Families of arsenic transporters. *Trends in Microbiol.* **7**, 207-212.

61. Liu, Z., Boles, E., and Rosen, B. P. (2004) Arsenic trioxide uptake by hexose permeases in *Saccharomyces cerevisiae*. *J. Biol. Chem.* **279**, 17312-17318.

62. Meng, Y. L., Liu, Z., and Rosen, B. P. (2004) As(III) and Sb(III) uptake by GlpF and efflux by ArsB in *Escherichia coli*. *J. Biol. Chem.* **279**, 18334-18341.

63. Kala, S. V., Neely, M. W., Kala G., Prater, C. I., Atwood, D. W., Rice, J. S., and Lieberman, M. W. (2000) The MRP2/cMOAT transporter and arsenic-glutathione complex formation are required for biliary excretion of arsenic. *J. Biol. Chem.* **275**, 33404-33408.

64. Schwerdtle, T., Walter, I., Mackie, I., and Hartwig, A. (2003) Induction of oxidative DNA damage by arsenite and its trivalent and pentavalent methylated metabolites in cultured human cells and isolated DNA. *Carcinogenesis* **24**, 967-974.

65. Tei, T. K., Liu, S. X., and Waldren, C. (1998) Mutagenicity of arsenic in mammalian cells: Role of reactive oxygen species. *Proc. Natl. Acad. Sci. USA* **95**, 8103-8107.

66. Liu, S. X., Athar, M., Lippai, I., Waldren, C., and Hei, T. K. (2001) Induction of oxyradicals by arsenic: Implication for mechanism of genotoxicity. *Proc. Natl. Acad. Sci. USA* **98**, 1643-1648.

67. Chou, W. C., Jie, C. F., Kenedy, A. A., Jones, R. J., Trush, M. A., and Dang, C. V. (2004) Role of NADPH oxidase in arsenic-induced reactive oxygen species formation

and cytotoxicity in myeloid leukemia cells. *Proc. Natl. Acad. Sci. USA* **101,** 4578-4583.

68. Hartwig, A. and Schwerdtle, T. (2002) Interactions by carcinogenic metal compounds with DNA repair processes: toxicological implications. *Toxicol. Lett.* **127**, 47-54.

69. Tran, H. P., Prakash, A. S., Barnard, R., Chiswell, B., and Ng, J. C. (2002) Arsenic inhibits the repair of DNA damage induced by benzo(a)pyrene. *Toxicol. Lett.* **133**, 59-67.

70. Cunninghan, M. L., Zvelebil, M. J., and Fairlamb, A. H. (1994) Mechanism of inhibition of trypanothione reductase and glutathione reductase by trivalent organic arsenicals. *Eur. J. Biochem.* **221**, 285-295.

71. Schuliga, M., Chouchane, S., and Snow, E. T. (2002) Upregulation of glutathione-related genes and enzyme activities in cultured human cells by sublethal concentrations of inorganic arsenic. *Toxicol. Sci.* **70**, 183-192.

72. Wang, T. S., Shu, Y. F., Liu, Y. C., Jan, K. Y., and Huang, H. (1997) Glutathione peroxidase and catalase modulate the genotoxicity of arsenite. *Toxicol.* **121**, 229-237.

73. Chang, K. N., Lee, T. C., Tam, M. F., Chen, Y. C., Lee, L. W., Lee, S. Y., Lin, P. J., and Huang, R. N. (2003) Identification of galectin I and thioredoxin peroxidase II as two arsenic-binding proteins in Chinese hamster ovary cells. *Biochem. J.* **371**, 495-503.

74. Li, J. and Pickart, C. M. (1995) Binding of phenylarsenoxide to Arg-tRNA protein transferase is independent of vicinal thiols. *Biochemistry* **34**, 15829-15837.

Chapter 3 Accumulation of Trivalent Dimethyl Arsenical Complex of Hemoglobin in Rats Fed with Arsenic Species[1]

3.1 Introduction

Arsenic is classified as a human carcinogen by a number of international organizations (1, 2). Human epidemiological studies have demonstrated a consistent association between elevated arsenic exposure and the prevalence of skin, bladder, and lung cancers (2-7). More than 40 million people around the world may be at risk (8, 9). However, the mechanism or mode of action by which arsenic causes various cancers is very complex and has not been well delineated. Recent studies have investigated multiple plausible mechanisms, including reaction with sulfhydryl groups of critical cellular proteins, generation of oxidative damage by trivalent arsenic metabolites, inhibition of DNA repair, inhibition of several key enzymes, and many other mechanisms (6, 10-12). Many of the proposed mechanisms are interdependent and may vary with specific arsenic compounds, tumor sites, cell types, and animal species.

Clarifying arsenic toxicity is further complicated by the lack of a reliable animal model. Long-term treatment (e.g., a two-year bioassay) with high doses of inorganic arsenic or pentavalent arsenic metabolites has not been tumorigenic in most experimental animals tested (12, 13) unless there was also co-exposure of other carcinogens (14-17). The only convincing exception is the production of urinary bladder tumors in rats

[1] *A version of this chapter has been submitted for publication. Lu et al. Proc. Natl. Acad. Sci. USA*

(especially female rats) after long-term treatment with high doses (40–200 μg/g) of dimethylarsinic acid (DMA^V) in the diet (18, 19) or drinking water (20, 21). Therefore, there has been much interest in understanding the mode of action for DMA^V-induced bladder tumors in rats (19, 21-24). Tumors produced in mice after *in utero* exposure to arsenic have also attracted much attention (25, 26).

A significant difference in arsenic metabolism and disposition has been demonstrated between rats and most other animal species, including humans. In general, inorganic arsenic undergoes biomethylation that involves alternate reduction of pentavalent arsenic species to trivalent arsenic species followed by oxidative methylation of the trivalent arsenic species. In humans, the biomethylation process appears to stop at the dimethyl arsenicals. In rats, however, the biomethylation process proceeds further to the formation of trimethyl arsenicals, mainly trimethylarsine oxide. Furthermore, rats have shown a much longer retention time of arsenic in their blood compared to humans primarily because of the retention in RBC (27-32). Rat hemonglobin (rHb) in the RBC has been considered a possible target protein (33, 34). The work in Chapter 2 has suggested that arsenic binding to the rHb is a basis for accumulation of arsenic in rat blood. However, it is not known which arsenic species binds to the rHb treated with arsenic. In this chapter, arsenic will be shown to accumulate significantly in RBC by binding dimethylarsonic acid (DMA^{III}) to a reactive cysteine residue in rHb regardless whether the rats are fed arsenic in the form of inorganic arsenate (iAs^V), monomethylarsonic acid (MMA^V), or dimethylarsinic acid (DMA^V). It suggests the efficient biomethylation of arsenicals in rats and the high affinity of rHb for DMA^{III}.

Confirming DMA^{III} as the predominant protein-bound arsenic species in rHb is biochemically and toxicologically important because of the cytotoxic and possible indirect genotoxic effects of DMA^{III} (35-37). It is generally accepted that the genotoxicity of DMA^{III} does not involve direct interaction with DNA. However, indirect processes involving oxidative damage resulting from reactive oxygen species (36, 38-44) and inhibition of DNA repair (37, 45) have been demonstrated. DMA^{III} is also more cytotoxic (36, 38, 39, 46, 47) and a more potent enzyme inhibitor (48, 49) than its pentavalent counterpart and the inorganic arsenic species. Studies of its biochemical interactions *in vivo* will contribute to further understanding of the mode of action responsible for arsenic toxicity.

3.2 Materials and Methods

3.2.1 Arsenic compounds used for rat treatment

Sodium arsenate (iAs^V) was obtained from Sigma (St. Louis, MO) and stored at room temperature without further purification. Dimethylarsinic acid (DMA^V) and monomethylarsonic acid (MMA^V) were received from Luxembourg Industries (Pamol, Tel-Aviv, Israel). The purity was documented by the provider and the analysis of DMA^V was confirmed by NMR analysis at the University of Nebraska Medical Center. DMA^V and MMA^V were stored desiccated at room temperature. DMA^V and MMA^V of measured concentrations (2–100 μg/g) were mixed into Certified Rodent Diet 5002 (PMI Nutrition International, St. Louis, MO) prior to pelleting by Dyets (Bethlehem, PA).

Other materials involved in this chapter are the same as those in Section 2.2.1.

3.2.2 Rats treated with iAs^V, MMA^V, and DMA^V (done by Lora L. Arnold at UNMC)

The experimental protocol was approved by the Institutional Animal Care and Use Committee of the University of Nebraska Medical Center. One hundred forty female F344 rats, 4 weeks old at the time of arrival, were purchased from Charles River Breeding Laboratories (Raleigh, NC). The animals were housed in the same way as that described in Section 2.2.2.4. They were fed pelleted Certified Rodent Diet 5002. Food and tap water were available *ad libitum* throughout the study. Following quarantine, the rats were randomized into 7 groups by a weight stratification method. Group 1 was provided with tap water supplemented with 100 μg/g iAs^V; all other groups (2-7) were given untreated tap water. Analysis of the tap water by the Metropolitan Utilities District (Omaha, NE) showed an arsenic level of less than 0.1 μg/L. Group 2 was fed the basal diet supplemented with 100 μg/g MMA^V, Groups 1 and 3 (control) were fed the basal diet, and the other four groups (Groups 4 to 7) were fed the basal diet supplemented with 2, 10, 40, and 100 μg/g DMA^V, respectively. Analysis of the basal diet by Nutrition International showed an arsenic level of less than 0.2 μg/g. The average food and water consumption for each group of rats was recorded. The average achieved dosage of arsenic (mg/kgBW/day) was obtained from the food and water consumption values, the body weight of rats, and the concentration of the arsenic species in water and food. The dosage results are summarized in Table 3-1.

3.2.3 Bladder inflation and blood collection and separation (done by Lora L. Arnold at UNMC)

After 1, 2, 6, 8, 10, and 15 weeks of treatment with normal diet or arsenic supplemented diet or drinking water, the 5 rats in groups 1-3 and 7 were sacrificed. The 5 rats in groups 4-6 were sacrificed after 10 weeks of treatment. All rats were sacrificed between 0900 and 1400 by an overdose of Nembutal (50 mg/kg of body weight, i.p.). At each sacrifice, blood from the abdominal aorta was collected from non-fasted rats into tubes containing lithium heparin and stored on ice until all samples were collected. RBC and plasma were separated by centrifugation at 3200 rpm at 4 °C for 10 min. The resultant plasma and packed RBC were immediately frozen in liquid nitrogen, kept on dry ice during shipping, and stored at -80 °C until analysis. At all time points except after 15 weeks of treatment, the urinary bladder was inflated *in situ* with Bouin's fixative, removed, and placed in the same fixative. Half of the bladder from each animal was processed for examination by SEM and classified as previously described (50). Briefly, Class 1 bladders show flat, polygonal superficial urothelial cells; Class 2 bladders show occasional small foci of superficial urothelial necrosis; Class 3 bladders show numerous small foci of superficial urothelial necrosis; Class 4 bladders show extensive superficial urothelial necrosis, especially in the dome of bladder; and Class 5 bladders show necrosis and piling up of rounded urothelial cells. Normal bladders are usually Class 1 or 2, but may occasionally be Class 3. The other half of the bladder was cut longitudinally into strips, and with a slice of stomach, was embedded in paraffin, stained with hematoxylin and eosin, and examined histopathologically (50, 51).

Table 3-1. Achieved dosage (mg/kg BW/day) during week 2 of treatment

Treatment	Arsenic Compound (mg/kg)	Arsenic (mg/kg)
100 μg/g iAs^V in water	10.40	10.40
100 μg/g MMA^V in food	9.10	4.88
2 μg/g DMA^V in food	0.18	0.10
10 μg/g DMA^V in food	0.90	0.49
40 μg/g DMA^V in food	3.64	1.98
100 μg/g DMA^V in food	9.10	4.94

3.2.4 GFC-ICPMS analysis of arsenic in blood of rats

The GFC-ICPMS system and its operational conditions were the same as described in Section 2.2.2.1. The rat plasma was diluted 20 times and subjected to GFC-ICPMS analysis directly. The RBC were lysed the same way as Section 2.2.2.3. The resulting RBC lysate was diluted up to 3000 times and subjected to GFC-ICPMS analysis. The sample from each rat was analyzed twice and the results were averaged. The results for the 5 rats from each group were then averaged at each time point.

3.2.5 NanoESI-MS analysis of RBC lysates from rats exposed to arsenic

The RBC lysates from both control and arsenic exposed rats were desalted by a BioSpin-6 column. Immediately prior to nanoESI-MS analysis, the desalted protein fraction was diluted 10-fold with water, methanol, and formic acid to a final methanol

concentration of 10% and formic acid concentration of 0.002%. The resulting solution was then loaded on to a nanoelectrospray capillary tip and subjected to nanoESI-MS analysis as described in Section 2.2.2.2.

3.2.6 HPLC-HGAFS analysis of the arsenic species in the protein adducts

Hydride generation coupled with atomic fluorescence spectrometry (HGAFS) was used for detection of the arsenic species released from the protein. RBC lysates from control and arsenic exposed rats were precipitated using ice acetone (-20 °C), centrifuged, and dissolved in alkaline solutions. Most of the bound arsenic (>90%) was released from the protein, which was examined using GFC-ICPMS as described in Section 2.2.2.1. The released arsenic was separated from the protein by ultrafiltration using microcon-3 filters (Millipore, Bedford, MA). The filtrate (with the released arsenic) was then diluted with the mobile phase and injected into the HPLC-HGAFS system, which was described previously (52, 53). Briefly, a Phenomenex ODS-3 reversed-phase column (150 x 4.6 mm, 3 μm particle size) with a temperature maintained at 50 °C was used for separation. The mobile phase contained 5 mmol/L tetrabutylammonium hydroxide, 4 mmol/L malonic acid, and 5 % methanol (pH 6.0). The flow rate was 1.2 mL/min, and the injection volume was 20 μL.

3.2.7 Measurement of the oxygen affinity of the rat hemoglobin after arsenic exposure

RBC from the control group and the iAs^{V}-treated groups were lysed and a supernatant solution was obtained as described in Section 2.2.2.3. The supernatant

solution was then passed through a PBS equilibrated G-25 desalting column (Amersham Biosciences, CA). The rHb fraction was collected and the concentration was determined by Drabkin's method (54). The purified rHb samples were immediately subjected to oxygen affinity measurement.

The measurement of the oxygen affinity of rHb was carried out using a Hemox Analyzer (automatic blood oxygen dissociation analyzer from TCS Scientific, New Hope, PA). The Hemox Analyzer was assembled with on-line compressed nitrogen and air. A dual-wavelength spectrophotometer was used to measure the level of rHb oxygenation according to the optical properties of rHb, and a Clark electrode was used for continuous monitoring of the oxygen partial pressure (mmHg or torr). The experiment was carried out at 37 °C with appropriate stirring. Here dissociation curves were measured by saturation of rHb under air atmosphere, followed by purging nitrogen in and simultaneously reducing the oxygen partial pressure. The rHb samples prepared above were diluted to 20 μM in 5 mL Hemox buffer [135 mM NaCl, 5 mM KCl, and 30 mM N-tris(hydroxymethyl)methyl-2-aminoethanesulphonic acid (pH 7.4)] which contained 20 μL BSA and 10 μL antifoaming agent, and immediately transferred into the cuvette for oxygen dissociation measurement. The Adair equation (55) was applied to generate a complete oxygen-binding curve, which was used to determine the oxygen pressure at which rHb is half saturated (P_{50}) and the Hill coefficient (h) for oxygen binding.

3.3 Results

3.3.1 Distribution and accumulation of arsenic in rat blood

The arsenic distribution in blood obtained from rats exposed for up to 15 weeks to three different pentavalent arsenicals (iAs^V, MMA^V, and DMA^V) at a dose of 100 μg/g has been obtained. It was found that arsenic accumulated predominantly in rat RBC and not in plasma (Figure 3-1). The ratios of the measured total arsenic in the rat RBC to that in rat plasma over the 15-week exposure duration were 88–423 for rats fed iAs^V, 100–680 for rats fed MMA^V, and 185–1393 for rats fed DMA^V (Figure 3-1A). The maximum total arsenic in RBC of rats exposed to 100 μg/g iAs^V in water was about 3.5 (±1.3) mM after 6 weeks of exposure, and 2.6 (±0.4) mM and 2.5 (±0.2) mM in the 100 μg/g MMA^V and DMA^V groups of 8 weeks exposure, respectively (Figure 3-1B). In comparison, the arsenic level in the plasma of rats treated with the three pentavalent arsenic compounds at the same dose of 100 μg/g fluctuated around 10 μM during the treatment period from 1 to 15 weeks (Figure 3-1C). These results indicate that arsenic was effectively arrested in rat RBCs at mM concentration (Figure 3-1B) but not in plasma (only μM concentrations as shown in Figure 3-1C) for all three investigated pentavalent arsenic compounds, making the total amount of arsenic found in rat RBCs 88–1393-fold higher than that in rat plasma.

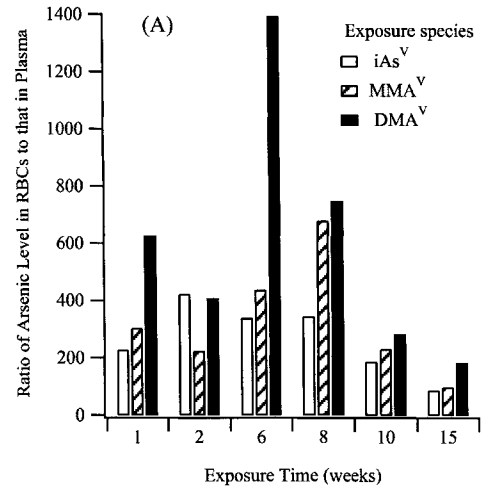

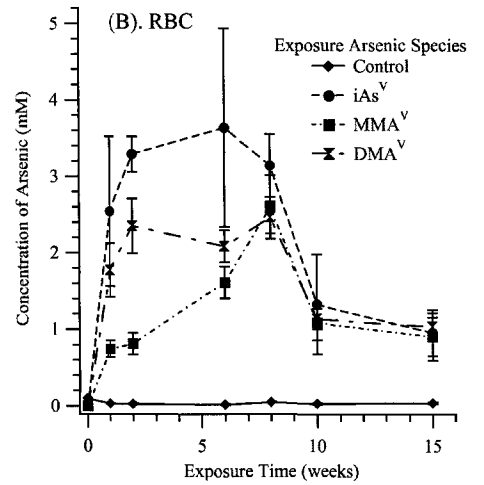

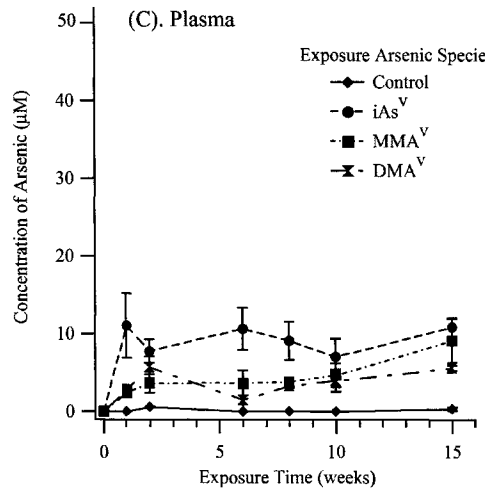

Figure 3-1. Arsenic concentration in the RBC and the plasma of control rats and rats fed iAs^V, MMA^V, and DMA^V over the 15-week exposure. (A) Ratio of total arsenic in RBC to that in plasma; (B) Total arsenic concentration in RBC of rats; and (C) Total arsenic concentration in plasma of rats. The total arsenic concentrations in RBC and plasma represent the sum of both free and protein-bound arsenic species obtained from GFC-ICPMS analysis. At each time point, data from the 5 rats in each group were averaged. Each sample from the same rat was analyzed twice and the data were averaged with a relative deviation of < 5%. Within each group of 5 rats, the relative standard deviation from the average value was mostly within 35%.

To understand the large difference of arsenic concentration in RBC and plasma, the protein-bound and the free arsenic species in RBC and plasma have been separately determined by the GFC-ICPMS method developed in Chapter 2. Figure 3-2 demonstrates the chromatograms obtained from GFC-ICPMS analysis of arsenic binding and distribution in RBC (A) and plasma (B) from the rats exposed to arsenic. The protein-bound arsenic migrated out faster (1.8 min) than free (unbound) arsenic (3.6 min). In rat RBC, protein-bound arsenic is the predominant fraction for all the rats exposed to iAs^V, MMA^V, or DMA^V (Figure 3-2A). Even in the control rats fed the basal diet (without supplemental arsenic), a small amount of protein-bound arsenic was detected in the RBC. However, very little free arsenic was observed in control or treated rat RBC (Figure 3-2A). In fact, the fraction of arsenic bound to protein in rat RBC is over 99% for all rats examined (n=138) regardless of the arsenic species (iAs^V, MMA^V, and DMA^V) administered to the rats, exposure dose (0–100 μg/g), or exposure duration (0–15 week). It is evident that the degree of protein binding of arsenic in RBC is independent of the speciation of the arsenicals used in the treatment of rats. In contrast, in the plasma of rats exposed to arsenic (100 μg/g iAs^V, MMA^V, or DMA^V, n=30 for each), the average protein-bound arsenic accounted for 40.1 (±15.6)%, 49.3 (±17.3)%, and 43.5 (±13.7)% of the total arsenic in plasma, respectively (Figure 3-2B). The results suggest that the higher degree of protein binding to arsenic in rat RBC may be responsible for the higher concentration of arsenic in rat RBC.

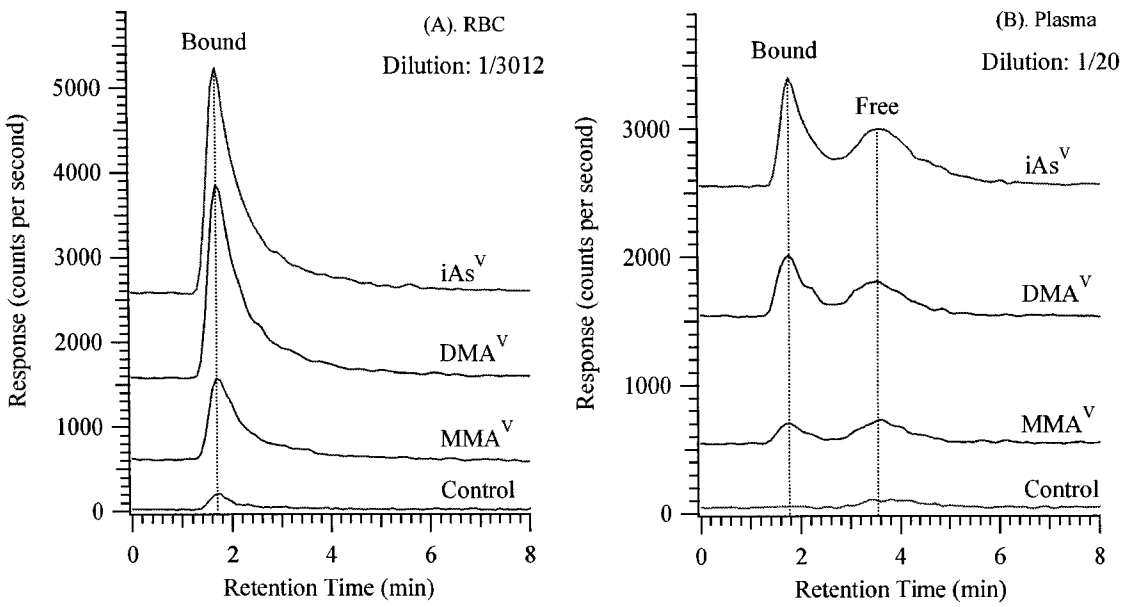

Figure 3-2. Chromatograms obtained from GFC-ICPMS analysis of protein-bound and free arsenic in the RBC and the plasma of control rats and rats fed pentavalent arsenic for 2 weeks. (A) RBC; (B) plasma. After separation of the plasma from the RBC, the plasma was diluted 20-fold and subjected to GFC-ICPMS analysis directly. The RBC was first lysed and subjected to high speed centrifugation. The supernatant solution were collected, diluted, and further subjected to GFC-ICPMS analysis. The total dilution factor for the RBC was 3012-fold and for the plasma was 20-fold. The detailed GFC-ICPMS conditions are described in Section 2.2.2.1.

3.3.2 Effect of exposure dose of DMA^V

To investigate the dose-response of arsenic in rat blood, rats that were exposed to DMA^V for 10 weeks with doses of 0, 2, 10, 40 and 100 μg/g were examined. The results demonstrate that arsenic content both in RBC and in plasma is dose-dependent (Figure 3-3). The protein-bound arsenic present in the RBC of the rats (n=5) significantly increased from 0.03(±0.01) mM (control level exposure, n=5) to 1.1 (±0.3) mM (40 μg/g DMA^V exposure, n=5). There was no further significant increase in the arsenic content of the RBC of the rats exposed to 100 μg/g DMA^V compared to the level in the 40 μg/g group (Figure 3-3A). This was probably caused by the decrease in the concentration of protein-bound arsenic in the 100 μg/g DMA^V group that started after 8 weeks of exposure (Figure 3-1B). In comparison, the total arsenic content in the plasma increased from undetectable levels to 2.1 (±0.94) μM (n=5) with increasing exposure doses from 0 to 10 μg/g. It reached over 4.0 (±1.4) μM (n=5) with increasing exposure doses from 10 to 100 μg/g (Figure 3-3B). Examination of the separate dose-response curves of the protein-bound arsenic and free arsenic in plasma showed that protein-bound arsenic increased with increasing exposure doses only when the doses were under 10 μg/g, and it approached a saturation point when the doses were above 10 μg/g (Figure 3-3B). Unlike protein-bound arsenic, the free arsenic level in the plasma continued to increase with increasing exposure doses (Figure 3-3B). In the entire dose range (0–100 μg/g DMA^V), the concentration of arsenic in the RBC was much higher (234–370-fold) than its concentration in the plasma, consistent with the exposure-time-dependent results shown in Figure 3-1.

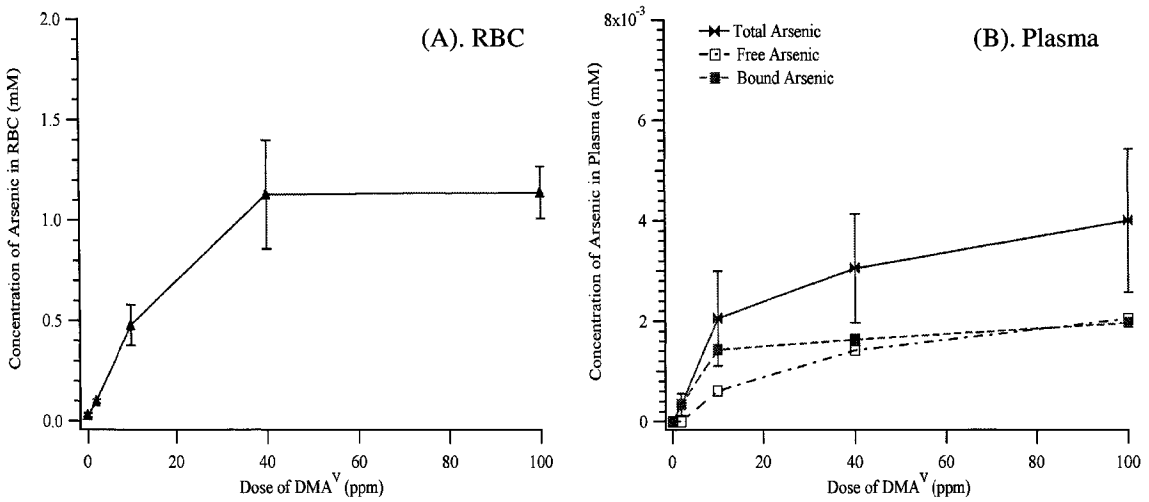

Figure 3-3. Arsenic concentration in the RBC and the plasma of rats fed either a basal diet or a diet supplemented with DMA^V at various doses. (A) RBC; (B) plasma. The rats (5 in each group) were exposed to control level, 2, 10, 40 or 100 μg/g DMA^V in the diet continuously for 10 weeks and were then sacrificed, and their blood was collected for arsenic analysis by GFC-ICPMS. The sample preparation methods and the GFC-ICPMS conditions are described in Sections 2.2.2.3 and 2.2.2.1, respectively.

3.3.3 Identification of the bound arsenic species in protein

To understand the biochemical basis of arsenic arrest and accumulation in rat RBC, protein-bound arsenic species were further identified and characterized using two techniques, nanoESI-MS and HPLC coupled with hydride generation atomic fluorescence spectrometry (HPLC-HGAFS). NanoESI-MS analysis can provide chemical information on the identities of bound proteins, reactive arsenic species, and *in vivo* pertinent binding

stoichiometry. Figure 3-4 demonstrates the deconvoluted mass spectra obtained from analysis of rat RBC lysates from the control rats and the rats exposed to 100 μg/g of iAs^V, MMA^V, or DMA^V. The identified mass spectral peaks are summarized in Table 3-2. The mass spectrum from a control rat demonstrated two major peaks of rHb α and β units with the corresponding molecular masses of 15813 Da and 16450 Da (trace D in Figure 3-4), resulting from the dissociated Hb tetramer. Under optimized conditions for sample preparation and MS analysis, the prosthetic group of the heme can be well-preserved complexed with most of the rHb α and β units. Only small amounts of the apo-α unit (MW 15197 Da) and apo-β unit (MW 15834 Da) were observed, which may be due to a loss of the heme group (MW 616.2 Da) from each Hb polypeptide chain during the desolvation process. In the mass spectrum from the rat exposed to DMA^V (trace A in Figure 3-4), a new peak of MW 15917 Da was observed, accompanied by a decrease in the peak of the rHb α unit (MW 15813 Da). This new peak has a mass increase of 104 Da from the intact rHb α unit (MW 15813 Da), indicating the formation of a rHbα-DMA^{III} complex. The mass increase of 104 Da is characteristic of an addition of one DMA^{III} molecule (MW 121.97 Da) with a loss of one water molecule (MW 18.01 Da), as demonstrated in Chapter 2. The binding stoichiometry of the observed rHbα-DMA^{III} complex is 1:1. Furthermore, no other arsenic-protein complex (different in binding stoichiometry or in bound arsenic species) was observed. Therefore, *in vivo* the predominant protein complex of arsenic in the RBC of rats exposed to DMA^V is the rHbα-DMA^{III} complex with stoichiometry of 1:1.

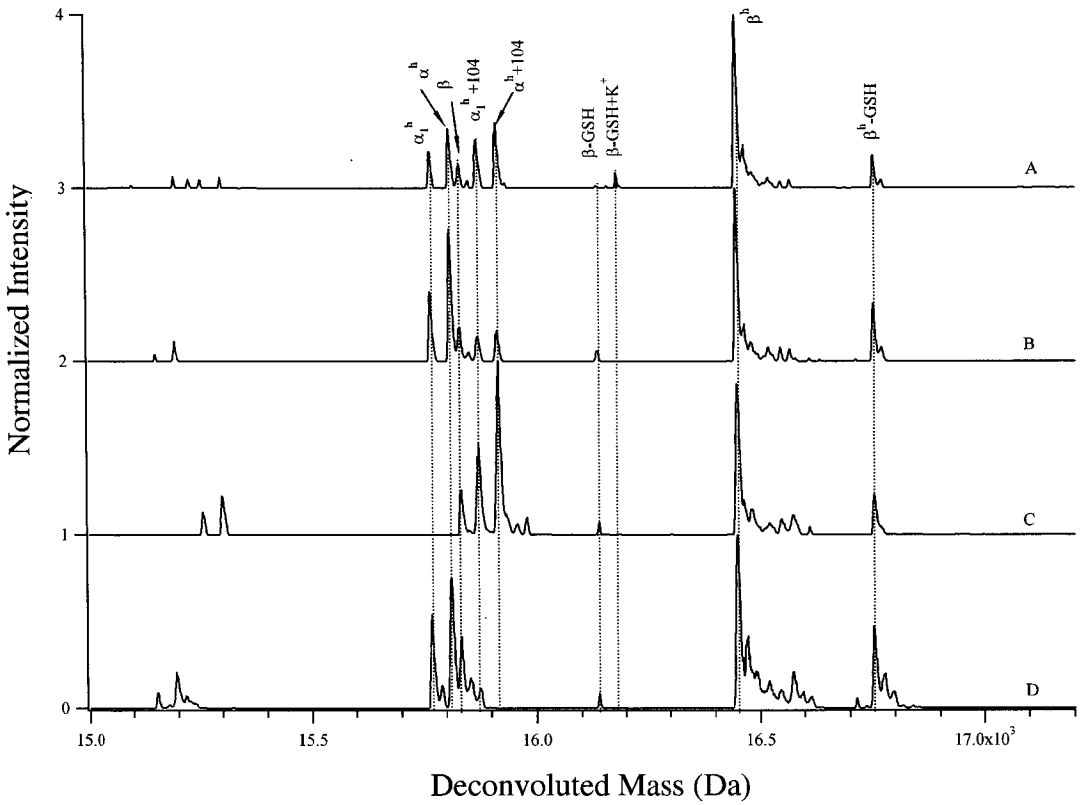

Figure 3-4. Deconvoluted nanoelectrospray mass spectra of the RBC lysates from rats exposed to different pentavalent arsenic species for 1 week. Rats were fed (A) 100 μg/g DMA^V in the diet; (B) 100 μg/g MMA^V in the diet; (C) 100 μg/g iAs^V in drinking water; (D) normal diet as control. The major peaks related to α and β chains rHb were labeled in the spectra. Peaks of α^h+104 and $\alpha_1{}^h$+104 are the complex of one α unit or α_1 unit (variant of the α unit) bound to one DMA^{III} molecule (mass increase of 104 Da from intact heme-α unit) with the heme group attached. As a result of exposure to pentavalent arsenicals (iAs^V, MMA^V, and DMA^V), a predominant protein adduct, rHbα-DMA^{III} with the stoichiometry of 1:1, was observed in rat RBC. There is no peak with mass increase of 104 Da from the β chain. However, the glutathione-conjugated β chain (β-GSH and β^h-GSH) was consistently observed in all rats, including the control rats, with mass increase of 305 Da from the β chain.

Table 3-2. Identified species in Figure 3-4 with corresponding molecular weight.

Identified Species		Mass Weight (Da)	Presence in Rats
α^h	α chain with heme (1:1)	15813.4	All rats
β	β chain without heme	15834.3	All rats
β^h	β chain with heme (1:1)	16450.3	All rats
β^h-GSH	Glutathione conjugate of β^h (1:1)	16755.4	All rats
$\alpha_1{}^h$	Variant of α chain (1:1)	15769.4	All rats
α^h+104	DMA^{III} bound to α^h (1:1)	15917.3	Only treated rats
$\alpha_1{}^h$+104	DMA^{III} bound to $\alpha_1{}^h$ (1:1)	15873.3	Only treated rats

Interestingly, the same protein complex (rHbα-DMA^{III}) with stoichiometry of 1:1 was also observed in rats exposed to MMA^V and iAs^V (traces B and C in Figure 3-4). There was no complex of monomethylarsonous acid (MMA^{III}) or inorganic arsenite (iAs^{III}) with the rHb from any of the treated rats. Consecutive monitoring of RBC from rats exposed to the arsenicals (0–15 weeks) further supported the conclusion that the rHbα-DMA^{III} complex with stoichiometry of 1:1 was predominant and persistent.

To confirm that DMA^{III} is the predominant arsenic species bound to the RBC of rats exposed to three different arsenicals, the arsenic species were further released from the Hb of rat RBC and determined using a well-established method for arsenic speciation analysis, HPLC-HGAFS (52, 53). This method can provide accurate speciation information for a number of arsenicals, including iAs^{III}, MMA^{III}, DMA^{III}, iAs^V, MMA^V, and DMA^V. In this experiment, bound arsenic was first released from the proteins in RBC

lysates (release efficiency >90%, see Figure 3-5), and analyzed for arsenic speciation using HPLC-HGAFS. As demonstrated in Figure 3-6, in all the rats exposed to iAs^V (trace B), MMA^V (trace C), or DMA^V (trace D), only two arsenicals, DMA^V (2.25 min) and DMA^{III} (4.38 min), were observed that had retention times consistent with the corresponding standard arsenicals (trace A). No significant amount of arsenic was detected in the rats fed the basal diet (trace E in Figure 3-6). *In vitro* experiments suggest that there is no direct reaction between rat Hb and DMA^V. The presence of DMA^V in the filtrate after releasing arsenic from protein may result from the oxidation of unstable DMA^{III} (56) during the release and follow-up separation process. The results further support the conclusion that DMA^{III} is the predominant arsenic species bound to rHb *in vivo* in the rats exposed to the arsenicals.

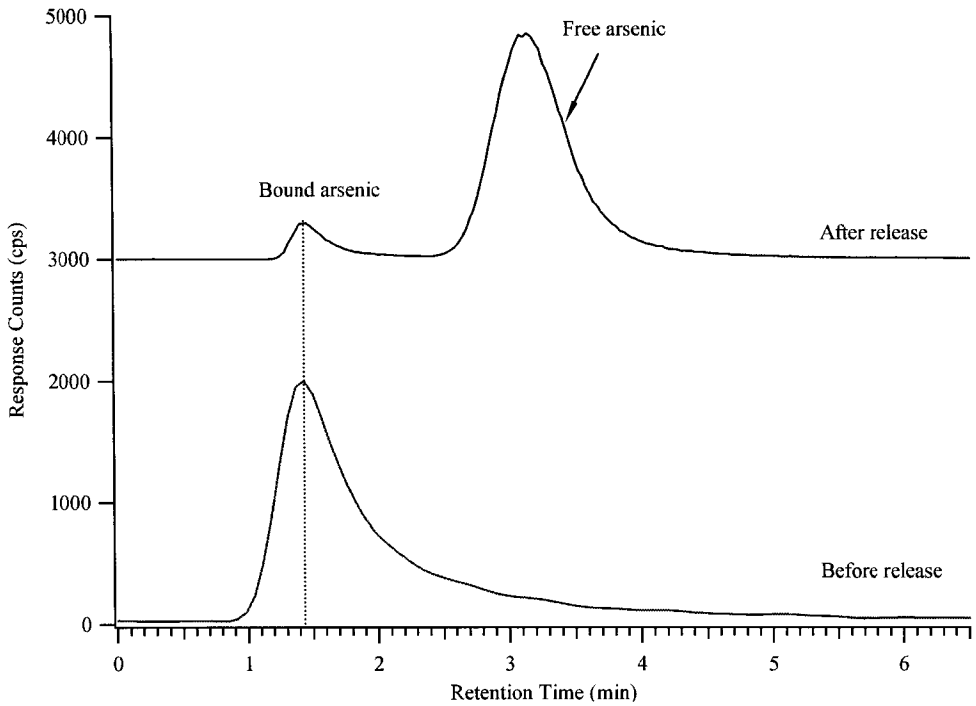

Figure 3-5. Comparison of GFC-ICPMS chromatograms before and after release of arsenic from protein in the RBC lysate. The RBC lysate was precipitated by ice acetone (-20 °C) for 1 hour and subjected to centrifugation. The protein pellet was then dissolved in a basic solution for about 20 min until it dissolved. The resulting solution was then subjected to GFC-ICPMS analysis. The experimental conditions for the GFC-ICPMS are described in Section 2.2.2.1.

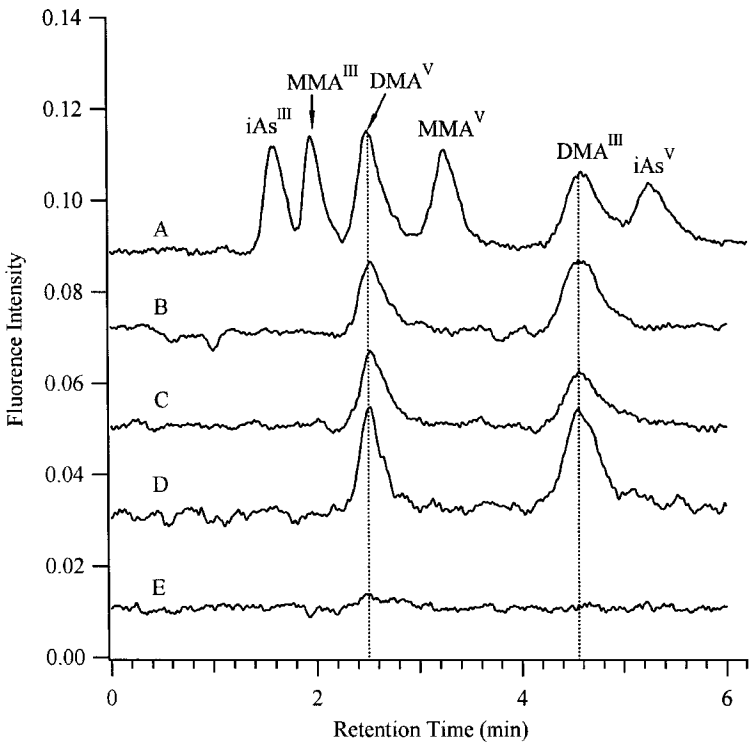

Figure 3-6. HPLC-HGAFS chromatograms showing the species of arsenic released from hemoglobin in the RBC lysate of rats exposed to different pentavalent arsenic species for 8 weeks. (A) A standard solution containing 6 arsenic species in deionized water; (B) rats fed 100 μg/g iAs^V in their drinking water; (C) rats fed 100 μg/g MMA^V in their diet; (D) rats fed 100 μg/g DMA^V in their diet; and (E) rats fed with normal diet as control. Detailed HPLC separation conditions are shown in Section 3.2.6.

3.3.4 Effect on oxygen binding affinity of rHb upon arsenic exposure

Since the main function of Hb is to carry oxygen from the lungs to other tissues and organs, it would be very interesting to see if the modification of rHb by the reactive metabolite, DMA^{III}, would have an effect on the capacity of rHb for oxygen transport. To examine this effect, the oxygen-binding isotherm of rHb from control and treated rats were determined. The results demonstrated that arsenic exposure slightly increased the oxygen-binding affinity of rHb. As shown in Figure 3-7, the rHb obtained from rats treated with 100 μg/g iAs^V for 8 weeks had a dissociation curve shifted slightly to the left of that from the control rats at the same time point, and the P_{50} value (the oxygen pressure where 50% of rHb is oxygenated) decreased about 6% from that of the control rats. The Hill coefficient (h) calculated for the rHb from arsenate-exposed rats was 2.6, which is a 7% decrease from the value for the Hb from control rats (h=2.8). The Hill coefficient is a characteristic parameter associated with Hb tetramer cooperativity for oxygen binding and release. The very close Hill coefficients indicate that the cooperativity of oxygen binding of rHb has not been significantly affected.

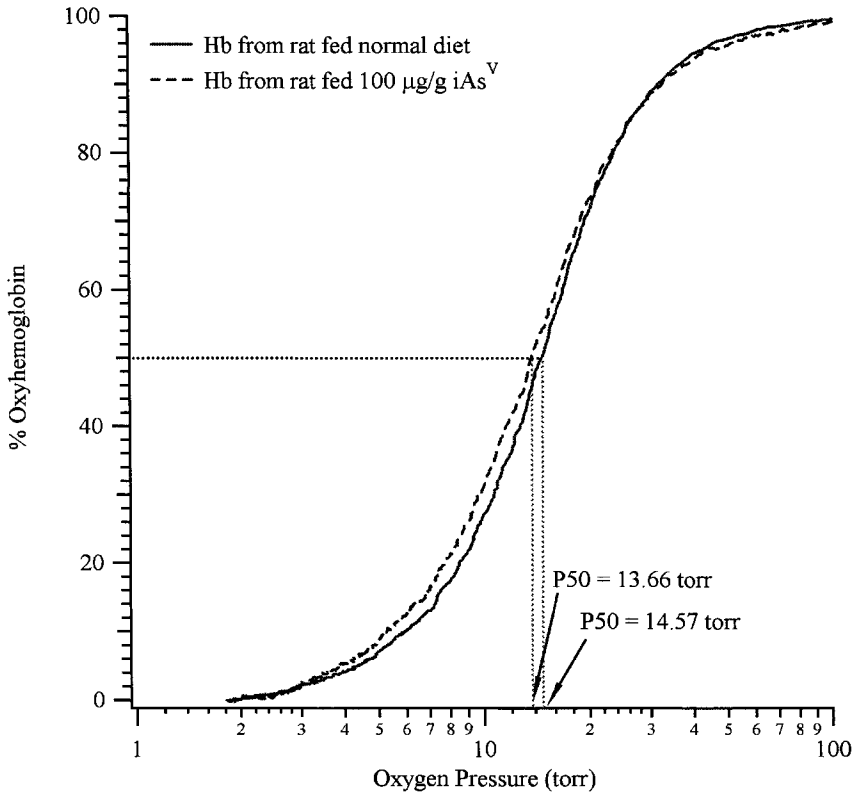

Figure 3-7. Oxygen isotherm curve of Hb from rats fed either the basal diet or 100 µg/g iAs^V. Hb from both groups of rats was extracted from rat RBC by lysis. The lysate was subjected to high speed centrifugation for 10 min. The supernatant solution was then passed through a PBS equilibrated G-25 column, and the protein fraction was collected and subjected to oxygen affinity measurement by the Hemox analyzer. Detailed experimental conditions are shown in Section 3.2.7.

3.3.5 Results of parameters measured in-life in the rats

Treatment with DMA^V and MMA^V had no effect on weight gain of the rats (Table 3-3). However, weight gain in the group treated with 100 μg/g iAs^V was significantly decreased by the end of week 2 compared to the weight gain in the control group. Although the mean body weight in the iAs^V-treated group remained significantly decreased compared to the control group throughout the experiment, the percent weight gain in the iAs^V-treated group was similar to the control group at 8 and 13 weeks. Food consumption (g/kg BW/day) was not affected by treatment with any of the three arsenicals (Table 3-3). Water consumption (g/kg BW/day) was significantly decreased throughout the study in the group treated with iAs^V in the water compared to the water consumption in the control group (Table 3-3). The mean achieved dosage for each group during week 2 of treatment is shown in Table 3-1. Since the rats consumed more water per kg body weight than diet, the consumption of arsenic compound (mg) per kg of body weight is higher in the 100 μg/g iAs^V group compared to the 100 μg/g MMA^V or 100 μg/g DMA^V group. When the achieved dosage is calculated for only the arsenic portion of the compounds, the dosage in the iAs^V group is much higher than in the MMA^V or DMA^V groups.

Examination with light microscopy showed that treatment with MMA^V and DMA^V did not cause an increase in the incidence of simple hyperplasia of the bladder epithelium at any time point (Table 3-4). However, there was an increase in the incidence of hyperplasia, as observed by light microscopy, in the group treated with 100 μg/g iAs^V in the drinking water starting as early as 1 week after the start of treatment and continuing

through 10 weeks of treatment. Treatment with iAs^V has not previously been reported to have an effect on the rat bladder epithelium.

By SEM, the rats treated with iAs^V showed significant changes as did the rats fed 100 μg/g of DMA^V. Only slight changes were detected in the MMA^V-treated group. There was a clear dose response for changes detected by SEM in rats fed various doses of DMA^V with a clear no-effect level at 2 ppm and only marginal changes at 10 ppm (Table 3-5 and Figure 3-8). The severity of the changes in rats administered DMA^V progressed over time whereas the changes in rats administered iAs^V did not. Further correlation of the lesion severity with protein-bound arsenic in the RBC showed a very good linear relationship with the regression coefficient of 0.995. The typical scanning electron micrographs from the bladders of rats fed 100 μg/g iAs^V supplemented diet and normal diet are shown in Figure 3-9.

Table 3-3. Effect of treatment with iAs^V, MMA^V, or DMA^V on body weight, food consumption, and water consumption[a].

	Body Weight			Food Consumption g/kg BW/day			Water Consumption g/kg BW/day		
Treatment	Wk 2	Wk 8	Wk 13	Wk 2	Wk 8	Wk 13	Wk 2[b]	Wk 8	Wk 13
100 μg/g iAs^V in water	110±1[c]	148±3[c]	160±6[c]	87±1	58±2	49[d]	104±4	95±4[c]	66[c,d]
100 μg/g MMA^V in food	128±1	171±2	188±4	91±1	60±1	50[d]	---	124±3	99[c,d]
Control	128±1	172±2	191±3	92±1	60±1	52[d]	---	124±3	113[d]
2 μg/g DMA^V in food	129±2	173±3	[e]	90[d]	59[d]	[e]	---	122[d]	[e]
10 μg/g DMA^V in food	124±2	167±3	[e]	90[d]	63[d]	[e]	---	133[d]	[e]
40 μg/g DMA^V in food	126±2	171±3	[e]	91[d]	60[d]	[e]	---	151[c,d]	[e]
100 μg/g DMA^V in food	125±1	170±2	187±2	91±2	63±1	51[b]	---	145±3[c]	109[d]

[a] Values expressed as the mean ± S.E.
[b] Wk 2 water consumption measurements for groups 2-7 not used due to procedural error
[c] Statistically significantly different from control group, $p<0.05$
[d] Only one cage in group
[e] All animals in group sacrificed after 10 weeks of treatment

Table 3-4. Effects of treatment with iAs^V, MMA^V, or DMA^V on the bladder epithelium.

Treatment	Bladder Histology		SEM Classification				
	Normal	Simple Hyperplasia	1	2	3	4	5
After treatment for 1 week							
100 mg/mL IAs^V [b]	2	3	0	0	0	0	3
100 mg /g MMA^V [b]	5	0	0	1	0	0	2
Control	4	1	2	2	1	0	0
100 mg /g DMA^V	4	1	0	0	3	0	2
After treatment for 2 weeks							
100 mg/mL IAs^V	1	4	0	0	1	0	4
100 mg /g MMA^V [c]	5	0	0	1	3	0	0
Control	4	1	0	5	0	0	0
100 mg /g DMA^V [c]	4	1	0	0	0	0	4
After treatment for 6 weeks							
100 mg/mL IAs^V	0	5[a]	0	0	0	0	5
100 mg /g MMA^V	5	0	0	2	3	0	0
Control	5	0	4	1	0	0	0
100 mg /g DMA^V	4	1	0	0	0	0	5
After treatment for 8 weeks							
100 mg/mL IAs^V	2	3	0	0	0	0	5
100 mg /g MMA^V	5	0	0	1	4	0	0
Control	5	0	3	2	0	0	0
100 mg /g DMA^V	5	0	0	0	0	0	5
After treatment for 10 weeks							
100 mg/mL IAs^V	0	5[a]	0	0	0	0	5
100 mg /g MMA^V [d]	4	1	0	0	0	0	2
Control	5	0	3	2	0	0	0
2 mg /g DMA^V	5	0	1	4	0	0	0
10 mg /g DMA^V	5	0	0	2	3[e]	0	0
40 mg /g DMA^V	2	3	0	0	0	0	5
100 mg /g DMA^V	4	1	0	0	0	0	5

[a] Statistically significantly different from control group, $p<0.05$

[b] Two bladders unobservable

[c] One bladder unobservable

[d] Three bladders unobservable

[e] Moderate cytotoxicity present

Table 3-5. Correlation of the Hb-arsenic complex with urothelial lesion severity.

Treatment for 10 weeks	SEM Classification[a]					Urothelial Lesion Severity[b]	Hb-Arsenic Adduct (mM)
	1	2	3	4	5		
100 mg/L iAs^{V}	0	0	0	0	5	5	1.33
100 ppm MMA^{V}	0	0	0	0	2	5	1.09
Control	3	2	0	0	0	1.4	0.03
2 ppm DMA^{V}	1	4	0	0	0	1.8	0.10
10 ppm DMA^{V}	0	2	3	0	0	2.6	0.48
40 ppm DMA^{V}	0	0	0	0	5	5	1.13
100 ppm DMA^{V}	0	0	0	0	5	5	1.14

[a] The use of 1-5 in the SEM classification scheme is arbitrary. Changes in Class 5 bladders are not five times more severe compared to Class 1 bladders. See Section 3.2.3 for the definition of each class.

[b] The urothelial lesion severity was calculated as the average SEM value for the rats in each treatment group (n=5 in all groups except the 100 ppm MMA group where n=2).

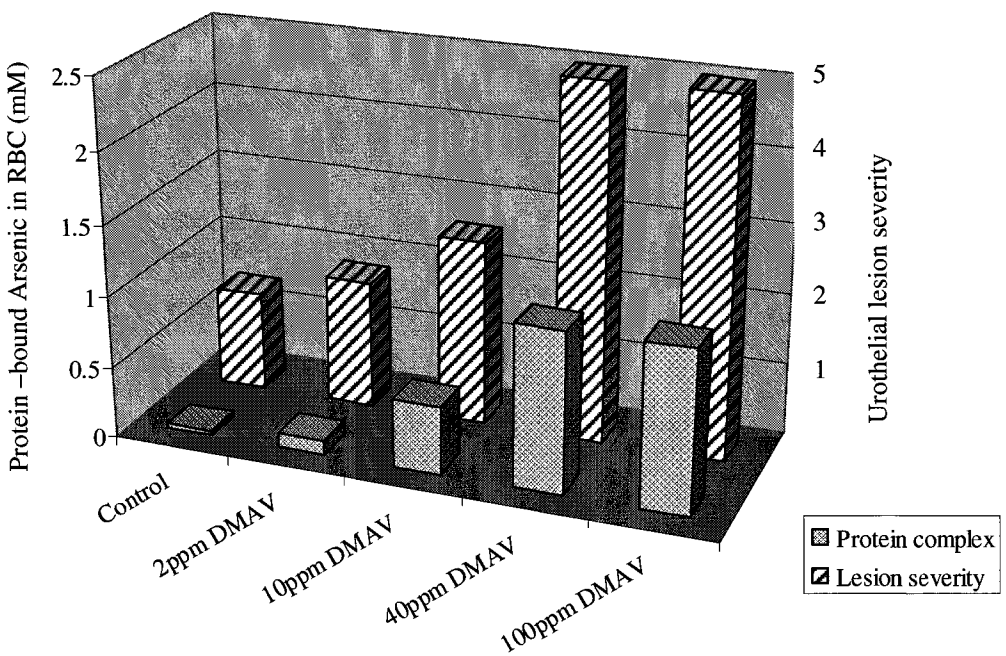

Figure 3-8. Urothelial lesion severity changes over the concentration of protein-bound arsenic in rat RBC. The data are shown in Table 3-5.

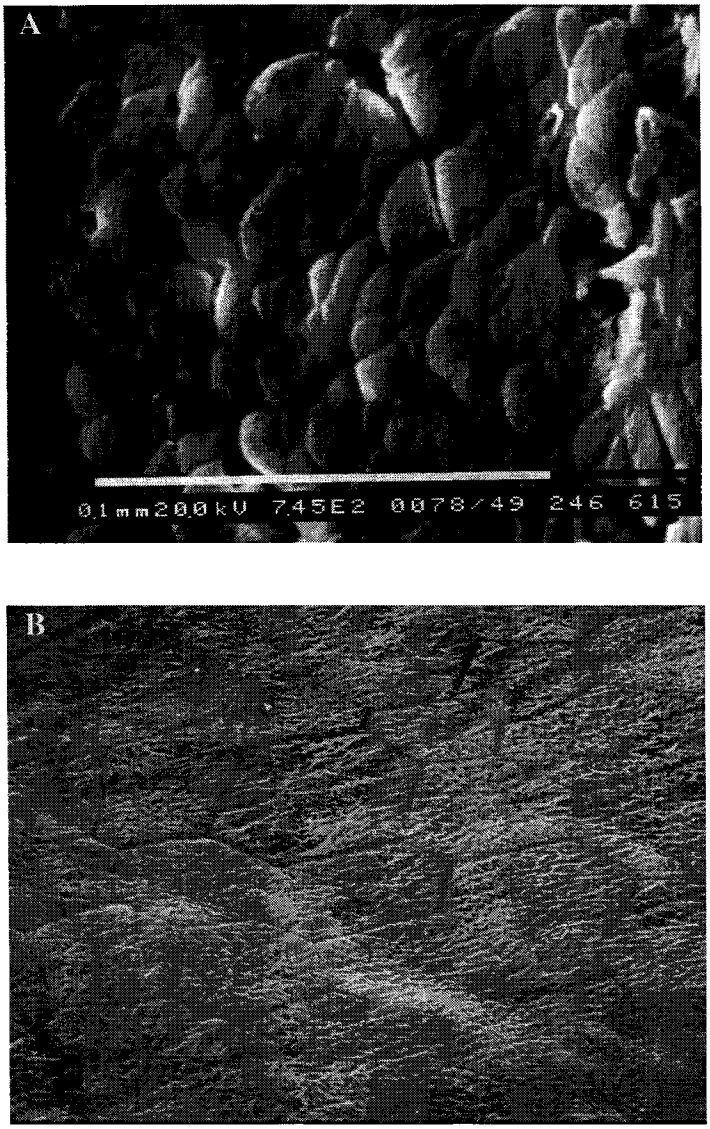

Figure 3-9. Scanning electron micrographs of the surface of the urinary bladders. (A) a bladder epithelium from a female F344 rat treated with 100 μg/g iAs^V for 8 weeks showing piling up of round cells indicative of hyperplasia. X745; (B) a normal urinary bladder from a female control F344 rat showing large, flat polygonal cells on the surface. X406.

3.4 Discussion and conclusions

It has been shown that arsenic significantly accumulated in the RBC of rats (elevated levels) in the form of rHb complexed with DMA^{III}, regardless of whether the rats were treated with iAs^{V}, MMA^{V}, or DMA^{V}. The presence of a rHb-DMA^{III} complex as the predominant arsenic species in rat RBC is probably because of the combination of rapid methylation of arsenic species (30) and strong binding of DMA^{III} to rHb (Chapter 2). iAs^{V} undergoes biomethylation that involves alternate steps of two-electron reduction of pentavalent arsenic to trivalent arsenic followed by oxidative methylation of the trivalent arsenic (57). The reactive trivalent arsenic metabolites include iAs^{III}, MMA^{III}, and DMA^{III}. MMA^{V} can be metabolized in rats to form MMA^{III}, DMA^{V}, DMA^{III}, and trimethylarsine oxide ($TMAO^{V}$). Although MMA^{III} is an intermediate reactive metabolite that can be formed in rats treated with iAs^{V} and MMA^{V}, any rHb-bound MMA^{III} in the rat blood was not observed (Figures 3-4 and 3-6). The absence of a rHb-MMA^{III} complex in the rats is probably due to the lower affinity of rHb for MMA^{III} than for DMA^{III} (5 times lower) (Chapter 2). An alternative explanation is that MMA^{III} is rapidly metabolized further to DMA^{V}, DMA^{III}, and $TMAO^{V}$ in the liver and kidneys of rats — the major organs for arsenic metabolism — before it is fluxed into the blood stream. Likewise, a rHb-iAs^{III} complex in the rat blood was not observed although iAs^{III} can be formed in the iAs^{V}-treated rats. *In vitro*, the binding affinity of iAs^{III} for rat Hb is 20 and 95 times lower than for MMA^{III} and DMA^{III}, respectively (Chapter 2). In rats, iAs^{III} undergoes further methylation to MMA^{V}, MMA^{III}, DMA^{V}, DMA^{III}, and $TMAO^{V}$. Therefore, whether the rats were treated with iAs^{V}, MMA^{V}, or DMA^{V}, the common reactive trivalent arsenic end metabolite was DMA^{III}, which bound to the Hb of the rats.

Much recent research has focused on the carcinogenic effects of DMA^{III} and DMA^{V} (20, 21, 58). DMA^{III} can generate free radicals; such reactive oxygen species (ROS) can cause oxidative stress *in vivo* (36, 39, 40, 43, 59-61). DMA^{III} has also been shown to be an indirect genotoxic agent (62-64). Possible forms of DNA damage caused by DMA^{III} include the formation of single strand DNA breaks, oxidative base damage of DNA, DNA-protein crosslinks, and chromosomal aberrations. In addition, the binding of trivalent arsenicals to sulfhydryl groups of proteins could significantly alter cellular processes and/or lead to cytotoxicity and cell death. Therefore, the characterization of DMA^{III} binding to Hb *in vivo* is biochemically and toxicologically significant, although the fate of the Hb-DMA^{III} complex in blood needs further study. Because the binding of DMA^{III} to Hb stabilizes DMA^{III}, the Hb-DMA^{III} complex may serve as a reservoir that gradually releases DMA^{III} as the RBC regenerate.

Chronic exposure to high levels of arsenic could lead to binding site saturation, such as those observed during the 8–10 weeks of rat treatment, leading to serious health effects. Among the rats treated with three pentavalent arsenic species, the iAs^{V}-treated group (with the highest arsenic concentration) showed the highest protein-bound arsenic and earliest saturation in RBC (Figure 3-1B). Hyperplasia of the bladder urothelium of iAs^{V}-treated rats developed as early as 1 week after the start of exposure as observed by light microscopy (Table 3-4). This is the first report of rat bladder urothelial proliferation produced by iAs^{V} administration. DMA^{V} has previously been demonstrated to produce similar bladder changes in rats at doses of 40 and 100 μg/g in the diet. MMA^{V} has generally not shown effects on the bladder in such studies (22, 65) although mild hyperplasia has been reported in rats administered 50 and 200 μg/g MMA^{V} in a two-year

bioassay (66). Additional studies are necessary to confirm these findings. Nonetheless, the results here suggest a correlation between protein-bound arsenic and bladder hyperplasia in rats.

The binding of DMA^{III} to Hb may also change arsenic metabolism and the profiles of free arsenic distribution because it changes the biologically available dose and the kinetic properties of the accumulation and excretion of arsenic. It may play an important role in the toxicokinetics and toxicodynamics of arsenic. The significant interception of DMA^{III} by rHb may potentially protect the cells from oxidative stress by reducing the available free DMA^{III} species in the cells. This would be consistent with the fact that rats are much more resistant and tolerant to acute arsenic toxicity than humans.

Previous reports have documented the accumulation of arsenic in rat blood (30, 31, 67-69). The binding of DMA^{III} to rHb was demonstrated to be responsible for this accumulation in this chapter. The preservation of the protein-bound arsenic species and the direct mass spectrometric measurement provide clear evidence that the reactive trivalent metabolite DMA^{III} is bound to the α chain of rHb. In subsequent investigations, the cys-13 in the α chain of rHb has been identified as the reactive binding site of DMA^{III} (Chapter 4). Cys-13α is present in rHb but not in hHb. This may explain the much weaker binding of hHb to the same trivalent arsenic species. The capacity for arsenic accumulation in the RBC of different animal species may be determined by the difference in the affinity of their Hb.

In conclusion, results from the GFC-ICPMS analysis of the protein-bound and free arsenicals in RBC and plasma (Figures 3-1 to 3-3) indicate that arsenic is predominantly accumulated in RBC. This appears to be due to the higher affinity of rHb

compared to plasma proteins for arsenic species. In rats treated with iAs^V, MMA^V, and DMA^V, the rHb-DMA^{III} complex is the predominant arsenic species in RBC, and is responsible for the accumulation of arsenic in rat blood. This complex species could play an important role in the metabolism of arsenic, the distribution of a biologically effective dose of arsenic, the retention and biochemical interaction of reactive arsenic species, and the overall toxicity of arsenic.

3.5 References

1. IARC (International Agency for Research on Cancer) (1980) *Some Metals and Metallic Compounds*, in *IARC Monographs on the Evaluation of the Carcinogenic Risks to Humans*. World Health Organization, Lyon, France.
2. National Research Council (2001) *Arsenic in the Drinking Water* (update), National Academy Press, Washington, DC.
3. Chen, C. J., Chuang, Y. C., Lin, T. M., and Wu, H. Y. (1985) Malignant neoplasms among residents of a blackfoot disease endemic area in Taiwan — high arsenic artesian well water and cancers. *Cancer Res.* **45**, 5895-5899.
4. Chiou, H-Y., Chiou, S-T., Hsu, Y. H., Chou, Y. L., Tseng, C. H., Wei, M. L., and Chen, C. J. (2001) Incidence of transitional cell carcinoma and arsenic in drinking water: a follow-up of 8,012 residents in an arseniasis-endemic area in northeastern Taiwan. *Am. J. Epidemiol.* **153**, 411-418.
5. Smith, A. H., Goycolea, M., Haque, R., and Biggs, M. L. (1998) Marked increase in bladder and lung cancer mortality in a region of Northern Chile due to arsenic in drinking water. *Am. J. Epidemiol.* **147**, 660-669.

6. Abernathy, C. O., Liu, Y. P., Longfellow, D., Aposhian, H. V., Beck, B. D., Fowler, B. A., Goyer, R. A., Menzer, R., Rossman, T., Thompson, C., and Waalkes, M. (1999) Arsenic: health effects, mechanisms of actions, and research issues. *Environ. Hlth. Perspect.* **107**, 593-597.

7. Chakraborti, D., Rahman, M. M., Paul, K., Chowdhury, U. K., Sengupta, M. K., Lodh, D., Chanda, C. R., Saha, K. C., and Mukherjee, S. C. (2002) Arsenic calamity in the Indian subcontinent — What lessons have been learned? *Talanta* **58**, 3-22.

8. Nordstrom, D. K. (2002) Worldwide occurrences of arsenic in ground water. *Science* **296**, 2143-2145.

9. Chakraborti, D., Sengupta, M. K., Rahman, M. M., Ahamed, S., Chowdhury, U. K., Hossain, M. A., Mukherjee, S. C., Pati, S., Saha, K. C., Dutta, R. N., and Quamruzzaman, Q. (2004) Groundwater arsenic contamination and its health effects in the Ganga-Meghna-Brahmaputra plain. *J. Environ. Monit.* **6**, 74N-83N.

10. Rosen, B. (2002) Biochemistry of arsenic detoxication. *FEBS Lett.* **529**, 86-92.

11. Miller, W. H., Schipper, H. M., Lee, J. S., Singer, J., and Waxma, S. (2002) Mechanisms of action of arsenic trioxide. *Cancer Res.* **62**, 3893-3903.

12. NRC (1999) *Arsenic in the Drinking Water*, National Research Council, National Academy Press, Washington, DC.

13. Kitchin, K. T. (2001) Recent advances in arsenic carcinogenesis: Modes of action, animal model systems, and methylated arsenic metabolites. *Toxicol. Appl. Pharmacol.* **172**, 249-261.

14. Rossman, T. G., Uddin, A. N., Burns, F. J., and Bosland, M. C. (2001) Arsenite is a cocarcinogen with solar ultraviolet radiation for mouse skin: An animal model for arsenic carcinogenesis. *Toxicol. Appl. Pharmacol.* **176**, 64-71.

15. Moser, G. J., Goodwin, R., and Germolec, D. (2002) Carcinogenic studies with arsenical species in female Tg.AC (z-globin-promoted v-Ha-Ras) transgenic mice. *Toxicologist* **66**, 183.

16. Popovicova, J., Moser, G. J., Goldsworthy, T. L., and Tice, R. R. (2000) Carcinogenicity and co-carcinogenicity of sodium arsenate in p53+- male mice. *Toxicologist* **54**, 134.

17. Nishikawa, T., Wanibuchi, H., Ogawa, M., Kinoshita, A., Morimura, K., Hiroi, T., Funae, Y., Kishida, H., Nakae, D., and Fukushima, S. (2002) Promoting effects of monomethylarsonic acid, dimethylarsinic acid and trimethylarsine oxide on induction of rat liver preneoplastic glutathione S-transferase placental form positive foci: A possible reactive oxygen species mechanism. *Int. J. Cancer* **100**, 136-139.

18. Van Gemert, M. and Eldan, M. (1998) Chronic carcinogenicity assessment of cacodylic acid. In: Society for Environmental Geochemistry and Health (SEGH) Third International Conference on Arsenic Exposure and Health Effects, Book of Abstracts, p.113. San Diego, CA, July 12-15.

19. Cohen, S. M., Arnold, L. L., Uzvolgyi, E., St. John, M., Yamamoto, S., Lu, X., and Le, X. C. (2002) Possible role of dimethylarsinous acid in dimethylarsinic acid-induced urothelial toxicity and regeneration in the rat. *Chem. Res. Toxicol.* **15**, 1150-1157.

20. Wei, M., Wanibuchi, H., Yamamoto, S., Li, W., and Fukushima, S. (1999) Urinary bladder carcinogenicity of dimethylarsinic acid in male F344 rats. *Carcinogenesis* **20**, 1873-1876.

21. Wei, M., Wanibuchi, H., Morimura, K., Iwai, S., Yoshida, K., Endo, G., Nakae, D., and Fukushima, S. (2002) Carcinogenicity of dimethylarsinic acid in male F344 rats and genetic alterations in induced urinary bladder tumors. *Carcinogenesis* **23**, 1387-1397.

22. Wanibuchi, H., Salim, E. I., Kinoshita, A., Shen, J., Wei, M., Morimura, K., Yoshida, K., Kuroda, K., Endo, G., and Fukushima, S. (2004) Understanding arsenic carcinogenicity by the use of animal models. *Toxicol. Appl. Pharmacol.* **198**, 366-376.

23. Cohen, S. M., Yamamoto, S., Cano, M., and Arnold, L. L. (2001) Urothelial cytotoxicity and regeneration induced by dimethylarsinic acid in rats. *Toxicol. Sci.* **59**, 68-74.

24. Okina, M., Yoshida, K., Kuroda, K., Wanibuchi, H., Fukushima, S., and Endo, G. (2004) Determination of trivalent methylated arsenicals in rat urine by liquid chromatography-inductively coupled plasma mass spectrometry after solvent extraction. *J. Chromatogr. B* **799**, 209-215.

25. Waalkes, M. P., Liu, J., Chen, H., Xie, Y., Achanzar, W. E., Shou, Y-S, Cheng, M-L, and Diwan, B. A. (2004). Estrogen signaling in livers of male mice with hepatocellular carcinoma induced by exposure to arsenic in utero. *J. Natl. Cancer Inst.* **96**, 466-474.

26. Waalkes, M. P., Ward, J. M., and Diwan, B. A. (2004) Induction of tumors of the liver, lung, ovary and adrenal in adult mice after brief maternal gestational exposure to inorganic arsenic: Promotional effects of postnatal phorbol ester exposure on hepatic and pulmonary, but not dermal cancers. *Carcinogenesis* **25**, 133-141.

27. Mealey, J., Brownell, G. L., and Sweet, W. H. (1959) Radioarsenic in plasma, urine, normal tissue, and intracranial neoplasms. *Arch. Neurol. Psychiatr.* **81**, 310-320.

28. Pomroy, C., Charbonneau, S. M., McCullough, R. S., and Tam, G. K. H. (1980) Human retention studies with ^{74}As. *Toxicol. Appl. Pharmacol.* **53**, 550-556.

29. Odanaka, Y., Matano, O., and Goto, S. (1980) Biomethylation of inorganic arsenic by the rat and some laboratory animals. *Bull. Environ. Contam. Toxicol.* **24**, 452-459.

30. Lerman, S. A., and Clarkson, T. W. (1983) The metabolism of arsenite and arsenate by the rat. *Fundam. Appl. Toxicol.* **3**, 309-314.

31. Lerman, S. A., Clarkson, T. W., and Gerson, R. J. (1983) Arsenic uptake and metabolism by liver cells is dependent on arsenic oxidation state. *Chem.-Biol. Interact.* **45**, 401-406.

32. Styblo, M., Del Razo, L. M., LeCluyse, E. L., Hamilton, G. A., Wang, C., Cullen, W. R., and Thomas, D. J. (1999) Metabolism of arsenic in primary cultures of human and rat hepatocytes. *Chem. Res. Toxicol.* **12**, 560-565.

33. Winski, S. L. and Carter, D. E. (1995) Interactions of rat red blood cell sulfhydryls with arsenate and arenite. *J. Toxicol. Environ. Health* **46**, 379-397.

34. Delnomdedieu, M., Basti, M. M., Styblo, M., Otvos, J. D., and Thomas, D. J. (1994) Complexation of arsenic species in rabbit erythrocytes. *Chem. Res. Toxicol.* **7**, 621-627.

35. Basu, A., Mahata, J., Gupta, S., and Giri, A. K. (2001) Genetic toxicology of a paradoxical human carcinogen, arsenic: a review. *Mutat. Res.* **488**, 171-194.

36. Kitchin, K. T. and Ahmad, S. (2003) Oxidative stress as a possible mode of action for arsenic carcinogenesis. *Toxicol. Lett.* **137**, 3-13.

37. Rossman, T. G. (2003) Mechanism of arsenic carcinogenesis: an integrated approach. *Mutat. Res.* **533**, 37-65.

38. Mass, M. J., Tennant, A., Roop, B. C., Cullen, W. R., Styblo, M., Thomas, D. J., and Kligerman, A. D. (2001) Methylated trivalent arsenic species are genotoxic. *Chem. Res. Toxicol.* **14,** 355-361.

39. Nesnow, S., Roop, B. C., Lambert, G., Kadiiska, M., Mason, R. P., Cullen, W. R., and Mass, M. J. (2002) DNA damage induced by methylated trivalent arsenicals is mediated by reactive oxygen species. *Chem. Res. Toxicol.* **15**, 1627-1634.

40. Ahmad, S., Kitchin, K.T., and Cullen, W. R. (2002) Plasmid DNA damage caused by methlated arenicals ascorbic acid and human liver ferritin. *Toxicol. Lett.* **133**, 47-57.

41. Kato, K., Yamanaka, K., Hasegawa, A., and Okada, S. (2003) Active arsenic species produced by GSH-dependent reduction of dimethylarsinic acid cause micronuclei formation in peripheral reticulocytes of mice. *Mutat. Res.* **539**, 55-63.

42. Kligerman, A. D., Doerr, C. L., Tenant, A. H., Harrington-Brock, K., Allen, J. W., Winkfield, E., Poorman-Allen, P., Kundu, B., Funasaka, K., Roop, B. C., Mass, M.

J., and DeMarini, D. M. (2003) Methylated trivalent arsenicals as candidate ultimate genotoxic forms of arsenic: Induction of chromosomal mutations but not gene mutations. *Environ. Mol. Mutagen.* **42**, 192-205.

43. Liu, S. X., Athar, M., Lippai, I., Waldren, C., and Hei, T. K. (2001) Induction of oxyradicals by arsenic: Implication for mechanism of genotoxicity. *Proc. Natl. Acad. Sci. USA* **98**, 1643-1648.

44. Liu, S. X., Davidson, M. M., Tang, X., Walker, W. F., Athar, M., Ivanov, V., and Hei, T. K. (2005) Mitochondreal damage mediates genotoxicity of arsenic in mammalian cells. *Cancer Res.* **65**, 3236-3242.

45. Schwerdtle, T., Walter, I., and Hartwig, A. (2003) Arsenite and its biomethylated metabolites interfere with the formation and repair of stable BPDE-induced DNA adducts in hman cells and impair XPAzf and Fpg. *DNA Repair* **2**, 1449-1463.

46. Aposhian, H. V., Zakharyan, R. A., Avram, M. D., Kopplin, M. J., and Wollenberg, M. L. (2003) Oxidation and detoxification of trivalent arsenic species. *Toxicol. Appl. Pharmacol.* **193,** 1-8.

47. Styblo, M., Del Razo, L. M., Vega, L., Germolec, D. R., LeCluyse, E. L., Hamilton, G. A., Reed, W., Wang, C., Cullen, W. R., and Thomas, D. J. (2000) Comparative toxicity of trivalent and pentavalent inorganic and methylated arsenicals in rat and human cells. *Arch. Toxicol.* **74**, 289-299.

48. Schuliga, M., Chouchane, S., and Snow, E. T. (2002) Upregulation of glutathione-related genes and enzyme activities in cultured human cells by sublethal concentrations of inorganic arsenic. *Toxicol. Sci.* **70**, 183-192.

49. Chang, K. N., Lee, T. C., Tam, M. F., Chen, Y. C., Lee, L. W., Lee, S. Y., Lin, P. J., and Huang, R. N. (2003) Identification of galectin I and thioredoxin peroxidase II as two arsenic-binding proteins in Chinese hamster ovary cells. *Biochem. J.* **371**, 495-503.

50. Cohen, S. M., Fisher, M. J., Sakata, T., Cano, M., Schoenig, G. P., Chappel, C. I., and Garland, E. M. (1990) Comparative analysis of the proliferative response to the rat urinary bladder to sodium saccharin by light and scanning electron microscopy and autoradiography. *Scan. Microsc.* **4**, 135-142.

51. Cohen, S. M. (1983) Pathology of experimental bladder cancer in rodents. In: S. M. Cohen and G. T. Bryan (eds.), *The Pathology of Bladder Cancer.* CRC Press, Boca Raton, vol. II, 1-40.

52. Le, X.C., Lu, X., Ma, M., Cullen, W.R., Aposhian, H. V., and Zheng, B. (2000) Speciation of Key Arsenic Metabolic Intermediates in Human Urine. *Anal. Chem.* **72**, 5172-5177.

53. Le, X.C., Lu, X., and Li, X.-F. (2004) Arsenic speciation. *Anal. Chem.* **76**, 27A-33A.

54. Drabkin, D.L. and Austin, J.H. (1935) Spectrophotometric studies. II. Preparations from washed blood cells; nitric oxide hemoglobin and sulfhemoglobin. *J. Biol. Chem.* **112,** 51.

55. Cornish-Bowden, A. (1995) *Fundamentals of Enzyme Kinetics.* Portland Press, London.

56. Gong, Z., Lu, X., Cullen, W. R., and Le, X.C. (2001) Unstable trivalent arsenic metabolites, monomethylarsonous acid and dimethylarsinous acid. *J. Anal. At. Spectrom.* **16**, 1409-1413.

57. Challenger, F. (1945) Biological methylation. *Chem. Rev.* **36**, 315-361.

58. Arnold, L. L., Cano, M., Margaret, St J., Eldan, M., van Gemert, M., and Cohen, S.M. (1999) Effects of dietary dimethylarsinc acid on the urine and urothelium of rats. *Carcinogenesis* **20**, 2171-2179.

59. Ahmad, S., Kitchin, K.T., and Cullen, W. R. (2000) Arsenic species that cause release of iron from ferritin and generation of activated oxygen. *Arch. Biochem. Biophys.* **382**, 195-202.

60. Florea, A.M., Yamoah, E.N., and Dopp, E. (2005) Intracellular calcium disturbances induced by arsenic and its methylated derivatives in relation to genomic damage and apoptosis indction. *Environ. Health Perspective.* **113**, 659-664.

61. Felix, K., Manna, S. K., Wise, K., Barr, J., and Ramesh, G. T. (2005) Low levels of arsenite activates nuclear factor-kappa B and activator protein-1 in immortalized mesencephalic cells. *J. Biochem. Mol. Toxicol.* **19**, 67-77.

62. Sordo, M., Herrera, L.A., Ostrosky-Wegman, P., and Rojas, E. (2001) Cytotoxic and genotoxic effects of As, MMA, and DMA on leukocytes and stimulated human lymphocytes. *Teratog. Carcinog. Mutagen* **21**, 249-260.

63. Schwerdlt, T., Walter, I., Mackiw, I., and Hartwig, A. (2003) Induction of oxidative DNA damage by arsenite and its trivalent and pentavalent methylated metabolites in cultured human cells and isolated DNA. *Carcinogenesis* **24**, 967-974.

64. Dopp, E., Hartmann, L.M., Florea, A.M., von Rechlinghausen, U., Pieper, R., and Shokouhi, B (2004) Uptake of inorganic and organic derivatives of arsenic associated with induced cytotoxic and genotoxic effect in Chinese hamster ovary (CHO) cells. *Toxicol. Appl. Pharmacol.* **201**, 156-165.

65. Shen, J., Wanibuchi, H., Waalkes, M. P., Salim, E. I., Kinoshita, A., Yoshida, K., Endo, G., and Fukushima, S. (2005) A comparative study of the sub-chronic toxic effects of three organic arsenical compounds on the urothelium in F344 rats; gender-based differences in response. *Toxicol. Appl. Pharmacol.* In press.

66. Shen, J., Wanibuchi, H., Salim, E.I., Wei, M., Doi, K., Yoshida, K., Endo, G., Morimura, K., and Fukushima, S. (2003) Induction of glutathione *S*-transferase placental form positive foci in liver and epithelial hyperplasia in urinary bladder, but no tumor development in male Fischer 344 rats treated with monomethylarsonic acid for 104 weeks. *Toxicol. Appl. Pharmacol.* **193**, 335-345.

67. Hunter, F. T., Kip, A. F., and Irvine, J.W. (1942) Radioactive tracer studies on arsenic injected as potassium arsenate. I. excretion and localization in tissues. *J. Pharmacol. Exp. Ther.* **76**, 207-220.

68. Lanz, H., Wallace, P. C., and Hamilton, J. G. (1950) The metabolism of arsenic in laboratory animals using As^{74} as a tracer. *Univ. of Calif. Publis. In Pharmacol.* **2**, 263-282.

69. Fuentes, N., Zambrano, F., and Rosenmann, M. (1981) Arsenic contamination: metabolic effects and localization in rats. *Comp. Biochem. Physiol.* **70C**, 269-272.

Chapter 4 Identification of a Highly Reactive Cysteine-13 Residue in the α Chain of Rat Hemoglobin by Collision Activated Dissociation/Tandem Mass Spectrometry

4.1 Introduction

The binding of ligand to proteins is crucial for the conformation, function, and activity of many proteins. For example, many enzymes are metal-containing proteins or require cofactors to function properly (1-4). The importance of protein-ligand binding has led to the continued development of a wide range of techniques to study the binding affinity and stoichiometry, and the specific binding sites (5-9). Tremendous advances have been made in recent years in the area of mass spectrometry (MS) (10, 11), making studies of proteomes possible.

While the identification and characterization of proteins have been the primary focus in many recent proteomics studies (10-13), locating the specific protein binding sites is also an important issue since it is an essential step toward understanding the properties and functions of proteins that are of particular interest to biologists (10). However, it is far more challenging due to the complexity arising from numerous protein modifications, including diverse post-translational modifications (>200 types) (10, 14), and endogenous and exogenous substrates bindings. Most previous work used enzyme digestion of proteins before using mass spectrometry to identify the binding sites of protein modifications (10, 11, 15-18). These approaches, however, are not suitable for

labile covalent bindings and low affinity non-covalent bindings due to breakdown of the protein's native conformation or incompatible enzymatic digestion conditions.

Recent advances in top-down MS techniques may provide promising methods for identification of protein modifications, by direct fragmentation of intact proteins in the gas phase without the need of prior enzymatic digestion (14, 19-23), particularly infrared multi-photon dissociation (IRMPD) and electron capture dissociation (ECD) developed for FT-ICRMS. The main advantages include potential 100% sequence coverage and improved identification of post-translational modifications (14, 20, 21, 23). These approaches require the use of large, expensive FT-ICRMS instruments, which limits their wide application.

A common gas-phase fragmentation technique, collision-activated dissociation (CAD), which is able to couple with mass spectrometry, has been widely applied in sequencing of biopolymers such as peptides, oligonucleotides, and oligosaccharides, and identification of binding site in these biopolymers and other small molecules (18, 22, 24-29). However, it has limited capability for direct identification and characterization of a large protein. It is difficult to generate enough ions to cover the whole protein. It becomes more difficult as the size of proteins become larger. On the other side, there is serious overlapping of mass clusters of fragment ions in the low mass to charge range. The common atoms normally present in proteins, ^{12}C (12.0000), ^{1}H (1.0078), ^{14}N (14.0031), ^{16}O (15.9949), and ^{32}S (31.9721), have very small values of mass defect from the unit mass (ranging from -0.005 to 0.007 except -0.028 for ^{32}S). Therefore, protein fragments from different amino acid compositions but with the same nominal mass cannot be easily resolved by the common CAD MS/MS. For example, CAD fragmentation of the α unit of

rat hemoglobin (rHb) can theoretically produce up to 380 peaks that are distributed within a window of 100 mass units (m/z range of 300-400) (Figure 4-1). Therefore, there is more than one peak (up to 12 peaks) at most nominal mass. The overlap becomes more serious with increasing protein mass. For very large protein (over 1 million Da), it is very difficult to resolve mass fragments even using the highest resolution MS currently available due to the complexity of the fragment ions.

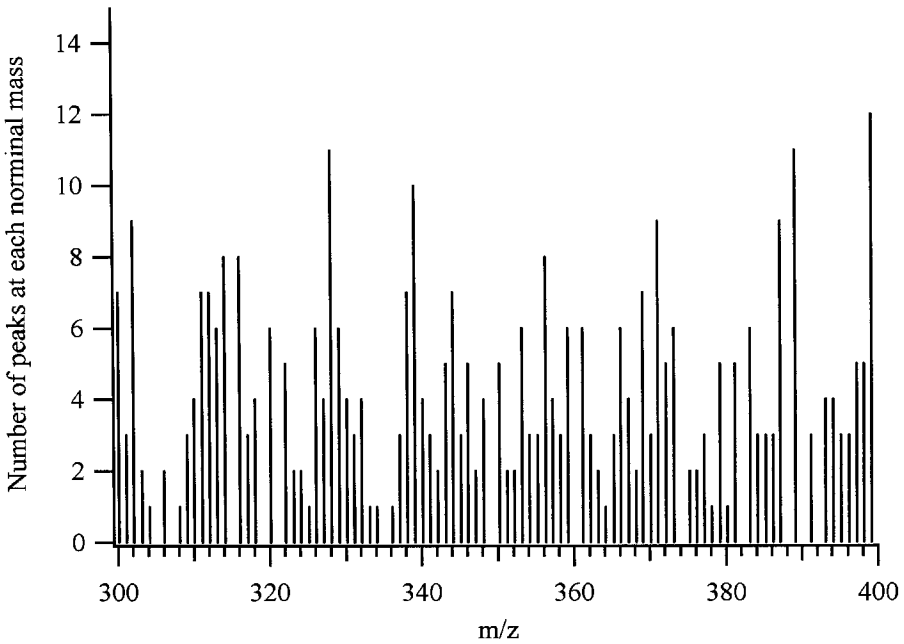

Figure 4-1. Possible fragment ions generated from CAD MS/MS of the rat hemoglobin α unit by theoretical calculation. The possible fragment ions were generated using the sequence database searching programs-MS Product (http://prospector.ucsf.edu/). The number of fragment ions with the same nominal mass were then calculated, and plotted against the nominal mass at every amu in the range of 300-400. The left axis represents the number of peaks that would appear at each nominal mass.

To overcome this limitation, I have developed a stable arsenic labeling technique for identification of protein binding site using CAD MS/MS. Arsenic has a single isotope of non-integer value (74.9216 amu) with mass defect of -0.0784 amu, which is distinct from the mass defect of the commonly present atoms in the protein. The labeling of arsenic to the protein increases the negative mass defect, and shifts the labeled fragment ions away from the unlabeled fragment ions. The unique arsenic signature allows easy and fast identification of the specific arsenic-labeled fragment ions (internal and immonium ions) from a large number of other fragment ions that are usually serious overlapped. The arsenic-sulfur bond is very stable in the gas phase, therefore, it can survive collision activated fragmentation in the gas phase, which preserves the sequence information.

To demonstrate the proof of principle, I present here the identification of a highly reactive cysteine residue in the α chain of rHb that preferentially binds to dimethylarsinous acid (DMA^{III}).

4.2 Materials and Methods

4.2.1 Materials

Iododimethylarsine [$(CH_3)_2AsI$] was synthesized according to the previous procedure (30, 31) in Dr. W. R. Cullen's laboratory at the University of British Columbia, and was kept at -20 °C. A dilute solution of the precursor was freshly prepared using deionized water in which it was spontaneously hydrolyzed to dimethylarsinous acid (DMA^{III}, $(CH_3)_2AsOH$). Other materials are the same as those in Sections 2.2.1 and 3.2.1.

4.2.2 Red blood cells (RBC) samples of rats

Rat treatment procedures were carried out by Dr. S. Cohen and Ms. L. Arnold at University of Nebraska Medical Centre, and the protocols were reviewed and approved by the Institutional Animal Care and Use Committee of the University of Nebraska Medical Center. Rats were given a basal diet (control) or arsenic supplemented diet or drinking water for 1, 2, 6, 8, 10, and 15 weeks, as described in Section 3.2.2. The data presented in this chapter are from the rats treated with 100 μg/g inorganic arsenate (iAs^V) in drinking water for 8 weeks. At the end of treatment period, equal number of control and treated rats were sacrificed, and blood samples were collected. RBC were separated from plasma by centrifugation at 3200 rpm at 4 °C for 10 min.

4.2.3 Mass spectrometry identification of Hb-arsenic complex in rat RBC

A QSTAR Pulsar i mass spectrometer (Applied Biosystems/MDS Sciex, Concord, Ontario, Canada) equipped with a nanoelectrospray ionization (nanoESI) source (Protana, Denmark) was used to analyze the Hb complex of arsenic in rat RBC, as described in Section 2.2.2.2.

RBC samples from rats with or without exposure to arsenic were first lysed, as described in Section 2.2.2.3. The resultant lysates were then analyzed by nanoESI-MS. The preparation of RBC lysate for nanoelectrospray and the parameters for nanoESI-MS analysis were the same as those in Sections 3.2.5 and 2.2.2.2, respectively.

4.2.4 CAD MS/MS analysis of protein complex

The second quadrupole in the QSTAR system was used to select the protein and its complex as parent ions, and the third quadrupole was used as a collision-activated dissociation (CAD) cell. Collision energy was 110 eV, and the flow rate of collision gas was set at 6 (relative value). In MS/MS mode, the instrument was calibrated by the synthesized peptides as shown in Section 4.2.6.

4.2.5 MS and MS/MS analysis of the *in vitro* complex between rHb with excess DMA^{III}

rHb was first extracted from RBC of control rats by lysis of the RBC as described in Section 2.2.2.3. The rHb concentration in the lysate was measured by Drabkin's method (32). The lysate was then mixed with 100-fold molar excess of DMA^{III} in 20 mM ammonium acetate buffer (pH 7.0) at room temperature for 1 hour. The resultant solution was subjected to BioSpin-6 column to remove the salt and free DMA^{III}. The filtrate was then loaded onto a capillary tip for nanoESI-MS and MS/MS analysis. The experimental conditions were the same as those for the *in vivo* formed rHb-DMA^{III} complex except that rat Hbα-$(DMA^{III})_3$ complex was selected as the parent ion.

4.2.6 Synthetic peptides

Three cysteine-containing peptides with sequences adapted from the α unit of rHb (Scheme 4-1) were synthesized at the Alberta Peptide Institute (Edmonton, AB). The peptides were then purified by HPLC with the purity of greater than 95%. The molecular

weights of these peptides were determined by electrospray mass spectrometry with a relative standard deviation from the theoretical values of less than 0.01%. The sequences of the peptides were also determined using a HP G1005A protein sequencer.

rHbα:

P1

1 VLSADDKT**NI KNCWGKI**GGH GGEYGEEALQ RMFAAFPTTK
13

41 TYFSHIDVSP GSAQVKAHGK KVADALAKAA DHVEDLPGAL

P2 111

81 STLSDLHAHK LRVDPVNFK**F LSHCLLVTLA CHHPG**DFTPA
104 P3

121 MHASLDKFLA SVSTVLTSKY R

Peptide synthesis:

P1: NH_2-**NIKNCWGKI**-COOH (cys-13 α)

P2: NH_2-**FLSHCLLVT**-COOH (cys-104 α)

P3: NH_2-**VTLACHHPG**-COOH (cys-111 α)

Scheme 4-1. Sequences of rat hemoglobin α chain and the synthesized peptides.

4.2.7 MS and MS/MS analysis of peptide-DMA^{III} complex

The synthesized peptides (5 μM) were prepared in aqueous solution (1 mM ammonium acetate, pH 7.0), and incubated with excess DMA^{III} (100 times more concentrated than the peptides) at room temperature for 1 hour. The reaction solution was

then subjected to mass spectrometric analysis and CAD MS/MS analysis. The parameters for MS and MS/MS analysis using the QSTAR system were the same as that for analysis of rat RBC lysates with the exception of the scanning range (100–1500), collision energy (30–60 eV), and collision gas flow rate (CAD of 5).

4.3 Results

4.3.1 Identification of the highly reactive binding site in rat Hb

As shown in Chapter 3, regardless whether rats were fed with iAs^V, MMA^V, or DMA^V, the rats were able to metabolize these arsenic species to dimethylarsinous acid (DMA^{III}) and accumulate DMA^{III} in their red blood cells in the form of Hb-DMA^{III} complex. Hb tetramers consist of two α and two β units. Mass spectrometry showed that DMA^{III} was bound to the α chain but not to the β chain (Figure 3-4 in Chapter 3).This is an interesting finding, and the reasons for this preferential binding were not known. Therefore, I have carried out additional experiments to identify if there is a highly reactive binding site in the α chain of rat Hb.

4.3.2 Identification of the targeting amino acid residues

To identify the binding sites of DMA^{III} in rHb, DMA^{III} was first shown to selectively bind to cysteine residues in the protein. Figure 4-2 shows the multicharged nanoESI-MS spectra from the analyses of RBC lysates of a control rat and a rat fed iAs^V in drinking water. The α and β units of rat Hb are observed from the samples of both the

control and treated rats. The main difference between the two spectra is the series of peaks corresponding to $(\alpha+104)^{n+}$ (n=9, 10, and 11) from the arsenic-treated rats. For example, the ion at m/z 1758.0 in the bottom spectrum from the control rat is the α unit of rat Hb with the heme group intact $[(\alpha^h)^{9+}]$. The corresponding ion in the top spectrum from the iAs^V-treated rat is at m/z 1769.6. The difference in m/z between these two species (1769.6-1758.0), suggests that the ion at 1769.6 corresponds to $(\alpha^h+104)^{9+}$. This distinct mass spectral feature is consistently observed from 90 rats that were fed arsenic species compared to 30 control rats. The mass shift of 104 is due to the binding of DMA^{III} $[(CH_3)_2AsOH$, FW 122], with the loss of a H_2O molecule, as it has been discussed in Chapter 2.

Figure 4-3 demonstrates CAD MS/MS analysis of the *in vivo* rHbα-DMA^{III} complex from the treated rat and the rHbα from the control rat. Two characteristic fragment ions with the corresponding masses of 136.942 Da and 179.978 Da were observed from the rHbα-DMA^{III} complex (dashed trace in Figure 4-3), but were absent from the rHbα chain without the DMA^{III} complex (solid trace in Figure 4-3). These two fragment ions are associated with the DMA^{III}-tagged cysteine residue. Their structures and molecular weights are illustrated in Scheme 4-2. No DMA^{III}-tagged immonium ions of other amino acids were observed. Fragment of the parent ions at other charge states showed the same characteristic ions. The results indicate that DMA^{III} is selectively bound to cysteine residue.

The results of DMA^{III} binding to a cysteine residue were further confirmed by examining the fragment ions of DMA^{III} complexes with cysteine and glutathione (GSH, a cysteine-containing tripeptide). The expected fragment ion of 136.94 Da was observed

from CAD MS/MS analysis of DMA^{III} complex of cysteine (Figure 4-4). This suggests the binding of the dimethyl arsenical to the sulfur atom of cysteine, as shown in Scheme 4-2. Both characteristic fragment ions (136.94 and 179.98) were observed from CAD MS/MS analysis of the DMA^{III} complex of GSH (Figure 4-5). The formation of the second fragment ion (immonium ion: 179.98) requires the breakage of the neighboring peptide bond as shown in Scheme 4-2. The results in Figures 4-3, 4-4, and 4-5 confirm that DMA^{III} is selectively bound to a cysteine residue in the rHbα by forming an arsenic-sulfur bond.

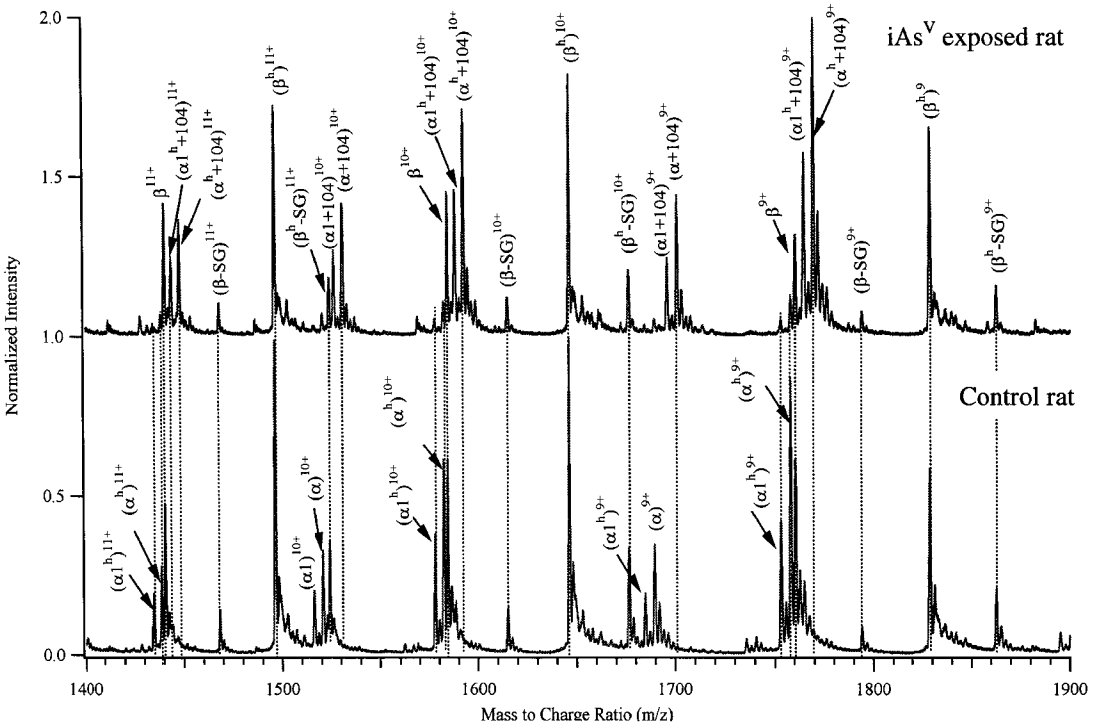

Figure 4-2. Multiply-charged nanoESI-MS spectra of the RBC lysates from rats with and without exposure to iAs^V showing that DMA^{III} is specifically bound to rHbα, forming a complex with stoichiometry of 1:1. The preparation for nanoelectrospray solution and other detailed MS and MS/MS conditions are described in Section 4.2.3.

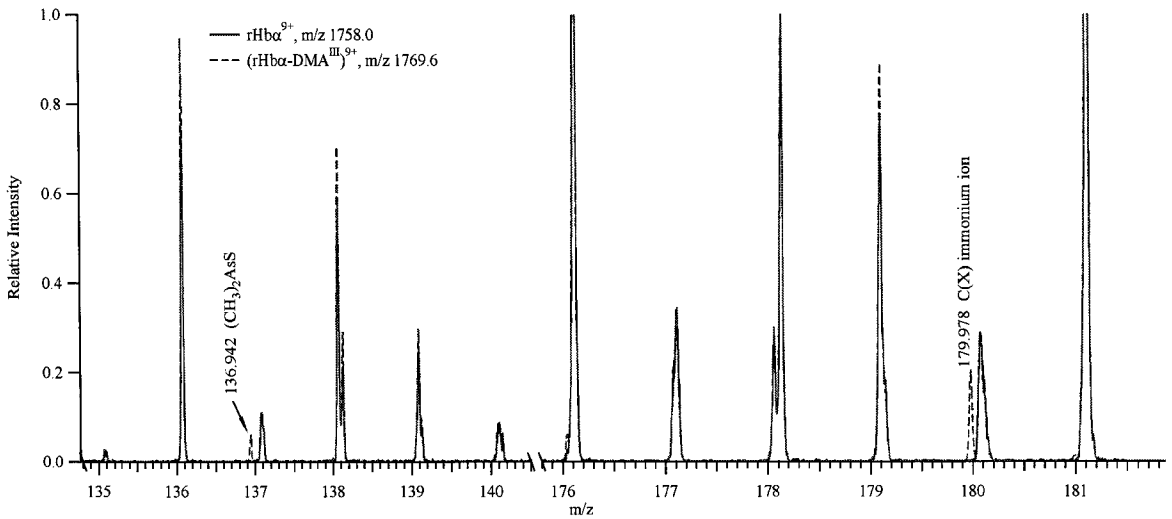

Figure 4-3. Comparison of the CAD MS/MS spectra of the parent ions of the rHbα-DMA^{III} complex (m/z=1769.6, 9^+) and rHbα (m/z=1758.0, 9^+) showing that two characteristic ions with amu of 136.942 and 179.978 are uniquely present in the MS/MS spectrum of the rat Hbα-DMA^{III} complex. This suggests that DMA^{III} is selectively bound to the cysteine residue in rHb. For MS/MS analysis, the collision energy (CE) was 110 eV, and the CAD gas setting was 6. The m/z range for monitoring was 130-210. The preparation for the nanoelectrospray solution and other detailed MS and MS/MS conditions were described in Sections 4.2.3.and 4.2.4.

(A).

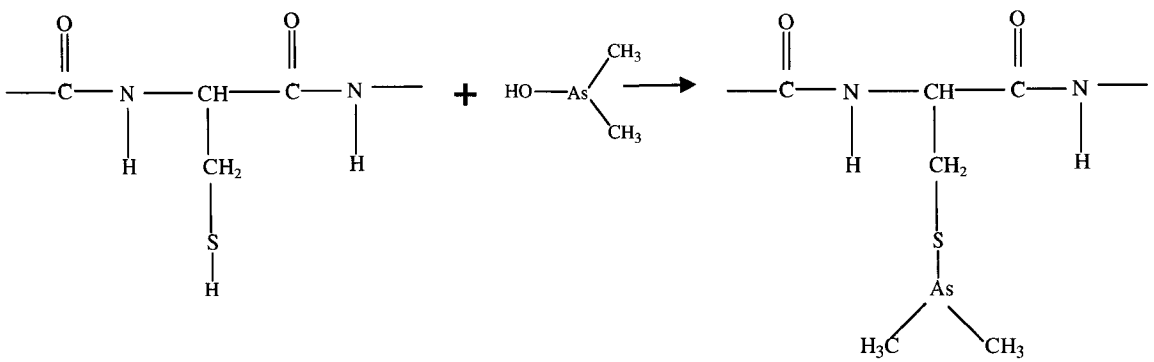

(B).

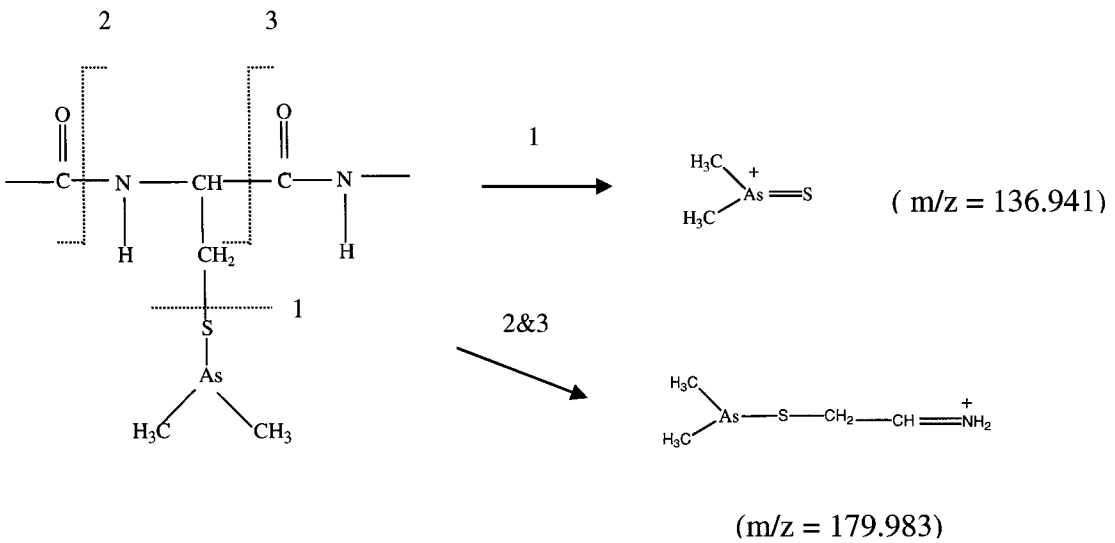

Scheme 4-2. Generation of the characteristic fragment ions under collision-activated dissociation of the DMA^{III}-cysteine complex in a single amino acid residue.

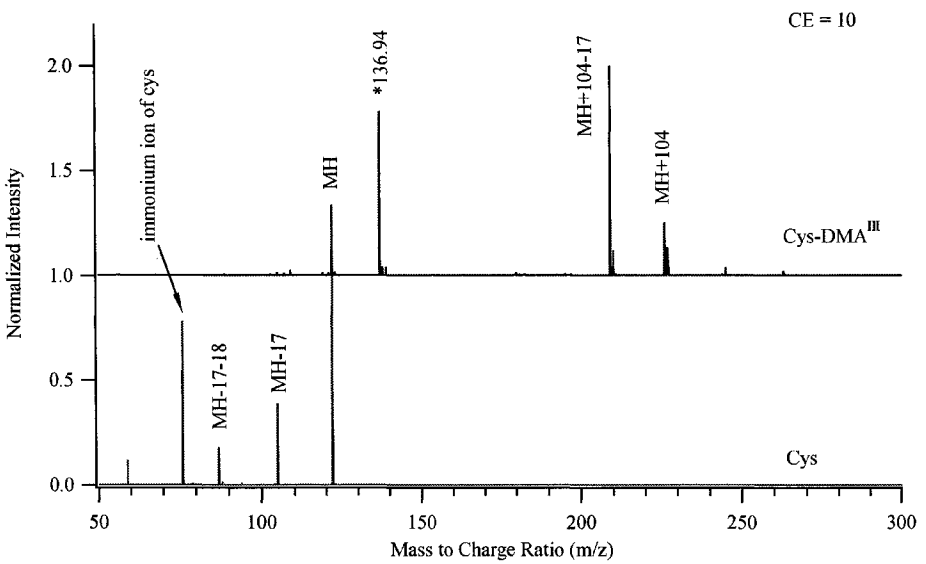

Figure 4-4. MS/MS spectra of the cysteine-DMA^{III} complex. Ten times molar excess DMA^{III} was incubated with cysteine in 1 mM ammonium acetate buffer (pH 7.0) for 30 min. The reaction solution was then diluted 10 times by methanol, formic acid, and water to final concentrations of 50% methanol, 0.1% formic acid, and cysteine 5μM. The electrospray conditions were the same as those for the protein complex in Sections 4.2.3 and 4.2.4 except for the collision energy of 10 eV, and the CAD setting of 5.

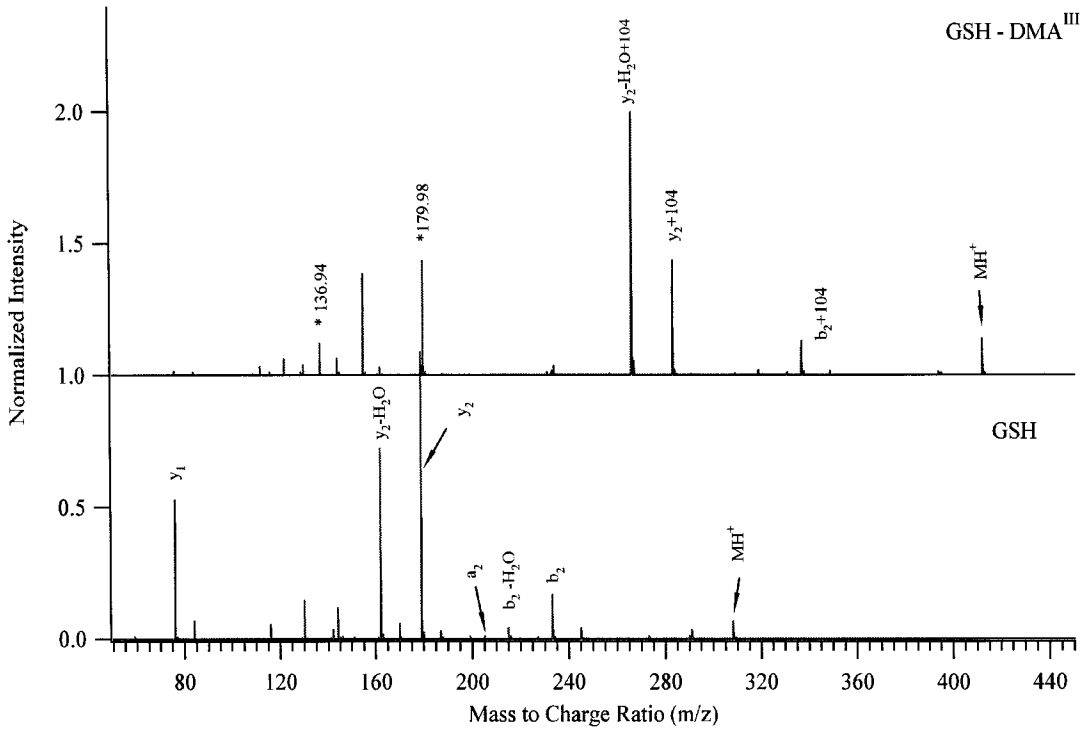

Figure 4-5. MS/MS spectra of the GSH-DMA^{III} complex. Ten times molar excess DMA^{III} was incubated with GSH in 1 mM ammonium acetate buffer (pH 7.0) for 30 min. The reaction solution was then diluted 10 times by methanol, formic acid, and water to final concentrations of 50% methanol, 0.1% formic acid, and 5μM GSH. The electrospray conditions were the same as those for the protein complex in Sections 4.2.3 and 4.2.4 except for the collision energy of 20 eV, and the CAD setting of 5.

4.3.3 Identification of the position of DMA^{III} binding in rHb

Although each α unit of the rHb contains three free cysteines and each β unit contains two free cysteines, the MS evidence shows that DMA^{III} binds only to one of the three cysteines in the α chain (Figure 3-4 in Chapter 3). To identify which of these cysteines in the α unit of the rHb is the reactive binding site for DMA^{III}, I have developed a unique MS technique based on arsenic labeling. This technique is used for the direct analysis of RBC samples with no need of enzymatic digestion of the protein.

The principle and approach of this technique is described with rat RBC as an example. Binding of DMA^{III} to rHb leads to an increase of 103.9607 mass unit in the protein, which has a mass defect of -0.0393 from the unit mass. Upon fragmentation, the DMA^{III}-tagged internal ions would provide information specific to the local sequence of each cysteine residue. These ions possess a negative mass shift from the common fragment ions of protein. As an example, the formation of DMA^{III}-tagged internal dipeptide ions is illustrated in Scheme 4-3. For each non-terminal cysteine residue in a protein, there are two possible internal dipeptide ions tagged with DMA^{III} (Scheme 4-3). Their molecular weights are the sum of 189.961 Da (DMA^{III} binding to a cysteine residue) and the molecular weight of the neighboring amino acid. Based on this scheme and combined with the known rHbα sequence, the expected internal dipeptide ion species with the DMA^{III} tag for all three cysteine residues (cys-13, 104 and 111) in the rHbα unit were derived and are listed in Table 4-1. The presence of any pair of internal dipeptide ions with a DMA^{III} tag combined with the absence of other pairs of internal dipeptide ions with a DMA^{III} tag allows the identification of the specific cysteine residue that is

highly reactive to DMA^{III}. The fragmentation analysis of the rHbα unit (without the DMA^{III} complex) under the same conditions can be examined as a negative control. Because small internal ions usually give strong response and better resolution, internal dipeptide ions were chosen as indicators of the binding sites. Larger internal peptide ions with a DMA^{III} tag can be used to further support the identification.

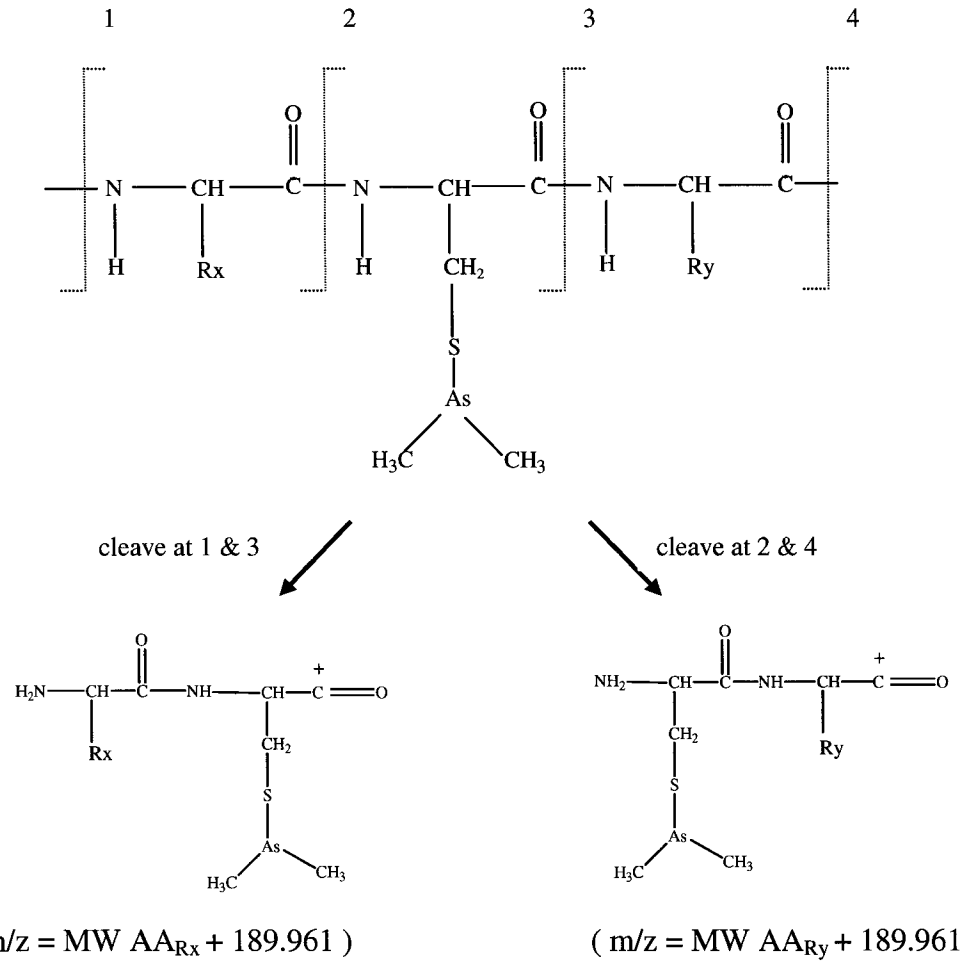

Scheme 4-3. Generation of characteristic internal dipeptide ions with DMA^{III} tag under collision-activated dissociation of the DMA^{III}-protein complex.

Table 4-1. List of major internal ions with a DMA^{III} tag and their expected and measured mass values from MS/MS analysis of DMA^{III} complexes of rHbα unit.

Site	Internal Ions with DMA^{III} tag	Formula	Expected (amu)	Measured *in vivo* complex (1:1)[a]	Measured *in vitro* complex (1:3)[b]	Mass Accuracy (ppm)	
						a	b
cys13 α	NC(X)	$C_9H_{17}N_3O_3SAs$	322.021	322.020	322.024	-3	9
	NC(X) - CO	$C_8H_{17}N_3O_2SAs$	294.026	294.034	294.033	27	24
	NC(X) - NH_3	$C_9H_{14}N_2O_3SAs$	304.994	304.998	305.004	13	33
	NC(X) - CO- NH_3	$C_8H_{14}N_2O_2SAs$	276.999	277.002	277.010	11	40
	C(X)W	$C_{16}H_{21}N_3O_2SAs$	394.057	394.057	394.052	0	-13
	C(X)W - CO	$C_{15}H_{21}N_3OSAs$	366.062	366.066	366.066	11	11
	C(X)W – NH_3	$C_{16}H_{18}N_2O_2SAs$	377.031	377.032	377.037	3	16
	C(X)W - CO– NH_3	$C_{15}H_{18}N_2OSAs$	349.036	349.038	349.041	6	14
	KNC(X)-NH_3	$C_{15}H_{26}N_4O_4SAs$	433.089	433.082	433.078	-16	-25
	C(X)WG	$C_{18}H_{24}N_4O_3SAs$	451.079	451.090	451.058	24	-47
	NC(X)W	$C_{20}H_{27}N_5O_4SAs$	508.100	508.085	508.107	-29	14
	NC(X)W - CO– NH_3	$C_{19}H_{24}N_4O_3SAs$	463.079	463.094	463.078	32	-2
	(KNC(X)WG/ NC(X)WGK)-CO-NH_3	$C_{28}H_{39}N_7O_6SAs$	676.190	676.217	N/D	40	N/A
cys104 α	HC(X)	$C_{11}H_{18}N_4O_2SAs$	345.037	N/D	345.041	N/A	12
	HC(X) - CO	$C_{10}H_{18}N_4OSAs$	317.042	N/D	317.050	N/A	25
	HC(X)- CO– NH_3	$C_{10}H_{15}N_3OSAs$	300.015	N/D	300.025	N/A	33
	C(X)L	$C_{11}H_{22}N_2O_2SAs$	321.062	N/D	321.064	N/A	6
	C(X)L -CO	$C_{10}H_{22}N_2OSAs$	293.067	N/D	293.076	N/A	31
	SHC(X)	$C_{14}H_{23}N_5O_4SAs$	432.069	N/D	432.064	N/A	-12
	HC(X)L	$C_{17}H_{29}N_5O_3SAs$	458.121	N/D	458.120	N/A	-2
cys111 α	AC(X)	$C_8H_{16}N_2O_2SAs$	279.015	N/D	279.024	N/A	32
	AC(X) - CO	$C_7H_{16}N_2OSAs$	251.020	N/D	251.010	N/A	-40
	AC(X) – CO - NH_3	$C_7H_{13}NOSAs$	233.993	N/D	234.009	N/A	68
	C(X)H	$C_{11}H_{18}N_4O_2SAs$	345.037	N/D	345.040	N/A	9
	C(X)H -CO	$C_{10}H_{18}N_4OSAs$	317.042	N/D	317.052	N/A	32
	HC(X)- CO– NH_3	$C_{10}H_{15}N_3OSAs$	300.015	N/D	300.023	N/A	27
	AC(X)H	$C_{14}H_{23}N_5O_3SAs$	416.074	N/D	416.062	N/A	-29
	C(X)HH	$C_{17}H_{25}N_7O_3SAs$	482.096	N/D	482.074	N/A	-46
	AC(X)HH	$C_{20}H_{30}N_8O_4SAs$	553.133	N/D	553.137	N/A	7
	AC(X)HH – CO	$C_{19}H_{30}N_8O_3SAs$	525.138	N/D	525.110	N/A	-53
	LAC(X)HH	$C_{26}H_{41}N_9O_5SAs$	666.217	N/D	666.250	N/A	50

Note: (a) Results on the measured *in vivo* complex were from the analysis of RBC samples of arsenic-treated rats. One DMA^{III} molecule was found to bind with each α unit of rat Hb.

(b) Results on the measured *in vitro* complex were from the analysis of incubation mixtures containing excess DMA^{III} over purified rat Hb. The excess amount of DMA^{III} lead to the binding of three DMA^{III} molecules to a single α unit of rat Hb.

Mass accuracy in the a column is calculated by the relative deviation of the *in vivo* complex (1:1 stoichiometry) from the expected value, and in the b column it is calculated by the relative deviation of the *in vitro* complex (1:3 stoichiometry) from the expected value.

Figure 4-6 shows the CAD MS/MS spectrum of the *in vivo* DMA^{III}-Hbα complex superimposed with that of the Hbα. These were obtained from the analyses of RBC samples from the arsenic-treated rat and the control rat. Two strong internal dipeptide ions of NC and CW with the DMA^{III} tag were observed with corresponding m/z of 322.020 and 394.057 (dashed trace in Figure 4-6). Internal ions with a loss of NH_3 (304.998 and 377.032), CO (294.034 and 366.066), and a simultaneous loss of NH_3 and CO (277.002 and 349.038) were also observed for each internal dipeptide ions containing the DMA^{III} tag (Table 4-1). These same internal dipeptide ions with DMA^{III} tag are absent in the MS/MS spectrum from the analysis of the RBC samples from the control rat (solid trace in Figure 4-6). Since only cys-13α has N and W as the neighboring amino acid residues (as shown in Scheme 4-1), it indicates that DMA^{III} is bound to cys-13α. A number of internal ions of higher molecular weight that contain the cysteine-DMA^{III} tag were also observed from fragmentation analysis of DMA^{III}-Hbα complex. Internal tripeptide ions with DMA^{III} tags were observed with m/z of 433.082, 451.090, and 508.085, corresponding to internal ions of KNC, CWG, and NCW, each with a DMA^{III} tag, respectively. An internal pentapeptide ion of 676.218 amu was also observed, which may result from two possible DMA^{III}-tagged fragments, KNCWG and NCWGK, with a simultaneous loss of CO and NH_3. Fragment of parent ions at other charge states showed the same results. These internal oligopeptide ions with DMA^{III} tags are associated with cys-13α in the protein sequence context, supporting that cys-13α is the *in vivo* reactive binding site.

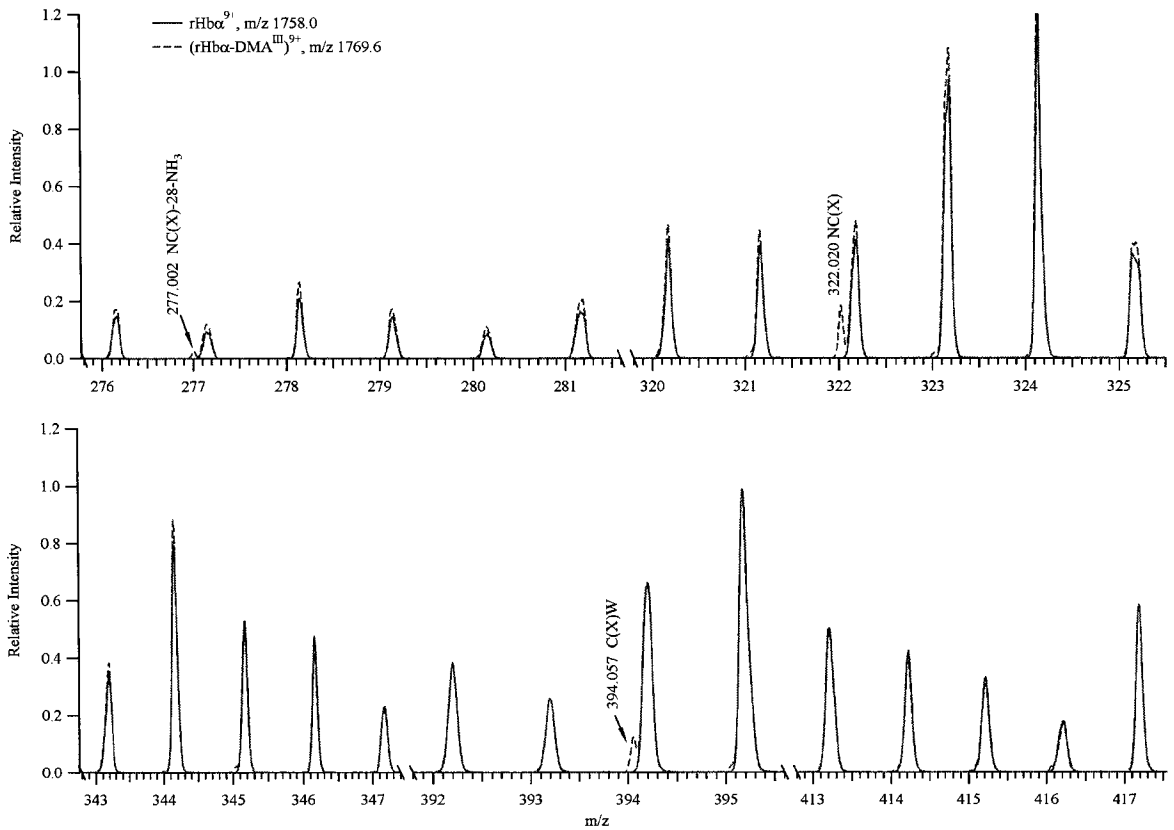

Figure 4-6. Comparison of the MS/MS spectra of the parent ions of the *in vivo*-formed rHbα-DMA^{III} complex (m/z=1769.6, 9^+) and rHbα (m/z=1758.0, 9^+) in the m/z range of 250–420. It shows that two characteristic internal dipeptide ions with DMA^{III} tag at 322.020 and 394.057 amu are uniquely present in the MS/MS spectrum of the rHbα-DMA^{III} complex but not in that of rHbα itself. The experimental conditions are described in Sections 4.2.3 and 4.2.4. Note: C(X) represents that the cysteine residue contains one DMA^{III} tag [$(CH_3)_2As$].

Furthermore, despite that 90% of the α unit of rHb in the sample chosen for CAD MS/MS analysis formed a covalent 1:1 complex with DMA^{III} *in vivo* (Figure 4-2), no significant internal dipeptide ions with DMA^{III} tags that associated with cys-104α (HC, CL) or cys-111α (AC, CH) were observed in its CAD MS/MS spectrum (Figure 4-6 and Table 4-1). To demonstrate that the absence of these internal ions is not due to differential production by CAD fragmentation, a non-physiological protein complex [rHbα– $(DMA^{III})_3$] with saturated stoichiometry (1:3) formed *in vitro* was examined under the same MS and MS/MS conditions. This complex was obtained by incubating rHb with 100-fold molar excess of DMA^{III}, with which both α and β units of rHb can be saturated. Figure 4-7 demonstrates the CAD MS/MS analysis of the α unit bound to three DMA^{III} molecules [rHbα-$(DMA^{III})_3$]. The derived internal ions with the DMA^{III} tag are listed in Table 4-1. In the presence of three DMA^{III} molecules simultaneously bound to the α chain of rHb, the DMA^{III}-tagged internal dipeptide ions associated with cys-13α, cys-104α, and cys-111α were all observed. The internal dipeptide ion of HC or CH with DMA^{III} tag (345.045 amu from cys-104α and cys-111α) has a much stronger signal (~3 fold) than that of NC with DMA^{III} tag (from cys-13α). The intensity of CL with DMA^{III} tag at 321.064 is higher than that of DMA^{III}-tagged NC internal ions. The observed signal of the AC internal ion with DMA^{III} tag (279.015, associated with cys-111α) is very weak, but the alternate tripeptide ACH with DMA^{III} tag shows a strong signal, and its intensity is similar to that of the NC internal ion with DMA^{III} tag. These results indicate that the internal ions from all the three cysteine residues can be produced under the same conditions. Therefore, the absence of DMA^{III}-tagged internal ions of HC/CH, CL, AC,

and ACH is due to an absence of DMA^{III} binding to cys-104α or cys-111α, and not due to the instability to produce the internal ions from these species.

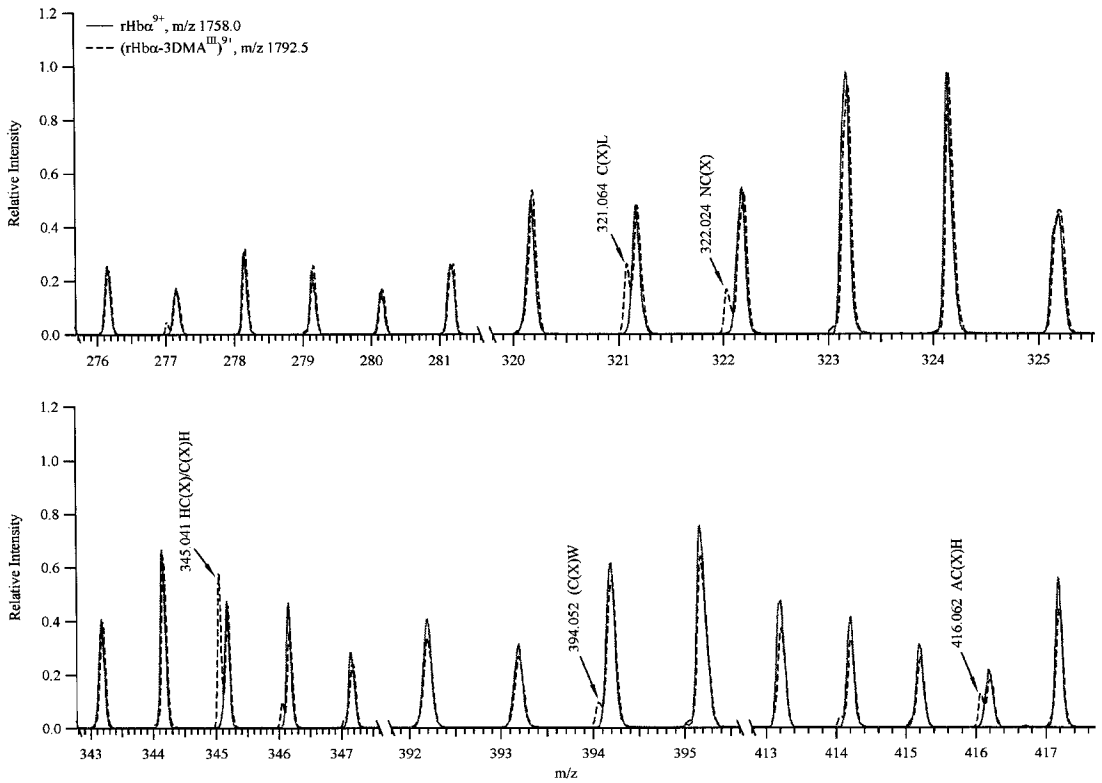

Figure 4-7. Comparison of the MS/MS spectra of rHbα unit (m/z 1758.0, 9+) and its *in vitro* complex with three DMA^{III} molecules (m/z 1792.6, 9+). The rHb-DMA^{III} complex was formed by incubating rHb purified from RBC lysate of control rats with 100-fold molar excess of DMA^{III}. The internal dipeptides at amu of 322.024 (NC-DMA^{III})and 394.052 (DMA^{III}-CW) are due to DMA^{III} binding to cys-13α. The internal peptides at amu of 416.062 [AC(DMA^{III})H] and 345.040 (DMA^{III}-CH) suggest DMA^{III} binding to cys-111. The internal dipeptides at amu of 321.064 (DMA^{III}-CL) and 345.041 (HC-DMA^{III}) suggest DMA^{III} binding to cys-104α. The preparation of the *in vitro* rHb complex with 3 DMA^{III} and the nanoESI-MS and MS/MS conditions were described in Section 4.2.5. Note: C(X) represents that the cysteine residue contains one DMA^{III} tag: $(CH_3)_2As$.

The experimentally measured mass values agreed well with the expected mass values, as shown in Table 4-1, and the mass measurement accuracy is within 70 ppm. Taken together, these results suggest that cys-13α is the highly reactive amino acid residue in native rHb.

4.3.4 Confirmation of the binding site by synthesized peptides

The identification of the reactive binding site cys-13 in the α chain of rat Hb is further supported by evidence from three synthetic peptides encompassing each of the cysteine residues in the α chain of rat Hb. The three nonapeptides were synthesized with sequences adapted from the rHbα unit that contain cys-13α, cys-104α, and cys-111α (Scheme 4-3), respectively. The cysteine residue is located in the center of each peptide. To produce a sufficient amount of peptide-DMA^{III} complex for MS/MS analysis, each synthesized peptide was incubated *in vitro* with 100-fold molar excess amount of standard DMA^{III}.

The nanoESI-MS analysis of the reaction mixture of short peptides with excess DMA^{III} demonstrates that all three peptides are able to react with DMA^{III} and form peptide-DMA^{III} complexes with stoichiometry of 1:1 (Figure 4-8A, B, and C). In a further CAD MS/MS analysis of the peptide-DMA^{III} complexes with a collision energy of 50 eV, two cysteine-bound characteristic fragment ions with m/z of 136.94 and 179.98 were clearly observed for all three peptide-DMA^{III} complexes, which supports that DMA^{III} is bound to cysteine (see Scheme 4-2). With a collision energy of 30 eV, the two specific ions with m/z of 136.94 and 179.98 were also observable, but less intense (Figure 4-9A, B, and C). However, a pair of internal dipeptide ions with a DMA^{III} tag for

each peptide was clearly observed. For peptide 1 (P1), which has a homologous sequence adapted from a local sequence of cys-13α, there was a pair of internal dipeptide ions at m/z of 322.028 and 394.078 (Figure 4-9A), which correspond to NC and CW with DMA^{III} tag. In contrast, both peaks were absent from the MS/MS spectra of P1, peptide 2 (P2), or peptide 3 (P3) without the DMA^{III} complex. The presence of the internal dipeptide ions of NC and CW with DMA^{III} tag is associated with DMA^{III} binding to P1. This pair of internal dipeptide ions with DMA^{III} tag has been observed in MS/MS fragmentation analysis of the *in vivo* DMA^{III}-Hbα complex (Figure 4-6). The paired presence of two internal ions of DMA^{III}-tagged HC and CL with the m/z of 345.03 and 321.01 is due to DMA^{III} binding to P2 (Figure 4-9B) and the paired presence of internal ions of DMA^{III} tagged CH and AC with the m/z of 345.03 and 279.01 is due to DMA^{III} binding to P3 (Figure 4-9C). The internal ions mainly present with DMA^{III} tags for three peptides are summarized in Table 4-2. These data suggest that DMA^{III}-tagged peptides can give characteristic internal ions that are dependent on the local sequences of the neighboring cysteine residues.

In summary, the same internal ions were observed from the binding of DMA^{III} to peptide 1 and from the RBC samples of the arsenic–treated rats. The DMA^{III}-tagged internal ions from DMA^{III} binding to P2 and P3 were not observed from the RBC samples of arsenic treated-rats. The synthetic peptides, P1, P2, and P3, have homologous sequence adapted from the local sequence of cys-13, cys-104, and cys-111, respectively. Taken together, these results further support that cys-13α in rat Hb is the *in vivo* preferential binding site for DMA^{III}.

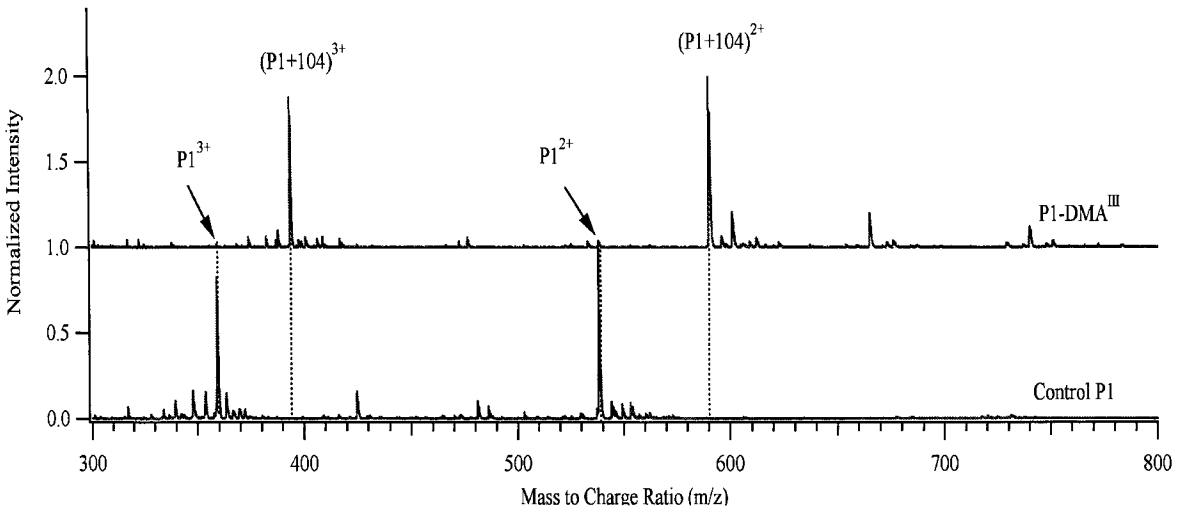

Figure 4-8A. MS analysis of peptide 1 (P1) containing one cysteine residue and its DMA^{III} complex showing that P1 can react with DMA^{III} and form complexes with stoichiometries of 1:1. The concentration of methanol and formic acid in the spray solution were 50% and 0.1%, respectively, and the concentration of the peptide was 5 μM. The ion spray voltage was 1000 V, the curtain gas was 25, and each spectrum was collected using the multichannel accumulation mode (MCA) for 2 min. The detailed reaction conditions were shown in the Section 4.2.7.

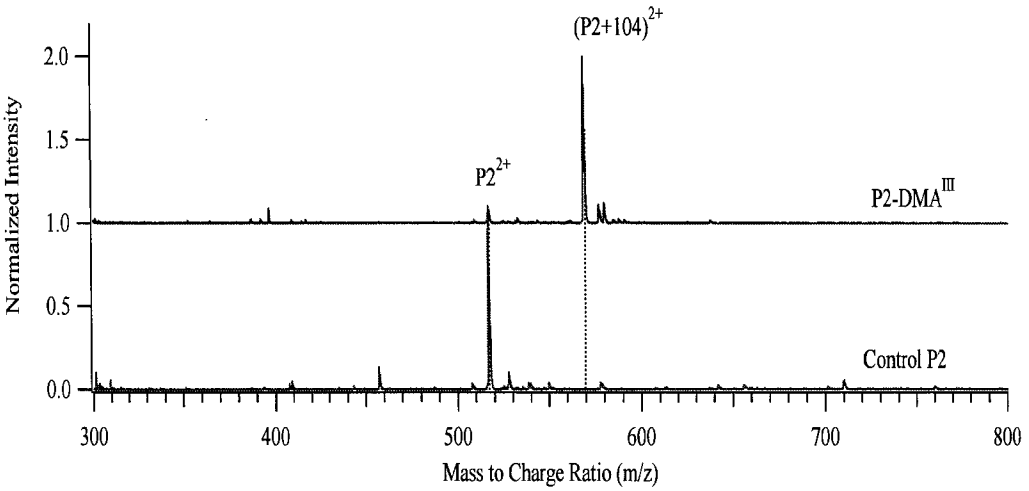

Figure 4-8B. MS analysis of peptide 2 (P2) containing one cysteine residue and its DMA^{III} complex showing that P2 can react with DMA^{III} and form complexes with stoichiometries of 1:1. The other conditions were the same as in Figure 4-8A.

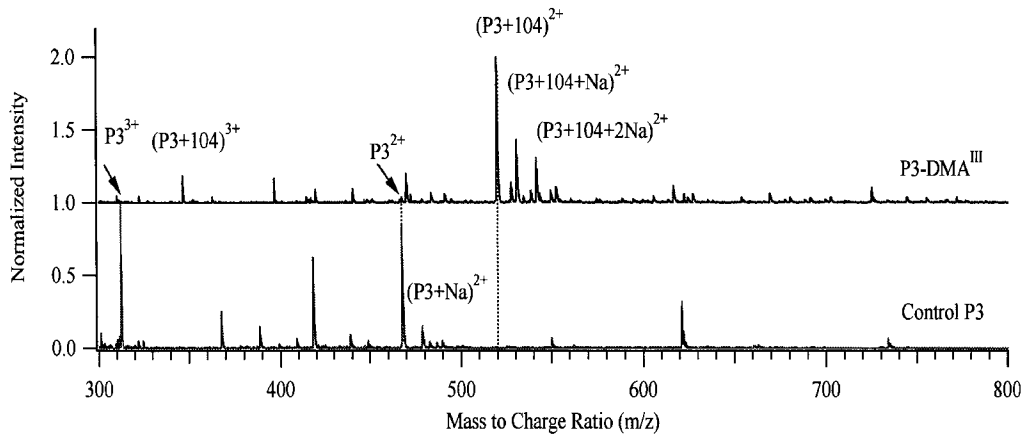

Figure 4-8C. MS analysis of peptide 3 (P3) containing one cysteine residue and its DMA^{III} complex showing that P3 can react with DMA^{III} and form complexes with stoichiometries of 1:1. The other conditions were the same as those in Figure 4-8A.

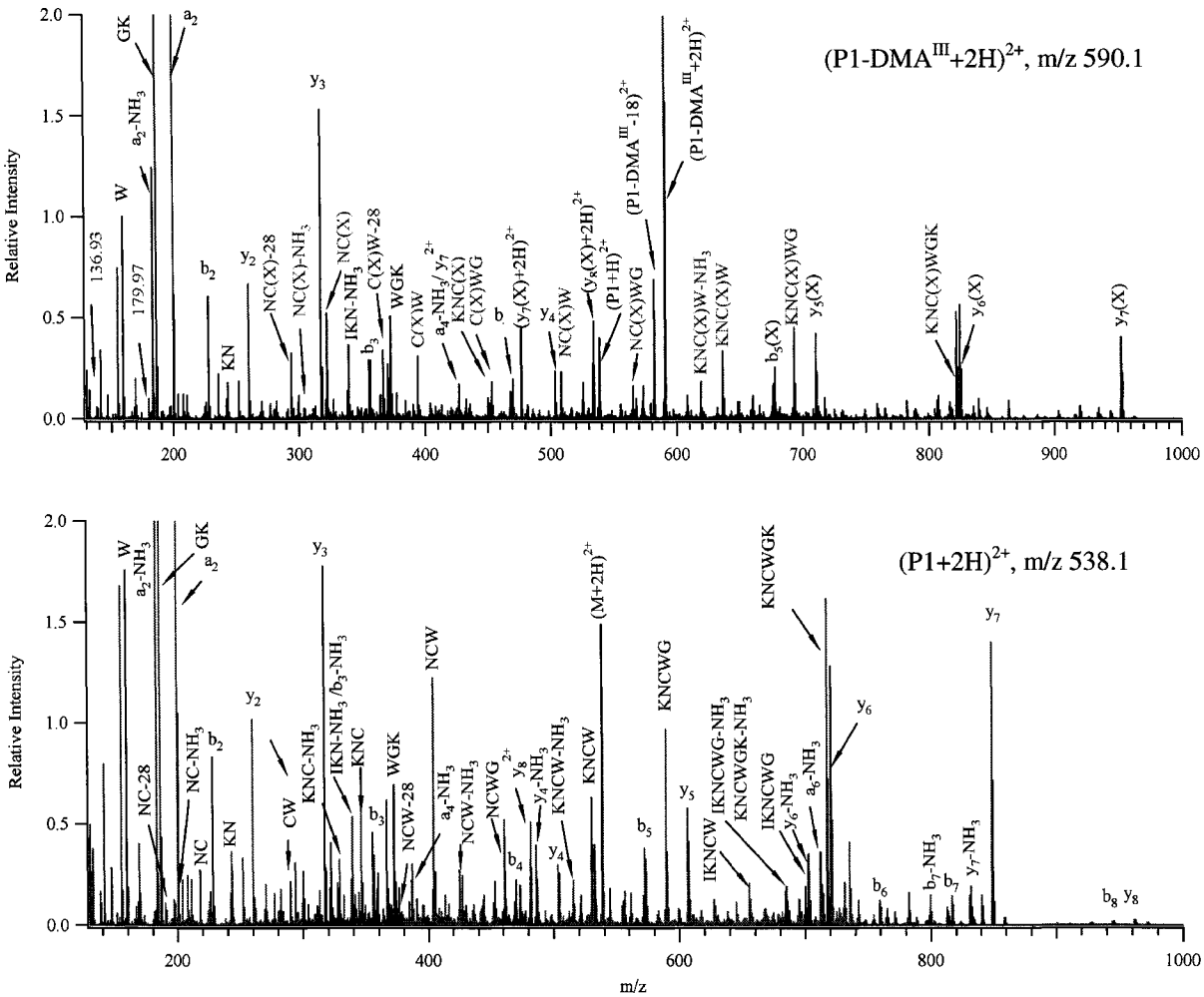

Figure 4-9A. MS/MS analysis of P1-DMA^{III} complexes and the control peptide P1. Parent ions were P1 (m/z 538.1, 2+) and its DMA^{III} complex (m/z 590.1, 2+), respectively. Information from both internal ions and b/y ions supports that DMA^{III} is bound to the cysteine residue in the fifth position of the peptide. Each peptide displays one pair of the unique internal dipeptide ions with DMA^{III} tag. The components for the nano-electrospray solution, the ion spray voltage, and curtain gas were the same as those in Figure 4-8A. The collision energy was 30 eV, and the collision gas setting was 5. Each spectrum was collected using the MCA mode for 5 min.

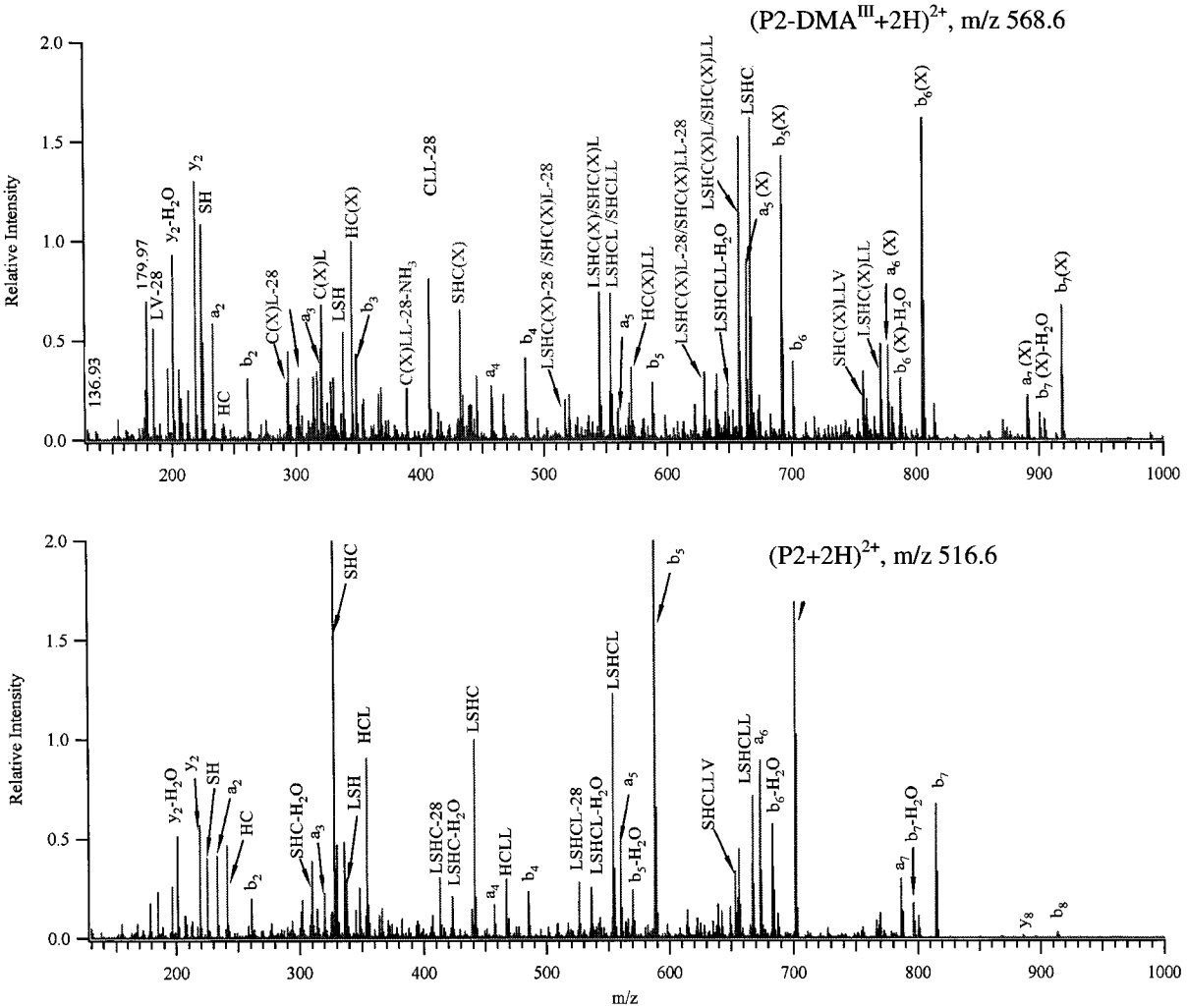

Figure 4-9B. MS/MS analysis of P2-DMA^{III} complexes and the control peptide P2. Parent ions were P1 (m/z 516.6, 2+) and its DMA^{III} complex (m/z 568.6, 2+), respectively. The other conditions were the same as in Figure 4-9A.

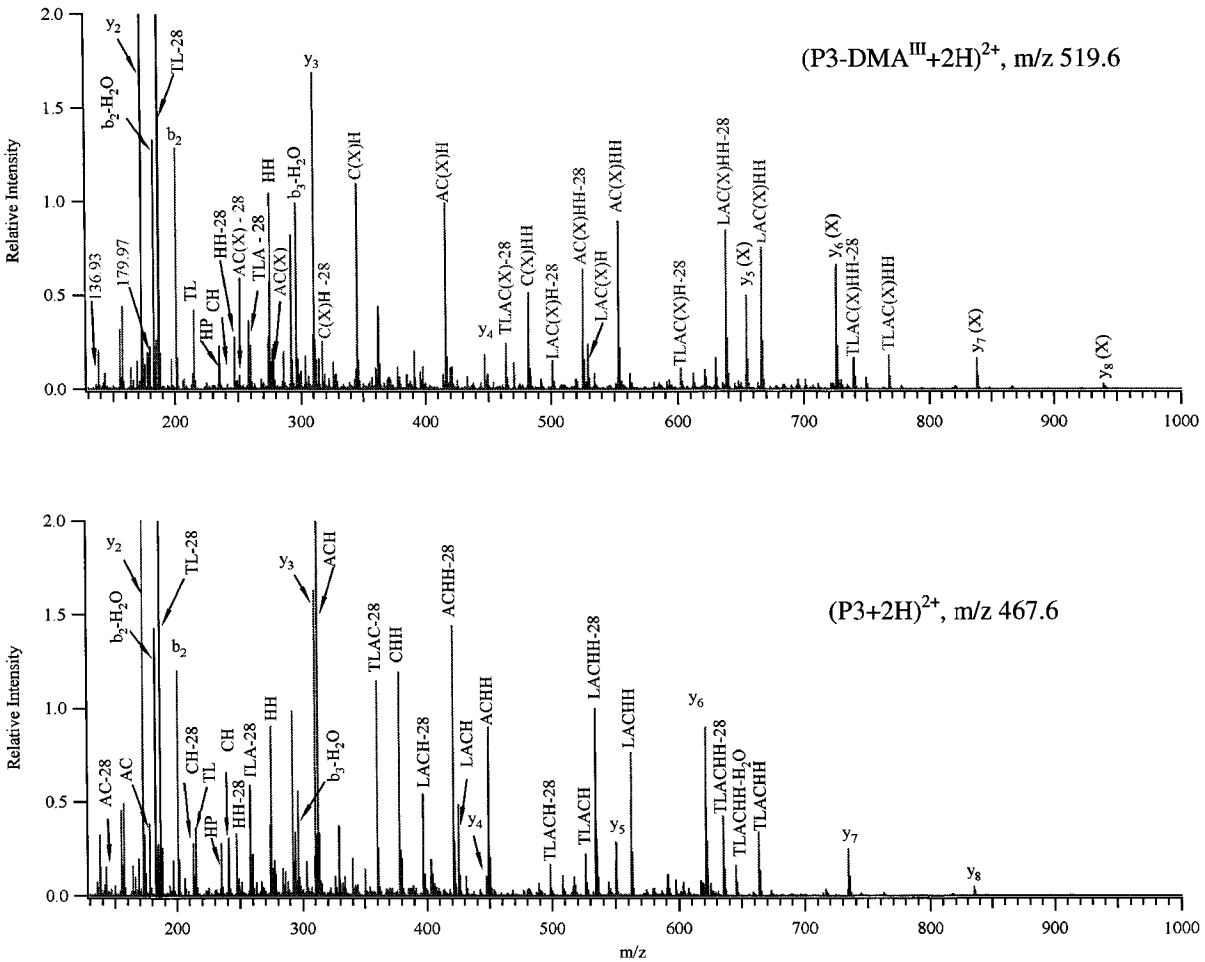

Figure 4-9C. MS/MS analysis of P3-DMA^{III} complexes and the control peptide P3. Parent ions were P3 (m/z 467.6, 2+) and its DMA^{III} complex (m/z 519.6, 2+), respectively. The other conditions were the same as in Figure 4-9A.

Table 4-2. List of major internal ions with DMA^{III} tags, and their expected and measured mass values from MS/MS analysis of DMA^{III} complexes of three synthetic peptides with sequences adapted from the rHbα.

Site	Internal Ions	Expected (amu)	Measured (amu)	Mass Accuracy (ppm)
P1 Cys-13α	NC(X)	322.021	322.028	22
	NC(X)-CO	294.026	294.037	37
	NC(X)-NH_3	304.994	305.008	46
	NC(X)-CO-NH_3	276.999	277.016	61
	C(X)W	394.057	394.078	53
	C(X)W-CO	366.062	366.052	-27
	C(X)W-NH_3	377.031	377.036	13
	C(X)W-CO-NH_3	349.036	349.032	-11
	KNC(X)	450.116	450.106	-22
	KNC(X)-NH_3	433.089	433.072	-39
	C(X)WG	451.078	451.062	-35
	NC(X)W	508.100	508.121	41
	KNC(X)W	636.195	636.192	-5
	KNC(X)W-NH_3	619.168	619.179	18
	KNC(X)WG/NC(X)WGK	693.216	693.220	6
	(KNC(X)WG/NC(X)WGK)-CO-NH_3	676.154	676.188	50
P2 Cys-104α	HC(X)	345.037	345.034	-9
	HC(X)-CO	317.042	317.043	3
	HC(X)-CO-NH_3	300.015	300.018	10
	C(X)L	321.0618	321.065	10
	C(X)L-CO	293.067	293.069	7
	SHC(X)	432.069	432.059	-23
	SHC(X)-CO	404.074	404.066	-20
	SHC(X)-NH3	415.042	415.046	10
	HC(X)L	458.121	458.094	-59
	C(X)LL	434.146	434.128	-41
	LSHC(X)	545.153	545.173	37
	HC(X)LL	571.205	571.215	18
	LSHC(X)L	658.237	658.242	8
	LSHC(X)L-CO	630.242	630.234	-13
P3 Cys-111α	AC(X)	279.015	279.028	47
	AC(X)-CO	251.020	251.027	28
	C(X)H	345.037	345.038	3
	C(X)H-CO	317.042	317.043	3
	C(X)H-CO-NH_3	300.015	300.023	27
	AC(X)H	416.074	416.062	-29
	C(X)HH	482.096	482.113	35
	AC(X)HH	553.133	553.143	18
	LAC(X)H	529.158	529.173	28
	LAC(X)HH-NH3	638.222	638.222	0
	LAC(X)HH	666.217	666.208	-14

Note: C(X) represents that the cysteine residue contains one DMA^{III} tag: $(CH_3)_2As$.

4.4 Discussion and Conclusions

A direct CAD MS/MS analytical method for the identification of an arsenic binding site in a large protein is presented. This method is based on the unique mass defect of arsenic, the high selectivity of arsenic to cysteine residues, and the excellent stability of arsenic-sulfur bonds in the gas phase. The arsenic signature in the fragment ions led to the successful identification of a highly reactive binding site in rHb, cys-13α, for the reactive arsenic metabolite-DMA^{III}. To my knowledge, no report has been made using CAD MS/MS to identify a binding site in such a large protein (~16 kDa, Hb monomer). This method is fast and efficient for the localization of binding sites of arsenic in proteins. The solvent hydrolysis that takes place very often in solution is avoided and the labile adduct tag can be preserved well in the fragment ions. This method does not require enzymatic digestion, which is problematic because it leads to the dissociation of DMA^{III} from rHb in solution. The requirement for mass resolution is not stringent, and identification of the binding sites can be achieved even at moderate mass resolution (~5000 at m/z of 500). Arsenic is not naturally present in proteins; therefore, the arsenic-labeled fragment ions have low background, which allows the detection of protein modifications at low frequencies, as presented here. Compared with other top-down methods, the presented approach is neither limited to the requirement of large, expensive FT-ICRMS instruments, nor is special fragmentation equipment such as ECD or IRMPD necessary. This method may be used in general mass spectrometric laboratories.

This method based on arsenic labeling is potentially useful for characterization and identification of the endogenous and exogenous protein complexes and post-

translational modification products, particularly for those that are labile to enzyme or chemical cleavage. This method may also be useful to quantitatively evaluate the reactivity of individual cysteine residues in the proteins, to identify the reactive cysteine for endogenous and exogenous conjugation, and to study the protein folding and conformation-dependent reactivity. The arsenic labeling method is also potentially useful in generation of cysteine-containing sequence tags for identification of proteomes, which would be complementary to bottom-up approaches by which the cysteine-containing peptides is very difficult to identify. Since arsenic is a ubiquitous environmental contaminant, this method may further the work on arsenic toxicity associated with arsenic binding to the key enzymes. The highly reactive cys-13 in the α chain of rHb has been shown associated with the accumulation of arsenic in rat blood (Chapter 3).

In conclusion, a method coupling arsenic labeling with CAD tandem mass spectrometry has been described in this chapter. It has been successfully used to identify a highly reactive cysteine residue in rHb by direct fragmentation of the large protein ions and monitoring of the unique arsenic signature on the fragment ions using a nanoESI-triple quadrupole time-of-flight mass spectrometer. The method overcomes the limitations of current MS approaches for the identification of chemically labile protein modifications and may have promising potential applications in proteomics and toxicological studies.

4.5 References

1. Giles, N. M., Watts, A. B., Giles, G. I., Fry, F. H., Littlechild, J. A., and Jacob, C. (2003) Metal and Redox modulation of cysteine protein function. *Chem. Biol.* **10**, 677-693.
2. Perry, D. K., Smyth, M.J., Stennicke, H. R., Salvesen, G. S., Duriez, P., Poirier, G. G., and Hannum, Y. A. (1997) Zinc is a potent inhibitor of the apoptotic protease, caspase-3 — a novel target for zinc in the inhibition of apoptosis. *J. Biol. Chem.* **272**, 18530-18533.
3. Maret, W., Jacob, C., Vallee, B. L., and Fischer, E. H. (1999) Inhibitory sites in enzymes: zinc removal and reactivation by thionein. *Proc. Natl. Acad. Sci. USA.* **96**, 1936-1940.
4. Mustacich, D. and Powis, G. (2000) Thioredoxin reductase. *Biochem. J.* **346**, 1-8.
5. Wang, H., Xing, J., Tan, W., Lam, M., Carnelley, T., Weinfeld, M., and Le, X.C. (2002) Binding stoichiometry of DNA adducts with antibody studied by capillary electrophoresis and laser-induced fluorescence. *Anal. Chem.* **74**, 1318-1323.
6. Tsunaka, Y., Takano, K., Matsumura, H., Yamagata, Y., and Kanaya, S. (2005) Identification of single Mn(2+) binding sites required for activation of the mutant proteins of *E. coli* RNase HI at Glu48 and/or Asp134 by X-ray crystallography. *J. Mol. Biol.* **345**, 1171-1183.
7. Mano, N., Nagaya, Y., Saito, S., Kobayashi, N., and Goto, J. (2004) Analysis of the antigen binding site of anti-deoxycholate monoclonal antibody using a novel affinity labeling reagent, acyl adenylate. *Biochemistry* **43**, 2041-2048.

8. Messens, J., Hayburn, G., Desmyter, A., Laus, G., and Wyns, L. The essential catalytic redox couple in arsenate reductase from Staphylococcus aureus. *Biochemistry.* **1999**, *38*, 16857-16865.

9. Wang, H. L., Zou, H. F., and Zhang, Y. K. (1998) Quantitative Study of Competitive Binding of Drugs to Protein by Microdialysis/High-Performance Liquid Chromatography. *Anal. Chem.* **70**, 373-377.

10. Aebersold, R. and Goodlett, D. R. (2001) Mass spectrometry in proteomics. *Chem. Rev.* **101**, 269-295.

11. Bogdanov, B. and Smith, R. D. (2005) Proteomics by FTICR mass spectrometry: top down and bottom up. *Mass Spectrom. Rev.* **24**, 168-200.

12. Bark, S. J., Muster, N., Yates, J. R., and Siuzdak, G. (2001) High-temperature protein mass mapping using a thermophilic protease. *J. Am. Chem. Soc.* **123**, 1774-1775.

13. Demirev, P.A., Ramirez, J., and Fenselau, C. (2001) Tandem mass spectrometry of intact proteins for characterization of biomarkers from *Bacillus cerus* T spores. *Anal. Chem.* **73**, 5725-5731.

14. Forbes, A. J., Patrie, S.M., Taylor, G.K., Kim, Y.-B., Jiang, L., and Kelleher, N. L. (2004) Targeted analysis and discovery of posttranslational modifications in proteins from methanogenic archaea by top-down MS. *Proc. Natl. Acad. Sci. USA.* **101**, 2678-2683.

15. Casagrande, S., Bonetto, V., Fratelli, M., Gianazza, E., Eberini, I., Massignan, T., Salmona, M., Chang, G., Holmgren, A., and Ghezzi, P. (2002) Glutathionylation of human thioredoxin: A possible crosstalk between the glutathione and thioredoxin systems. *Proc. Natl. Acad. Sci. USA.* **99**, 9745–9749.

16. Fratelli, M., Demol, H., Puype, M., Casagrande, S., Eberini, I., Salmona, M., Bonetto, V., Mengozzi, M., Duffieux, F., Miclet, E., Bachi, A., Vandekerckhove, J., Gianazza, E., and Ghezzi, P. (2002) Identification by redox proteomics of glutathionylated proteins in oxidatively stressed human T lymphocytes. *Proc. Natl. Acad. Sci. USA.* **99**, 3505-3510.

17. Cooper, H. J., Heath, J. K., Jaffray, E., Hay, R. T., Lam, T. T., and Marshall, A. G. (2004) Identification of sites of ubiquitination in proteins: a Fourier Transform ion cyclotron resonance mass spectrometry approach. *Anal. Chem.* **76**, 6982-6988.

18. Schweppe, R. E., Haydon, C. E., Lewis, T. S., Resing, K. A., and Ahn, N. G. (2003) The characterization of protein post-translational modifications by mass spectrometry. *Acc. Chem. Res.* **36**, 453-461.

19. Little, D. P., Speir, J. P., Senko, M. W., O'Connor, P. B., and McLafferty, F. W. (1994) Infrared multiphoton dissociation of large multiply charged ions for biomolecule sequencing. *Anal. Chem.* **66**, 2809-2815.

20. Sze, S. K., Ge, Y., Oh, H., and McLafferty, F. W. (2002) Top-down mass spectrometry of a 29-kDa protein for characterization of any posttranslational modification to within one residue. *Proc. Natl. Acad. Sci. USA.* **99**, 1777-1779.

21. Hogan, J. M., Pitteri, S. J., and McLuckey, S. A. (2003) Phosphorylation site identification via ion trap tandem mass spectrometry of whole protein and peptide ions: bovine r-crystallin α chain. *Anal. Chem.* **75**, 6509-6516.

22. Nemeth-Cawley, J. F., Tangarone, B. S., and Rouse, J. C. (2003) "Top Down" characterization is a complementary technique to peptide sequencing for identifying protein species in complex mixtures. *J. Proteome Res.* **2**, 495- 505.

23. Kelleher, N. L. (2004) Top-down proteomics. *Anal. Chem.* **76**, 196A-203A.

24. McLafferty, F. W. (1981) Tandem mass spectrometry. *Science* **214**, 280-287.

25. Nemirovskiy O. V. and Gross, M. L. (1998) Determination of calcium binding sites in gas-phase small peptides by tandem mass spectrometry. *J. Amer. Soc. Mass. Spectrom.* **9**, 1020-1028.

26. Chen, H., Tabei, K., and Siegel, M. M. (2001) Biopolymer sequencing using a triple quadrupole mass spectrometer in the ESI nozzle-skimmer/precursor ion MS/MS mode. *J. Amer. Soc. Mass. Spectrom.* **12**, 846-852.

27. Wan, K. X. and Gross, M. L. (2000) Gas-phase stability of double-stranded oligodeoxygnucleotides and their noncovalent complexes with DNA-binding drugs as revealed by collisional activation in an ion trap. *J. Amer. Soc. Mass. Spectrom.* **11**, 450-457.

28. Zaia, J. and Costello, C. E. (2002) Tandem mass spectrometry of sulfated heparin-like glycosaminoglycan oligosaccharides. *Anal. Chem.* **75**, 2445-2455.

29. Davis, B. D., and Brodbelt, J. S. (2004) Determining glycosylation site of flavonoids. *J. Am. Soc. Mass Spectrom.* **15**, 1287-1299.

30. Cullen, W. R., McBridge, B. B., Manji, H., Pickett, A. W., and Reglinski, J. (1989) The metabolism of methylarsine oxide and sulfide. *Appl. Organomet. Chem.* **3**, 71-78.

31. Burrows, G. J. and Turner, E. E. (1920) A new type of compound containing arsenic. *J. Chem. Soc. Trans.* **117**, 1373-1383.

32. Drabkin, D.L. and Austin, J.H. (1935) Spectrophotometric studies. II. Preparations from washed blood cells; nitric oxide hemoglobin and sulfhemoglobin. *J. Biol. Chem.* **112,** 51.

Chapter 5 Interaction of Human Hemoglobin with Arsenic Species

5.1 Introduction

Arsenic's reputation is that of a notorious toxin which causes a variety of both cancerous and noncancerous effects on humans (1-6). Paradoxically, arsenic compounds have been successfully used for clinical treatment of newly diagnosed, relapsed and refractory acute promyelocytic leukemia (APL) with higher remission rate (7-10). However, a number of adverse effects were also clinically observed including QTc prolongation, leukocytosis, hepatic dysfunction, peripheral neuropathies, and even clinical fatalities (7-14). To understand the benefit and risk profiles of arsenic, extensive research activities on arsenic's mechanisms of actions have been conducted. Most efforts have been focused on cellular differentiation, induction of apoptosis, degradation of specific APL transcripts, antiproliferation, and inhibition of angiogenesis (14-17). But little attention has been paid to arsenic speciation and their interactions with cellular proteins.

The studies in Chapter 3 have shown that DMA^{III} can be efficiently arrested by rat Hb, which reduces the acute toxicity of arsenic and greatly change arsenic metabolism profile. In the context of this research, it is very interesting to investigate the arsenic species interaction with human blood proteins.

To extend the previous studies to human, here interaction of arsenic species with hHb was conducted in both standard protein-arsenic incubation and *in vivo* exposure of arsenic trioxide of APL patients. It is demonstrated that trivalent arsenic can interact with hHb, and the reactivity is arsenic species dependent. Examination of blood from APL patients under arsenic trioxide treatment further demonstrates that arsenic-protein complexes can form *in vivo*, predominantly in the RBC.

5.2 Materials, Patients, and Methods

All procedures of sample collection and analysis were in compliance with the guidelines and regulations of both the Ethical Review Board of the University of Alberta and Harbin Medical University Hospital, China.

5.2.1 Materials

All the materials used have been described in Section 2.2.1.

5.2.2 Patient treatment protocols (done by the Harbin Medical University Hospital)

Four ongoing APL patients (already under treatment for some time) and two newly diagnosed APL patients had been registered in the Harbin Medical University Hospital (China) with signed informed consent for participation in this study. Their status is listed in Table 5-1. At the time of the study, all of the four ongoing patients had been treated with arsenic trioxide (10 mg/day) continuously on a daily basis by intravenous

injection since their admission to the Harbin Medical University Hospital. Prior to the first collection of blood samples for the present study, the four ongoing patients had been treated with arsenic trioxide for 18, 9, 35, and 25 days, respectively. When the project started, the four ongoing patients continued the treatment. A new adult patient (patient 5) was given the same treatment as the four ongoing patients. Patient 6, a newly admitted child, was also treated with the same procedure, except that the dose was reduced to 5 mg/day.

5.2.3 Blood collection protocols.

Blood was collected from the on-going patients for three consecutive days, 24 hours after the previous treatment with arsenic trioxide. For the two newly diagnosed patients, the blood was collected right before treatment with arsenic trioxide, and 24 hours after the first and the second treatment. The blood was then subjected to separation as described below.

Table 5-1. Summary of the APL patients participating in the study

Patient	Age	Sex	Past days of arsenic trioxide treatment (days)	Note
1	35	M	19	-
2	52	M	36	relapsed[a]
3	31	M	10	relapsed[b]
4	31	F	26	-
5	19	M	0	-
6	8	M	0	-

Note: a- patient #2 was diagnosed with APL and was treated with all-*trans* retinoic acid (ATRA) four years ago.
b- patient #3 was diagnosed with APL and was treated with arsenic trioxide (ATO) five years ago, relapsed one year ago, and was treated with ATO again until remission.

5.2.4 Blood separation and lysis of RBC

The blood was separated by centrifugation at 4000 rpm for 10 min at 4 °C. The separated plasma was transported on dry ice and stored at -80 °C before analysis. The RBC were preserved in AS-3 solution (18), and were transported and stored at 4 °C for no more than 42 days before analysis. The RBC were then lysed by addition of water, then subjected to centrifugation to remove the membrane as shown in Section 3.2.4. One portion of plasma and RBC lysates were diluted with 20 mM ammonium acetate (pH 7.0) to the appropriate concentration assigned for GFC-ICPMS analysis. Another portion of RBC lysates were subjected to BioSpin-6 column for purification. The protein fraction was then diluted 10 times by the addition of methanol (to a final concentration of 10% methanol), formic acid (to a final concentration of 0.002% fominc acid), and water. The resulting solution was then loaded on to a nanoelectrospray capillary for nanoESI-MS analysis in a QSTAR system.

5.2.5 Methods

The GFC-ICPMS and nanoESI-MS methods and the reaction between hHb and trivalent arsenic species have been described in detail in Chapter 2.

5.3 Results

5.3.1 Binding of arsenic species with pure hHb

The binding of the trivalent arsenic species to hHb was first examined by GFC-ICPMS. It was found that the percentage of protein-bound arsenic changing over the incubation time is arsenic species dependent (Figure 5-1). Only a small fraction of iAs^{III} (~0.4 %) was bound to hHb after 2 h of incubation (Figure 5-1). Extending the incubation time to 24 h did not substantially increase the binding of iAs^{III} to hHb (~1.6%). The fraction of MMA^{III} increased rapidly during the first 2 hours to 4(±0.2)%, then it continuously increased to 9.3(±0.5)% within 24 hours. The binding of DMA^{III} to hHb also increased very fast during the first 2 hours. However, after reaching its maximum (21(±0.4)%) after 4 h, it then decreased to 17.0(±0.4)% after 24 h. The slight decrease in the hHb-DMA^{III} complex was probably due to oxidation of DMA^{III} to the less reactive DMA^{V} (34), indicating that the formation of hHb-DMA^{III} complexes may be chemically reversible. The results indicate that all the three trivalent arsenic species have very low reactivity to hHb. Of the three arsenic species, DMA^{III} was more reactive, iAs^{III} was less reactive, and MMA^{III} was moderately reactive. The reactivity ratio for DMA^{III}, MMA^{III}, and iAs^{III} was 17:6.5:1.

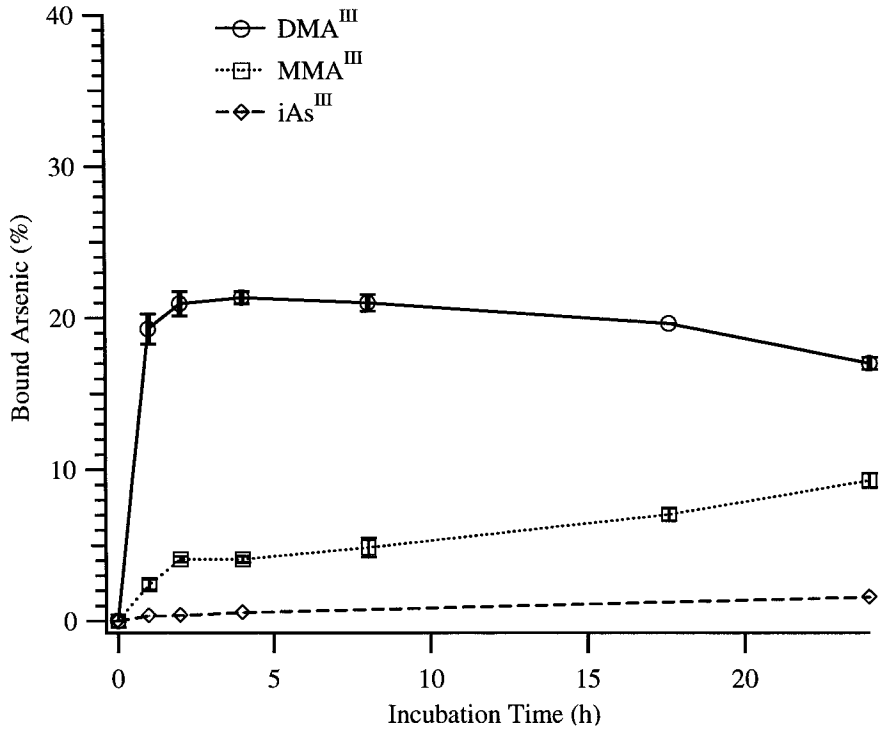

Figure 5-1. Percentage of protein-bound arsenic changing over the incubation time. hHb (20 μM) was incubated with iAs^{III}, MMA^{III}, or DMA^{III} (1 μM) at room temperature for up to 24 h in 20 mM ammonium acetate buffer (pH 7.0). An aliquot (30 μL) of each reaction mixture was then subjected to GFC-ICPMS analysis. The chromatograms obtained were integrated, and the percentage of protein-bound arsenic was calculated. The experimental conditions are described in Section 2.2.2.1

To characterize the possible binding products between hHb and the arsenic species, the molecular species of arsenic bound to the α and β units of hHb were further identified using nanoESI-MS. Figure 5-2A shows typical deconvoluted mass spectra from the nanoESI-MS analysis of hHb with or without reaction with DMA^{III}. In the absence of DMA^{III} (bottom spectrum of Figure 5-2A), the two major species are the α unit (peak 1, 15126 Da) and β unit (peak 3, 15867 Da). The measured molecular mass values are consistent with those reported in the protein bank database (Swiss-Prot). After incubation with excess DMA^{III}, the relative intensity of the α and β units (peaks 1 and 3) decreased, and three new major species appeared (peaks 2*, 4*, and 5*). The molecular mass of the peak 2* species (15230 Da) is 104 Da higher than that of the α unit (15126 Da), suggesting that this is due to the complex of one α unit to one DMA^{III} molecule (22). The peak 4* (15971 Da) and peak 5* (16075 Da) have mass shifts of 104 Da and 208 Da from the β unit (15867 Da), corresponding to complexes of one β unit with one and two DMA^{III} molecules, respectively.

The complexes of DMA^{III} with both the α and the β units of hHb are dependent on the relative concentrations of hHb and DMA^{III}. Figure 5-2B shows representative multicharged mass spectra from the analysis of reaction mixtures containing a constant concentration of hHb (2 μM) and varied concentrations of DMA^{III} (0-100 μM). The signal of the complex of one α and one DMA^{III} molecule (peak 2*) increased with increasing concentration of DMA^{III} up to 10 μM. Further increase of DMA^{III} concentration did not result in any significant increase in the signal of the complex (peak 2*). No other complex of the α unit with DMA^{III} was observed with excess of DMA^{III} (the DMA^{III} concentration ranging from 2 μM to 100 μM). These results suggest that the

reaction between the α unit of hHb and DMA^{III} has 1:1 stoichiometry. Two complexes of the β unit with DMA^{III} (peaks 4* and 5*) in Figure 5-3 had 1:1 and 1:2 stoichiometry, respectively. The complex of one β unit with one DMA^{III} (peak 4*) was favored at a lower concentration of DMA^{III} (2–10 μM), and the complex of one β unit with two DMA^{III} (1:2 stoichiometry, peak 5*) was dominant (peak 5*) at higher concentrations of DMA^{III} (50–100 μM). The stoichiometries were consistent with the available binding sites - free cysteine residues in hHb.

Using nanoESI-MS, the interaction between hHb and MMA^{III} was further examined to confirm the binding stoichiometry and the relative affinity of hHb for arsenic species. While DMA^{III} was able to bind with only one cysteine residue, MMA^{III} in principle can bind to two cysteine residues due to the presence of two free hydroxyl groups. It was found that a new peak (15955 Da, peak 3*) appeared after incubation with MMA^{III}, with a corresponding decrease in the intensity of the β unit (Figure 5-3A). The mass shift from the β chain was 88 Da, which represents the addition of one MMA^{III} molecule and the loss of two H_2O molecules. This is most likely due to the reaction of MMA^{III} with two cysteines (Cys93 and Cys112) in the β chain of hHb. There was no complex of MMA^{III} with the α chain of hHb, which contains only one cysteine. Experiments with a range of MMA^{III} concentrations (2–50 μM, Figure 5-3B) consistently showed that only one MMA^{III} was bound to the β chain of hHb.

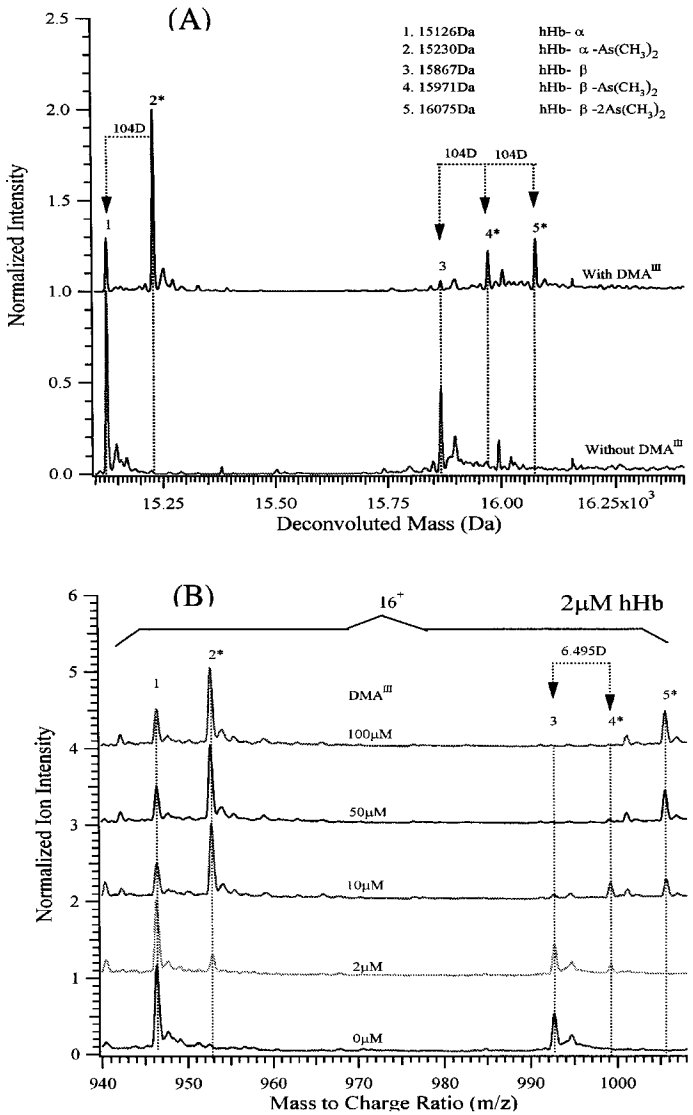

Figure 5-2. Nanoelectrospray mass spectra showing the interaction products between the α and β units of hHb and DMA^{III}. (A): Deconvoluted mass spectra showing molecular mass of the species. (B). The multiply charged mass spectra showing relative intensity changes in the interaction products between hHb and DMA^{III} with increasing concentration of DMA^{III}. The ions carry 16 positive charges. The reaction of hHb with DMA^{III} and the experimental conditions are described in Section 2.2.2.2.

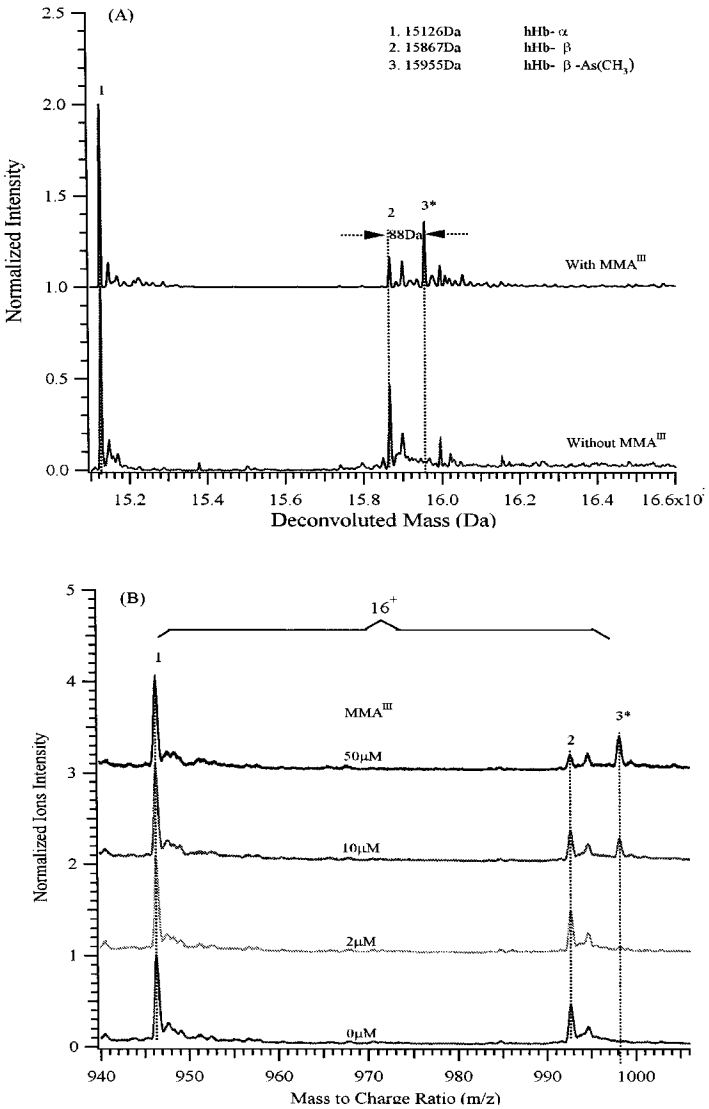

Figure 5-3. Nanoelectrospray mass spectra showing the interaction products between the α and β units of hHb and MMA^{III}. (A): Deconvoluted mass spectra showing molecular mass of the species. (B) The multiply charged mass spectra showing relative changes in the interaction products between hHb and MMA^{III} with increasing concentration of MMA^{III}. The reaction of hHb with MMA^{III} and the experimental conditions are described in Section 2.2.2.2.

Nanoelectrospray MS experiments showed that iAs^{III} had negligible binding to hHb with the molar ratio up to 50:1 (arsenic concentration : hHb). The extremely weak reactivity of iAs^{III} was consistent with the results revealed by GFC-ICPMS (Figure 5-1). Further experiments showed that pentavalent arsenic species (iAs^{V}, MMA^{V}, and DMA^{V}) did not react with hHb. The experimental evidence has shown that trivalent arsenic species can interact with hHb by forming hemoglobin complexes, and that their reactivity depends on the arsenic species.

5.3.2 Arsenic in the blood samples from APL patients undergoing arsenic trioxide treatment

Having established the interaction of trivalent arsenic species with hHb, the next step was to examine arsenic in the blood of APL patients under arsenic treatment.

The arsenic distribution in plasma and RBC of 6 APL patients under arsenic treatment for a duration of up to 38 days was first examined. Arsenic was observed in both the plasma and the RBC of the patients under arsenic treatment. With the increase of total arsenic concentration in plasma, the concentration of total arsenic in RBC increased rapidly (Figure 5-4A). This indicates that RBC can take up arsenic very efficiently from plasma. During the treatment, the arsenic levels in RBC was about ~1.9–4.5 times that in plasma (Figure 5-4B). For short treatment durations, the ratio of arsenic in RBC to that in plasma was as high as 4.5. With increase of the treatment duration, the ratio tended to decrease to a plateau with an average value of 2.5(±0.4). In comparison, the arsenic level in both plasma and RBC was under the detection limit in newly diagnosed patients before

arsenic treatment. The higher percentage of arsenic in RBC compared to plasma suggests that RBC have a higher affinity to arsenic.

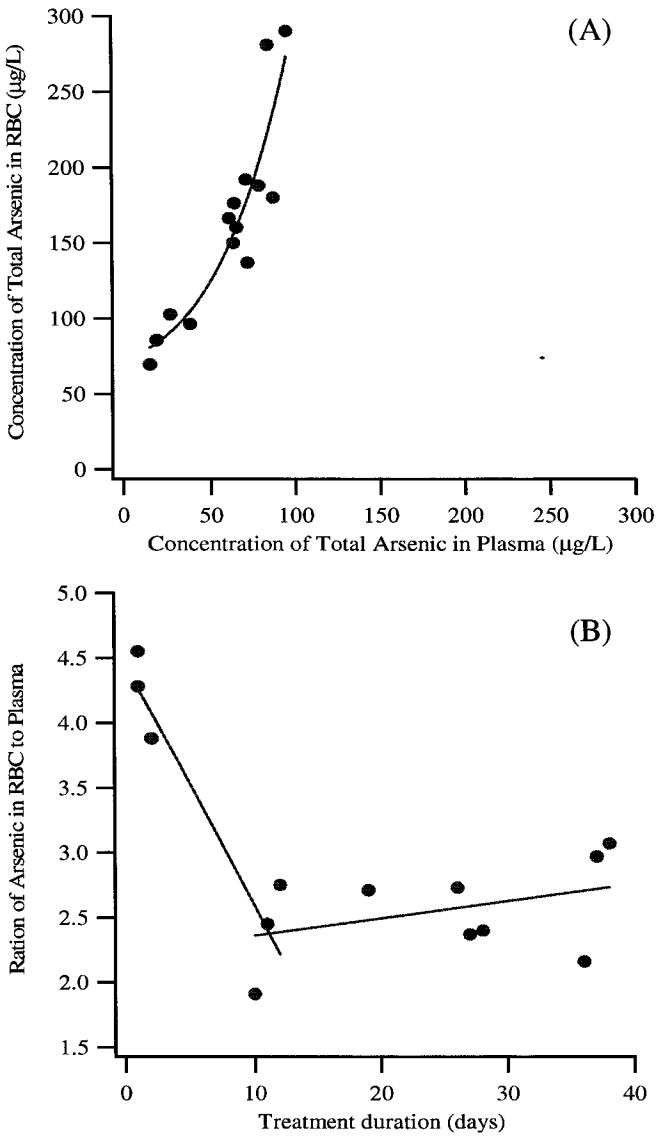

Figure 5-4. Distribution of total arsenic in the RBC and plasma of 6 APL patients. (A) Correlation of total arsenic in RBC with that in plasma, and (B) Change in ratio of arsenic in RBC to that in plasma over treatment time.

To further understand why RBC have a relatively higher amount of arsenic than plasma, GFC-ICPMS was applied to examine the protein-bound and free arsenic in both RBC and plasma of the patients. Figure 5-5 represents the typical chromatograms obtained from the patients. It was found that the major arsenic component in RBC was in protein-bound form (Figure 5-5A), while the major arsenic component in plasma was in the free form (Figure 5-5B). With an increase of total arsenic in RBC, both protein-bound and free arsenic increased, with protein-bound arsenic increasing more quickly than the free arsenic (Figure 5-6A). In comparison, with an increase in total arsenic in plasma, both protein-bound and free arsenic increased; the free arsenic increased faster than the protein-bound form (Figure 5-6B). The results indicate that proteins in RBC may have a higher affinity to arsenic compounds than proteins in plasma.

Protein-bound arsenic in RBC was further correlated with the treatment duration. It was found that binding of arsenic to RBC proteins may involve two phases: one is the fast phase probably related to a relatively strong binding site, and the other is the slow phase, which may correspond to a weak binding site (Figure 5-7).

RBC lysate from the blood of APL patients was further subjected to nanoESI-MS analysis. However, there was no significant change observed in the mass spectra of hHb of these patients after arsenic treatment. This is mainly due to the low reactivity of arsenic species with hHb.

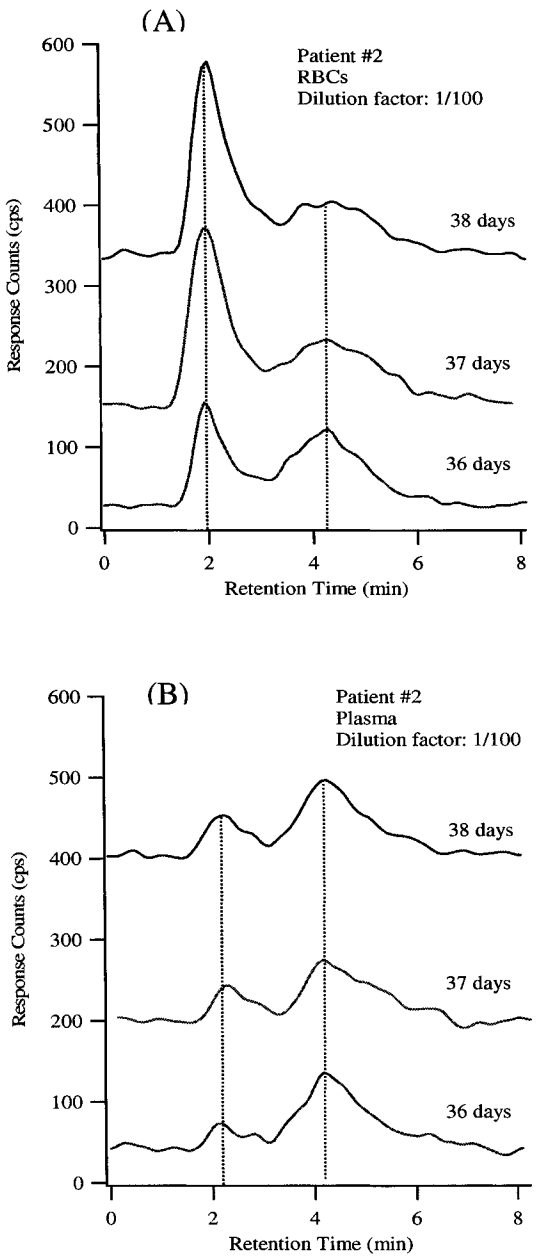

Figure 5-5. Typical chromatograms obtained from the RBC (A) and plasma (B) of APL patients under arsenic trioxide treatment. 20 μL RBC lysate or plasma samples were subjected to GFC-ICPMS analysis. The HPLC separation conditions were the same as those in Figure 2-1.

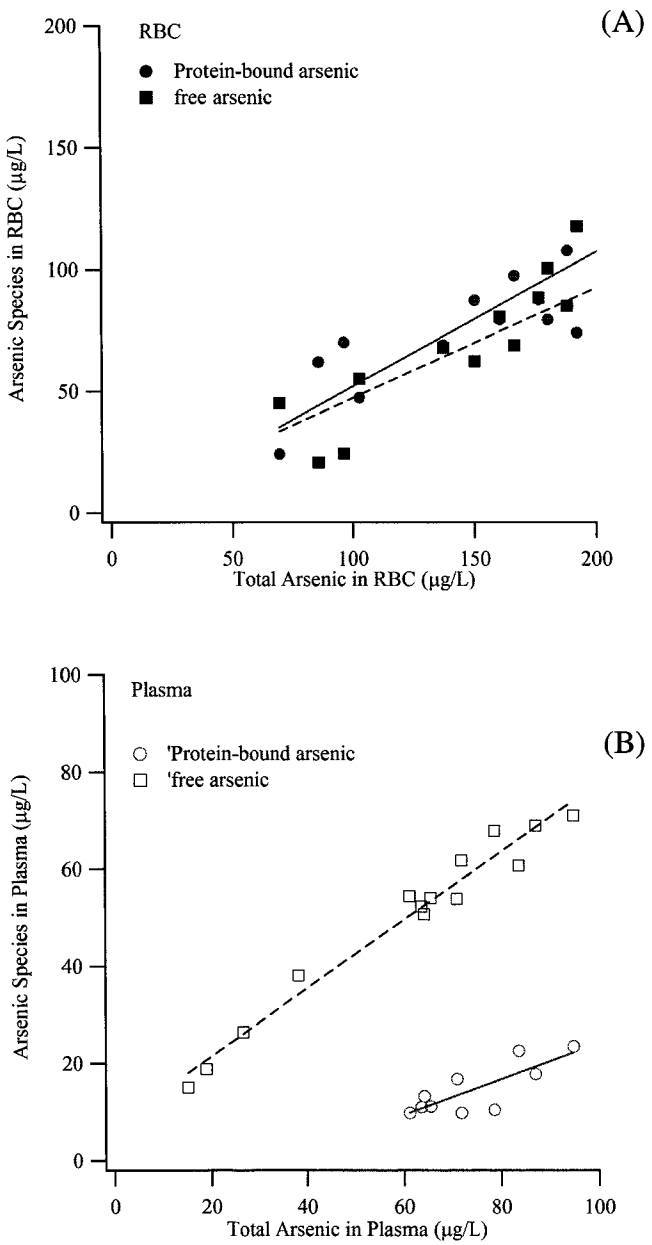

Figure 5-6. Change in the protein-bound and free arsenic with the total arsenic in (A) RBC and (B) plasma from 6 APL patients under arsenic trioxide treatment.

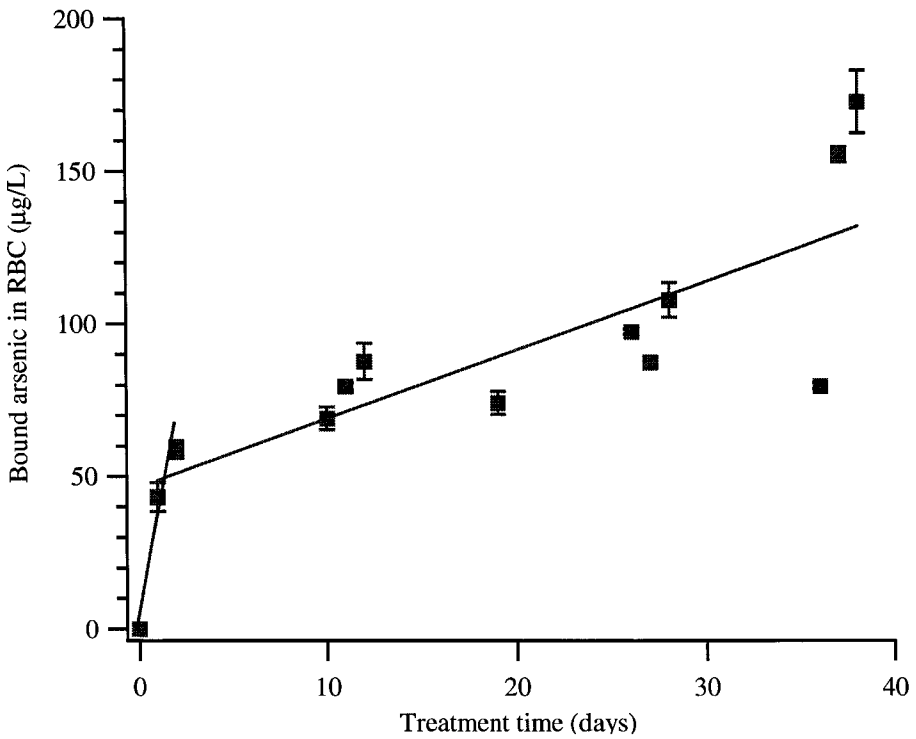

Figure 5-7. Change in the protein-bound arsenic in RBC of APL patients over arsenic trioxide treatment time.

5.4 Discussion and conclusions

Biomonitoring of arsenic has been based mainly on the speciation analysis of arsenic in urine (19-22). Although some attempts (23-25) have been made to perform speciation analysis of arsenic in human blood, little information is available on the protein-bound arsenic and free arsenic species in blood. In clinical APL studies involving arsenic trioxide, the pharmacokinetics of this compound have been examined; however, no arsenic species have ever been differentiated (7, 16). This chapter provided direct information on the protein-bound and free arsenic species in RBC and plasma of APL patients. The large fraction of arsenic present in RBC suggests that RBC should be emphasized for biomonitoring.

Hb has been demonstrated to react with the trivalent methylated arsenic metabolites, MMA^{III} and DMA^{III}, but the reactivity is very low. The binding constants for iAs^{III}, MMA^{III}, and DMA^{III} range from 7.69×10^{2} to 1.3×10^{4} M^{-1} (Chapter 2). The concentration of Hb is in the mM range, and that of the arsenic-bound protein is in the ~μM (hundreds μg/L) range in the APL patients under arsenic treatment. Therefore, the level of arsenic-bound protein is about 1000 times lower than the unbound protein. With the presence of such an abundant unbound protein, the arsenic-bound protein signal could be suppressed during the electrospray process, resulting in significant changes in the mass spectra. More effort could be made to separate the arsenic-bound protein from the unbound protein, in order to identify the protein species. The bound arsenic species could also be released from protein following by arsenic speciation analysis, so that the bound arsenic species could be identified.

Taken together, these preliminary results have shown that trivalent arsenic species involved in the arsenic metabolic pathway can interact with hHb and form characteristic hHb-arsenic complexes. Protein-arsenic complexes were also observed in the blood of APL patients who were under arsenic trioxide treatment, with the major arsenic complexes seen in the RBC of these patients. This may be due to the differences in the affinity of arsenic species for the proteins in RBC and for those in plasma.

5.5 References

1. World Health Organization (2001) Arsenic in drinking water. *WHO Fact Sheet*, **No 210**.
2. Bagla, P. and Kaiser, J. (1996) Epidemiology — India's spreading health crisis draws global arsenic experts. *Science* **274**, 174-175.
3. Chakraborti, D., Rahman, M. M., Paul, K., Chowdhury, U. K., Sengupta, M. K., Lodh, D., Chanda, C. R., Saha, K. C., and Mukherjee, S. C. (2002) Arsenic calamity in the Indian subcontinent — What lessons have been learned? *Talanta* **58**, 3-22.
4. Abernathy, C. O., Liu, Y. P., Longfellow, D., Aposhian, H. V., Beck, B. D., Fowler, B. A., Goyer, R. A., Menzer, R., Rossman, T., Thompson, C., and Waalkes, M. (1999) Arsenic: health effects, mechanisms of actions, and research Issues. *Environ. Health Perspect.* **107**, 593-597.
5. Smith, A. H., Goycolea, M., Haque, R., and Biggs, M. L. (1998) Marked increase in bladder and lung cancer mortality in a region of Northern Chile due to arsenic in drinking water. *Am. J. Epidemiol.* **147**, 660-669.

6. NRC (2001) *Arsenic in the Drinking Water* (update), National Research Council, National Academy Press, Washington, DC.

7. Shen, Z. X., Chen, G. Q., Ni, J. H., Li, X. S., Xiong, S. M., Qiu, Q. Y., Zhu, J., Tang, W., Sin, G. L., Yang, K. Q., Chen, Y., Zhou, L., Fang, Z. W., Wang, Y. T., Ma, J., Zhang, P., Zhang, T. D., Chen, S. J., Chen, Z., and Wang, Z. Y. (1997) Use of arsenic trioxide (As_2O_3) in the treatment of acute promyelocytic leukemia (APL): II. Clinical efficacy and pharmacokinetics in relapsed patients. *Blood* **89**, 3354-3360.

8. Soignet, S. L., Maslak, P., Wang, Z. G., Jhanwar, S., Calleja, E., Dardashti, L. J., Corso, D., DeBlasio, A., Gabrilove, J., Scheinberg, D. A., Pandolfi, P. P., and Warrell, R. P. (1998) Complete remission after treatment of acute promyelocytic leukemia with arsenic trioxide. *N. Engl. J. Med.* **339**, 1341-1348.

9. Niu, C., Yan, H., Yu, T., Sun, H. P., Liu, J. X., Li, X. S., et al (1999) Studies on treatment of acute promyelocytic leukemia with arsenic trioxide: remission induction, follow-up, and molecular monitoring in 11 newly diagnosed and 47 relapsed acute promyelocytic leukemia patients. *Blood* **94**, 3315-3324.

10. Soignet, S. L., Frankel, S. R., Douer, D., Tallman, M. S., Kantarjian, H., Calleja, E., Stone, R. M., Kalaycio, M., Scheinberg, D. A., Steinherz, P., Sievers, E. L., Coutre, S. , Dahlberg, S., Ellison , R., and Jr Warrell, R. P. (2001) United States multicenter study of arsenic trioxide in relapsed acute promyelocytic leukemia. *J. Clin. Oncol.* **19**, 3852-3860.

11. Lu, D. P., Qiu, J.-Y., Jiang, B., Wang, Q., Liu, K.-Y., Liu, Y.-R., Chen, S.-S. (2002) Tetra-arsenic tetra-sulfide for the treatment of acute promyelocytic leukemia: a pilot report. *Blood* **99**, 3136-3143.

12. Zhang, T.-D., Chen, G.-Q., Wang, Z.-G., Wang, Z. -Y., Chen, S. -J., and Chen, Z. (2001) Arsneic trioxide, a therapeutic agent for APL. *Oncogene* **20**, 7146-7153.

13. Westervelt, P., Brown, R. A., Adkins, D. R., Khoury, H., Curtin, P., Hurd, D., Luger, S. M., Ma, M. K., Ley, T. J., and DiPersio, J. F. (2001) Sudden death among patients with acute promyelocytic leukemia treated with arsenic trioxide. *Blood* **98**, 266-271.

14. Evens, A. M., Tallman, M. S., and Gartenhaus, B. (2004) The potential of arsenic trioxide in the treatment of malignant disease: past, present, and future. *Leukemia Res.* **28**, 891-900.

15. Miller, W. H., Schipper, H. M., Lee, J. S., Singer, J., and Waxman, S. (2002) Mechanisms of action of arsenic trioxide. *Cancer Res.* **62**, 3893-3903.

16. Chen, G. Q., Zhou, L., Styblo, M., Walton, F., Jing, Y. K., Weinberg, R., Chen, Z., and Waxman, S. (2003) Methylated metabolites of arsenic trioxide are more potent than arsenic trioxide as apoptotic but not differentiation inducers in leukemia and lymphoma cells. *Cancer Res.* **63**, 1853-1859.

17. Zhu, J., Chen, Z., Lallemand-Breitenbach, V., and de The, H. (2002) How acute promyelocytic leukaemia revived arsenic. *Nat. Rev. Cancer* **2**, 705-713.

18. Heaton, A., Keegan, T., and Holme, S. (1989) In vivo regeneration of red cell 2,3-diphosphoglycerate following transfusion of DPG-depleted AS-1, AS-3 and CPDA-1 red cells. *Br. J. Haematol.* **71**, 131-136.

19. Aposhian, H. V., Gurzau, E. S., Le, X. C., Gurzau, A., Healy, S. M., Lu, X. F., Ma, M. S., Yip, L., Zakharyan, R. A., Maiorino, R. M., Dart, R. C., Tircus, M. G., Gonzalez-Ramirez, D., Morgan, D. L., Avram, D., and Aposhian, M. M. (2000) Occurrence of monomethylarsonous acid in urine of humans exposed to inorganic arsenic. *Chem. Res. Toxicol.* **13**, 693-697.

20. Le, X. C., Lu, X., Ma, M., Cullen, W. R., Aposhian, H. V., and Zheng, B. (2000) Speciation of key arsenic metabolic intermediates in human urine. *Anal. Chem.* **72**, 5172-5177.

21. Mandal, R. K., Ogra, Y., and Suzuki, K. T. (2001) Identification of dimethylarsinous acid and monomethylarsonous acid in human urine of the arsenic-affected areas in West Bengal, India. *Chem. Res. Toxicol.* **14**, 371-378.

22. Wang, Z., Zhou, J., Lu, X., Gong, Z., and Le, X. C. (2004) Arsenic speciation in urine from acute promyelocytic leukemia patients undergoing arsenic trioxide treatment. *Chem. Res. Toxicol.* **17**, 95-103.

23. NRC (1999) *Arsenic in the Drinking Water*, National Research Council, National Academy Press, Washington, DC.

24. Zhang, X., Cornelis, R., De Kimpe, J., Mees, L., Vanderbiesen, V., De Cubber, A., and Older, R. (1996) Accumulation of arsenic species in serum of patients with chronic renal disease. *Clin. Chem.* **42**, 1231-1237.

25. He, B., Jiang, G. B., and Xu, X. (2000) Arsenic speciation based on ion exchange high-performance liquid chromatography hyphenated with hydride generation atomic fluorescence and on-line UV photooxidation. *Fresenius J. Anal. Chem.* **368**, 803-808.

26. Mandal, B. K., Ogra, Y., Anzai, K., and Suzuki, K. T. (2004) Speciation of arsenic in biological samples. *Toxicol. Appl. Pharmacol.* **198**, 307-318.

Chapter 6 Conclusions and Future Research

6.1 Discussion and conclusions

Arsenic is a complete carcinogen, causing various types of cancers in humans. To understand the mechanisms of action of arsenic, seeking an appropriate animal model has been one of the focuses. Rats are among the few animals in which bladder cancer can be induced by arsenic. However, rats have also shown significant differences from human in blood distribution, metabolism, and resistance to acute toxicity of arsenic. Understanding the chemical and biochemical basis of these differences could benefit human health risk assessment. I believe that the interaction of arsenic with hemoglobin may play some role in causing these differences. The objective of this research was to develop and apply analytical techniques to study the hemoglobin-arsenic interaction and its possible biological effects.

With the two main analytical methods, gel-filtration chromatography combined with inductively coupled plasma mass spectrometry and nanoelectrospray tandem mass spectrometry, I have successfully studied the major arsenic species involved in the arsenic metabolic pathway interacting with hemoglobin of rats and humans. I have found that methylated trivalent arsenic species (MMA^{III} and DMA^{III}) are more chemically reactive than their pentavalent forms and inorganic arsenic, and are ready to react with cysteine residues in hemoglobin by forming arsenic-sulfur bonds. The binding capacity depends on both the arsenic and the hemoglobin species. Further studies on some other arsenic species such as phenylarsine oxide have indicated that hydrophobicity may play

an important role in governing arsenic reactivity to hemoglobin. The significantly higher reactivity of the same arsenic species to rat hemoglobin compared to human hemoglobin led me to compare the differences on primary sequences and the microenvironment of the potential target sites of these two hemoglobin species. I have found that available binding sites and preferred position may account for the differences.

Studies on arsenic species interacting with red blood cells (RBC) of humans and rats *in vitro* have shown that the RBC of both can take up arsenic species efficiently. However, the species inside the cells are greatly different. The major arsenic species in human RBC remains free (unbound). In contrast, large amounts of rat Hb-MMA^{III} or -DMA^{III} complexes can form in rat RBC during *in vitro* exposure to arsenic. Further investigation from *in vivo* exposure showed that arsenic in rat RBC can be up to hundreds of times higher than that in plasma, but arsenic in human RBC is only 2.5–4.5 times higher than that in plasma. This further confirmed the higher affinity of rat RBC to arsenic compared to human RBC. Examination of rat RBC by mass spectrometry and tandem mass spectrometry has shown that cysteine 13 in the α unit of rat Hb is the unique target site for DMA^{III}.

The rat Hb-DMA^{III} complex is physiologically stable, and is probably not dissociated until the RBC degrade. It increases with the exposure duration and exposure dose until the RBC are saturated. With the degradation of RBC, DMA^{III} would be released into the blood, ready for further methylation to trimethylarsine, taken up again by RBC, or directly excreted in urine. Therefore, the significant interception of DMA^{III} in rat RBC by the formation of Hb-DMA^{III} complex can shift the arsenic distribution in blood, move the arsenic metabolic profile to higher methylated products, and also delay

arsenic elimination, which may result in the apparently dramatic differences in arsenic distribution, metabolism, and excretion between rats and humans.

Formation of the Hb-DMA^{III} complex has been correlated well with the occurrence of hyperplasia and with the urothelial lesion severity in the rat bladder. Therefore, the concentration of the rHb-DMA^{III} complex is probably directly related to the bioavailable dose of DMA^{III}, which may serve as a biomarker.

The laboratory rat is one of the traditional animal models. It has been widely used in medical, toxicological, and pharmacological studies. Because of its high reactivity and high concentration (~mM range), Cys-13α in rat Hb may have more profound impacts beyond the study of arsenic.

6.2 Future research

There are a number of potential projects that may be conducted to expand the current research. This may include further study on the toxicological response of arsenic compounds in the rat model system and analytical method development to investigate kinetic and metabolic change of arsenic species in blood over time.

6.2.1 Carcinogenic effect of inorganic arsenate in rat bladder

Exposure to inorganic arsenate via drinking water at the level of 100 μg/g induced bladder hyperplasia in rats. Inorganic arsenic is the major form of arsenic in drinking water, and it leads to various cancerous effects in humans. Elucidating the carcinogenic effect of inorganic arsenate in rat would be beneficial for understanding the health effects of arsenic in humans. In the current study, only one dose of inorganic arsenate was

included. More doses and long-term bioassays should be carried out to confirm this finding, establish the dose-response relationship, and investigate the possible mechanisms of action of arsenic.

6.2.2 The fate of hemoglobin-bound arsenic in rat blood and its role in the generation of bladder hyperplasia in rats

In the current project, hemoglobin-bound arsenic was found to be correlated well with bladder hyperplasia and urothelial lesion severity. However, the *in vivo* fate of hemoglobin-bound DMA^{III} was not clear. Tracing the *in vivo* fate of this hemoglobin-bound arsenic species may further our understanding on the carcinogenic effects of arsenic compounds.

6.2.3 Identification of the protein-bound arsenic species in APL patients

Although protein-bound arsenic was observed in human RBC and plasma of APL patients under arsenic treatment, the identities of the bound arsenic species need to be further identified. This could be done by arsenic speciation after releasing arsenic from protein using HPLC-HGAFS or HPLC-ICPMS. The identification of protein-bound arsenic species in RBC and plasma would help the understanding of the toxicokinetic and pharmacokinetic properties of arsenic trioxide, and provide useful information for the benefit and risk evaluation of arsenic in human medicine.

6.2.4 Kinetic study of arsenic-protein binding and arsenic species in blood of APL patients under arsenic trioxide treatment

Blood was collected 24 hours after arsenic trioxide treatment in our current study involving APL patients. Since the half-life of arsenic in blood is short, it is noteworthy to demonstrate the protein-arsenic binding and arsenic species changing over time, the peak arsenic concentration, and the half-life of arsenic in APL patients. It would further the understanding of the pharmacokinetics of arsenic trioxide, and provide useful information on the active drug components and the relative contribution of arsenic species in induced cell apoptosis.

6.2.5 Characterization and identification of arsenic species and involved proteins in epithelial cells of rat bladder

It has been observed that pentavalent arsenic such as iAs^V and DMA^V can induce rat bladder hyperplasia. Analysis of arsenic species in epithelial cells, its DNA adduct or protein adduct, its DNA damage biomarker such as 8-hydroxydeoxyguanosine, and its reactive oxygen species, would provide direct correlation between the arsenic in bladder epithelial cells and the bladder hyperplasia, which could further the understanding of the modes of action of arsenic.